Horizon 2020
Programme

GENIORS
Research and Innovation Action (RIA)
This project has received funding from the European Union's Horizon 2020 research and innovation programme under grant agreement No 755171.
Start date : 2017-06-01 Duration : 48 Months
http://geniors.eu/

GENIORS

optimized flowsheets for homogeneous recycling of advanced MOX fuel in GEN IV reactors

Authors : Dr. Robin TAYLOR (NNL), Robin Taylor (NNL), Thea Lyseid Authen (Chalmers), Andreas Geist (KIT), Andreas Wilden (Juelich), Giuseppe Modolo (Juelich), Bart Verlinden (Juelich), Wim Verboom (Twente), Santa Jansone-Popova (ORNL), Mike Carrott (NNL), Dan Whittaker (NNL), Billy Keywood (NNL)

GENIORS - Contract Number: 755171

Project officer: Roger Garbil

Document title	optimized flowsheets for homogeneous recycling of advanced MOX fuel in GEN IV reactors
Author(s)	Dr. Robin TAYLOR, Robin Taylor (NNL), Thea Lyseid Authen (Chalmers), Andreas Geist (KIT), Andreas Wilden (Juelich), Giuseppe Modolo (Juelich), Bart Verlinden (Juelich), Wim Verboom (Twente), Santa Jansone-Popova (ORNL), Mike Carrott (NNL), Dan Whittaker (NNL), Billy Keywood (NNL)
Number of pages	71
Document type	Deliverable
Work Package	WP6
Document number	D6.2
Issued by	NNL
Date of completion	2021-06-18 11:14:06
Dissemination level	Public

Summary

The Deliverable Report, D6.2, Optimized flowsheets for homogeneous recycling of advanced MOX fuel in GEN IV reactors, compiles optimization studies towards the development of GANEX processes for the homogeneous recycling of actinides performed within the GENIORS project focused on the two reference processes for the second transuranic separation cycle (GANEX-2): i. EURO-GANEX optimization studies ii. CHALMEX optimization studies

Approval

Date	By
2021-06-18 11:14:54	Dr. Robin TAYLOR (NNL)
2021-06-18 17:31:09	Dr. Jean-Marc ADNET (CEA)
2021-06-21 07:28:54	Mr. Stéphane BOURG (CEA)

CONTENT

This project has received funding from the EURATOM research and training programme 2014-2018 under grant agreement No 755171. The content of this deliverable reflects only the author's view. The European Commission is not responsible for any use that may be made of the information it contains.

INTRODUCTION

The Deliverable Report, *D6.2, Optimized flowsheets for homogeneous recycling of advanced MOX fuel in GEN IV reactors,* compiles optimization studies towards the development of GANEX processes for the homogeneous recycling of actinides performed within the GENIORS project focused on the two reference processes for the second transuranic separation cycle (GANEX-2):

i. EURO-GANEX optimization studies
ii. CHALMEX optimization studies

SCOPE

This report covers the work undertaken in Work Package 6 of GENIORS associated with GANEX process options for homogeneous recycling with a focus on activities that help to optimise the flowsheet designs. Note that it was decided at the GANEX Workshop, held at the GENIORS project meeting in Antwerp (October 2018), to focus on basic data for future flowsheet design rather than drive towards flowsheet testing. This was because the EURO-GANEX cycle had already been successfully tested in its current form and there was insufficient basic data to propose flowsheet testing of modified versions with the new ligands that were still under investigation. Likewise, it was agreed that further process chemistry studies of the CHALMEX option were needed in GENIORS before commitments to flowsheet testing should be considered.

REVIEW OF THE ‘STATE OF THE ART’ FOR HOMOGENEOUS RECYCLING

Robin Taylor, Thea Lyseid Authen, Andreas Geist

INTRODUCTION

Nuclear power reactors provide a safe, low-carbon and non-intermittent production of electricity. In 2019, 26.7% of the EU’s total net electricity generation was generated by 109 nuclear power reactors across 16 member countries. However, whilst the potential contribution nuclear energy can make towards a sustainable, low carbon future is being increasingly recognized, the challenges remain related to safe, secure, long term management of the spent nuclear fuels (SNF) that are highly radioactive over long timescales [1]. Altogether, 57,861 tHM SNF had been produced and stored by the end of 2016 in the EU [2-5] whilst globally, around 10,000 tonnes of SNF are generated per year [6]. Whilst SNF can be interim stored safely for extended periods, ultimately there are only two options for spent fuel management (SFM): disposal or recycling. Direct disposal in a deep geological repository (DGR), called the open or once through fuel cycle, is the accepted strategy for many countries such as Finland, Sweden and the United States [7, 8]. SNF recycling, based on reprocessing to recover re-usable nuclear materials and fabrication of new fuels from the reprocessed products, has been implemented industrially in some countries, e.g. France, UK and Japan. This is referred to as the closed nuclear fuel cycle and there are variations on the closed fuel cycle depending on which materials are recycled and whether the materials are recycled once or multiple times [9]. The advantages of recycling have been described elsewhere but, as might be expected, relate to improved use of natural resources, less wastes with reduced radiotoxicity for disposal leading to a smaller DGR and a smaller environmental footprint for nuclear energy [1, 7, 10-12].

Europe has a long history of reprocessing SNF with plants in Belgium, France, Germany, Russia and the UK [13]. France and the UK have operated commercial scale reprocessing plants at La Hague and Sellafield, respectively, with more than 34,000 and 65,000 tonnes of used nuclear fuels reprocessed at these sites [14, 15]. All these reprocessing programmes have used or still use the PUREX process [16-18] to separate fissile materials, uranium and plutonium, from irradiated fuel. Uranium and plutonium can be recycled in present-day light water reactors (LWRs) either as reprocessed uranium oxide (RepU) fuels or mixed oxide (MOX) fuels.

Advanced fuels and reactors, however, offer the prospect of multi-recycling of U and Pu which can substantially increase the benefits in terms of uranium utilisation and resource preservation [7]. Whilst multi-recycling in LWRs is possible, fast reactors (so-called Generation IV nuclear energy systems) [10] are optimised for this purpose. SNF recycling in the Generation IV reactors has the advantage of comprehensively addressing issues such as sustainability, proliferation resistance, reprocessing of non-oxide and high-burnup fuels and the efficient use of the DGR. The latter is supported by recycling minor actinides (MA = Np, Am, Cm) to reduce the heat loading and radiotoxicity of the final wastes [7, 19-21].

The recycling of uranium, plutonium and MA in fast reactor (FR) based fuel cycles can be via either homogeneous or heterogeneous routes, see Figure 1 [22, 23]. In heterogeneous recycling (often termed the partitioning and transmutation or P&T scenario), uranium, plutonium and potentially neptunium are recovered, usually by the PUREX process for the production of MOX fuels. The other MA, americium and curium, are then recovered from the PUREX high level waste (HLW) stream and converted to MA fuels or targets which can be transmuted in the FR. In this scenario, the (U,Pu) and MA fuels are separated in different stages in the reprocessing plant and the refabricated fuels are distributed heterogeneously in the reactor core.

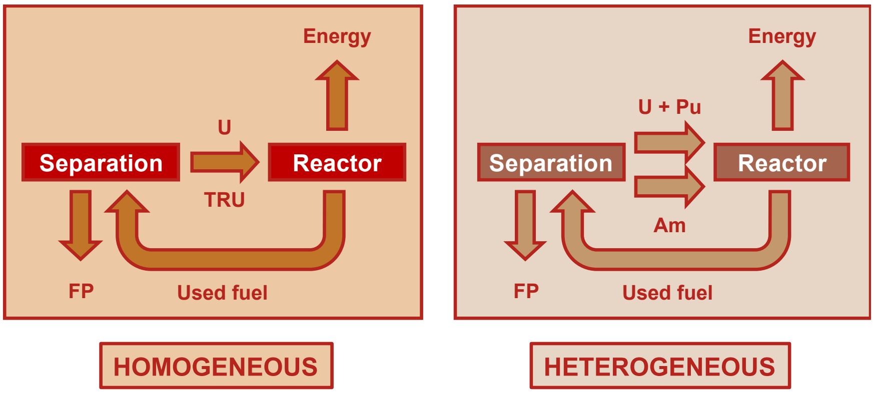

Figure 1: Schematic illustration of heterogeneous and homogeneous recycling. FP = fission products

In the homogeneous recycling option, uranium and the transuranic elements (TRU = Np, Pu, Am, Cm) are contained within a single fuel type and distributed homogeneously throughout the FR core. These fuels typically have between 1 – 5 % wt/wt MA compared to perhaps 30 wt% MA in the MA fuel in the heterogeneous recycle scenario. The homogeneous mode is beneficial in that there is no pure stream of plutonium, making the fuel production arguably more proliferation resistant. Simulation studies have also suggested that a higher degree of minor actinide transmutation is achieved with homogeneous fuels, compared to heterogeneous fuels. Whilst the homogeneous route is perhaps more straightforward with regards to fuel fabrication and reactor physics, the separations chemistry is more complicated than the heterogeneous reprocessing. Therefore, advanced fuel cycle R&D programmes commonly pursue both heterogeneous and homogeneous options.

The development of the chemical separations processes needed for the reprocessing (or partitioning) of the actinides is widely recognised as a key enabler of advanced fuel cycle technologies. In Europe, the development of the chemical separations required for such strategies was triggered by two French waste management acts (1991 and 2006) [24, 25] and has found support from EURATOM-funded research programmes since the early 1990s. Continuously evolving from initially small programmes, a sequence of programmes dedicated to developing actinide separation processes and the related chemistry was executed: NEWPART (1997–1999) [26], PARTNEW (2000–2003) [27], EUROPART (2004–2007) [28], ACSEPT (2008–2012) [29], SACSESS (2013–2016) [30-32], and the latest programme, GENIORS (2017–2021) [33]. These programmes have made substantial progress in developing the separation technologies towards the point at which they can be deployed and our previous paper [23] discussed the actinide separation processes developed in Europe addressing heterogeneous recycling. This paper reviews and assesses the respective processes for homogeneous recycling, once again focusing on the development in Europe.

RECYCLING STRATEGIES

The discussion so far has focused on how multi-recycling in FRs can derive optimum benefits from nuclear energy generation related to sustainability and waste management and how this multi-recycling can be achieved either in a heterogeneous or homogeneous mode. The heterogeneous recycling mode is primarily related to the aqueous reprocessing (hydrometallurgical) routes, involving:

a) An initial separation of U and Pu using the PUREX process or some variation thereof. If desirable, neptunium can be recovered with the U and Pu relatively easily [34].
b) A new extraction process to recover either americium and curium or americium alone from the aqueous HLW stream.

The different strategies for heterogeneous recycling of MA are described in the preceding paper [23]. Homogeneous recycling, on the other hand, can be achieved either by an aqueous route or by a non-aqueous pyrochemical processing of SNF in molten salt media [35, 36]. Indeed, pyro-processing is well suited to homogeneous recycling of FR fuels, being resilient to radiation from high burn up and short cooled FR fuels, based on electrorefining that is adapted to the metal fuels often considered for FRs and naturally producing a low purity mixed actinide product [37]. However, pyro-processing is generally a low throughput batch process and, as such, was originally developed as part of the Integral Fast Reactor programme in the United States [38]. Further discussion of the pyrochemical routes for homogeneous recycling are beyond the scope of this paper but the interested reader is referred to references [9, 35, 39-42].

AQUEOUS SEPARATION PROCESSES FOR HOMOGENEOUS RECYCLING

The basic requirement for homogeneous recycling is that it requires the recovery of the TRU elements as a group. Uranium could be co-recovered with the TRU or separated on its own in a dedicated solvent extraction cycle (or other process such as crystallisation [9, 43]). From this initial assumption, some secondary characteristics of the process become evident as well:

- A new extractant is required since tributyl phosphate (TBP), as used in the PUREX process, is not able to extract trivalent minor actinides.
- Adherence to the "CHON principle[1]" of degradable ligands in the process is preferred, particularly for the organic phase.
- Efficient extraction of TRU actinide ions in oxidation states III (Am, Cm), IV (Pu, Np) and VI (Np, potentially U and Pu) is required.
- The process must be able to cope with high concentrations of plutonium (~10 times that of the conventional PUREX process for thermal oxide fuel reprocessing) without third phase or precipitate formation. Therefore, avoiding Pu recovery by reductive stripping (as used in the PUREX process) is preferred.
- Elimination of hazardous reagents, such as hydrazine, is advisable.
- At some point in the process there must be selectivity in either the organic or aqueous phases for trivalent actinides over trivalent lanthanides otherwise effective decontamination from lanthanides (which are neutron poisons in the reactor) will not be achievable.
- Fast chemical and/or mass transfer kinetics are required for compatibility with next generation solvent extraction equipment such as centrifugal contactors.
- Ligands, particularly in the organic phase, must be sufficiently stable towards radiolysis and hydrolysis and extractants must be sufficiently soluble in the diluent to enable extraction of rather high concentrations of TRU elements.

In Europe, substantial challenges were met in early projects, NEWPART, PARTNEW and EUROPART, developing ligands that were able to achieve the challenging An(III)/Ln(III) separation [44, 45] and this led to defining and testing 'reference' processes for heterogeneous recycling in the later projects, namely ACSEPT and SACSESS [36, 46, 47]. The learning from these early projects was exploited, initially in the ACSEPT project, to start development of a European option for homogeneous recycling [48]. This pan-European development was in parallel to French efforts and indeed the first strategies for homogeneous recycling were developed by the French Atomic Energy Commission (CEA) and tested in their ATALANTE facility at Marcoule [36, 49, 50]. The process was termed GANEX (Grouped ActiNide Extraction) and, as of today, three GANEX options exist for homogeneous recycling and a fourth process variant for heterogeneous recycling has also been reported. These four GANEX-variants fall into three basic strategies, depending on how they recover the TRU actinides, as indicated in Figure 2:

1) Co-extraction of TRU and lanthanides followed by selective stripping of TRU
2) Selective extraction of TRU
3) Co-extraction of TRU and lanthanides followed by selective and sequential stripping of, firstly, Np and Pu and then trivalent MA

All three strategies presume an initial separation of most or all of the uranium to reduce the volume and complexity of the TRU recovery cycle. Figure 2 also indicates the types of ligands (O or N donor ligands in organic or aqueous phases) proposed for each strategy.

In brief, the GANEX process was first developed by the CEA and designed as a 2-stage solvent extraction process, where the bulk uranium is extracted in the primary stage (GANEX-1) [51], while the TRU/fission product separation is achieved in the secondary GANEX-2 stage – this has been termed CEA-GANEX [50]. In the ACSEPT project alternatives to CEA-GANEX were investigated and the EURO-GANEX cycle was developed and tested [52-54] as well as the initial formulation of the Chalmers-GANEX (CHALMEX) [55-58]. In the CEA-GANEX and the

---

[1] Ligands that contain carbon, hydrogen, oxygen and nitrogen only and, therefore, should be fully decomposable to gases.

EURO-GANEX processes, the actinides (An) and lanthanides (Ln) are co-extracted from the GANEX 1st cycle (GANEX-1) raffinate. The actinide/fission product separation is achieved through subsequent selective stripping. In the CHALMEX process, the An/Ln separation occurs by the selective extraction of An [55-57]. It is clear that the CHALMEX option, at least superficially, offers a simpler and more elegant solution to the challenge of recovering TRU actinides as a group. However, it is concomitantly more challenging from the process chemistry perspective and, for reasons that will become apparent later, the EURO-GANEX is considered to be the current reference process for the GANEX 2nd cycle (GANEX-2).

The individual processes will be briefly described below, focusing on aspects such as their basic principles, development status (technology readiness), upstream and downstream compatibilities, generation of secondary wastes and process safety. In line with our previous review [23], decontamination factors achieved in lab-scale process demonstration trials are not reported (stricter purity requirements can quite easily be met by e.g. increasing the number of stages); such data are found in the original literature. Acronyms for extracting and complexing agents, together with their molecular structures, are explained in the Appendix.

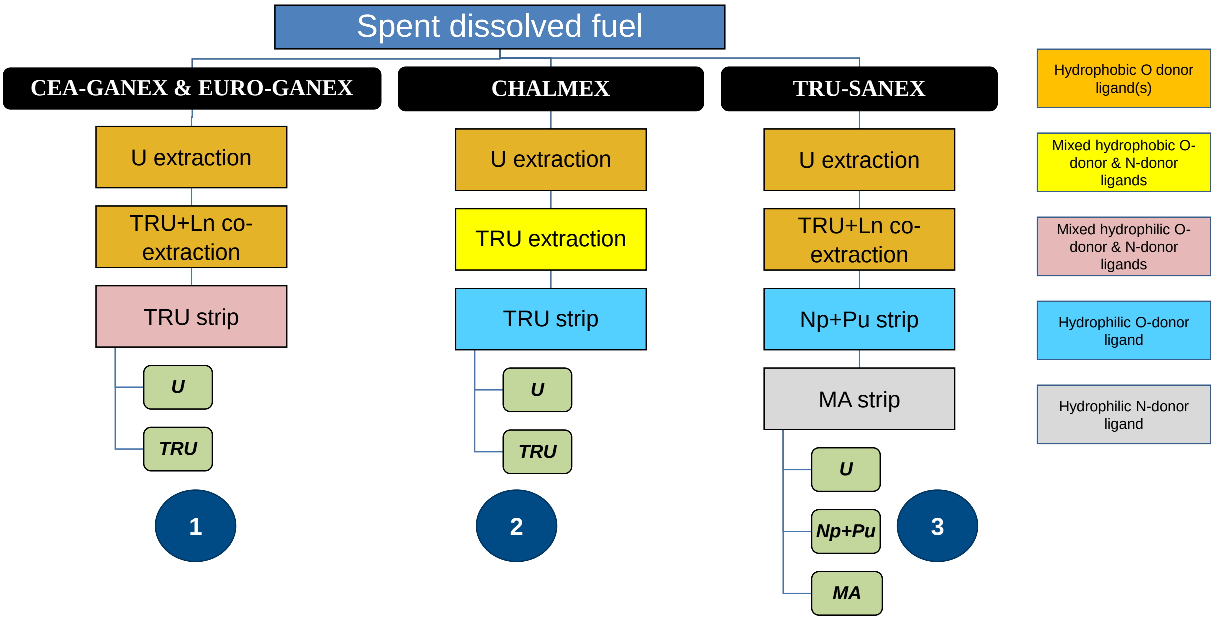

Figure 2: A schematic overview of GANEX solvent extraction processes for homogeneous recycling developed in Europe. The colour scheme indicates the kind of extracting or complexing agents used (see legend)

URANIUM EXTRACTION (GANEX-1 CYCLE)

The GANEX 1st cycle is common for all the variants of the GANEX processes and is aimed at the bulk recovery of uranium from a dissolved spent nuclear fuel solution. This is necessary as a high purity uranium product is required to enable tuning of the U/TRU ratios in the final fuel. It also reduces the volume (mass) of material that must be processed in the next cycle and simplifies the chemistry – since uranium is present as the very stable, linear, hexavalent dioxo-cation, UO_2^{2+}, which is quite different to the other An^{3+} and An^{4+} cations. The uranium separation is achieved by a solvent consisting of a N,N-dialkylamide that is selective for U(VI), N,N-di-(ethyl-2-

hexyl)isobutyramide (DEHiBA) in an aliphatic diluent such as hydrogenated tetrapropylene (HTP) or Exxsol D-80. N,N-dialkylamides have several advantages including adherence to the CHON-principle, high hydrolytic and radiolytic stability and a high loading capacity for uranium. DEHiBA degrades into carboxylic acids and secondary amines, which have little to no effect on the separation of uranium from the raffinate. DEHiBA delivers high values for $D_{U(VI)}$, high U/Pu separation factors (~80), and high decontamination factors (DF) for most fission products in nitric acid media [36, 59, 60].

Two hot tests with SNF have been performed on the GANEX-1 cycle. The flowsheet was initially developed at the CEA in France and tested in the ATALANTE facility at Marcoule with thermal oxide fuel [51]. Later, the flowsheet was adjusted by use of the CEA's PAREX model and tested at the Joint Research Centre (JRC) in Karlsruhe at the end of the ACSEPT project [54]. In both cases the aim was to generate the highly active (HA) raffinate stream for testing the GANEX-2 cycle and a full optimisation of the GANEX-1 cycle has not really been pursued. Nevertheless, both tests gave good results that are summarised in Table 1. The flowsheet for the JRC hot test was based on dissolved FR fuel and so had a different U:Pu ratio in the feed. The results of the JRC test with respect to Np, Pu and Tc decontamination were not as good as the CEA test. This is probably attributable to the use of short residence time centrifugal contactors and fewer scrubbing stages in the JRC test. Optimisation of the hydrazine scrubbing is evidently required. As with the PUREX process, technetium co-extraction with uranium was also a significant factor and accounted for in the PAREX model. The technical maturity for this cycle has been assessed through application of the widely used technology readiness level (TRL) assessment by the OECD-NEA [61]. Although it is noted that this assessment was made at the "system level" and so parts of the process (so-called "critical technology elements") may actually be at a lower level. GANEX-1 was assessed to be at TRL 5 (which was defined as "*Technology component or process step validated at bench scale under relevant conditions. Process models developed. Proof of principle hot tests using spent fuel*" [9, 61]).

Table 1: Key properties and results from the GANEX-1 hot tests at CEA and JRC [36, 51, 54]

Property	**CEA hot test**	**JRC hot test**
U in feed (g/L)	176	103.1
Pu in feed (g/L)	2.5	22.7
U in raffinate (%)	<0.02	0.06
Pu in U product (%)	0.024	0.38
Np in U product (%)	0.33	5.8
Tc in U product (%)	2.4	24.5
Contactor type	Mixer-settlers	Centrifugal contactors
Total stages	28	32

GANEX-2 CYCLE SCHEME 1: SELECTIVE ACTINIDE STRIPPING

The most developed formulation of the GANEX 2nd cycle is given in Scheme 1. This involves the co-extraction of TRU actinides and the trivalent lanthanides from the GANEX-1 aqueous raffinate. The co-extraction of the lanthanides is inevitable if an O-donor ligand is used as the extracting agent due to the chemical similarity of the trivalent actinides and lanthanides. The actinides are then selectively stripped from the organic phase by suitable hydrophilic ligands containing a soft donor ligand (usually N-donors). The lanthanides remain in the organic phase and are stripped in the next stage before the lean solvent is recycled.

CEA-GANEX

The GANEX-2 cycle was first proposed by CEA based on an adaptation of their DIAMEX-SANEX process [49, 50]; this being a process already developed and tested for separation of minor actinides [24, 62]. Therefore, the organic phase was based on the combination of the malonamide N,N'-dimethyl-N,N'-dioctyl-2-(2-hexylethoxy) malonamide (DMDOHEMA) and Di-(2-ethylhexyl)phosphoric acid (HDEHP) diluted in a kerosene diluent (TPH). N-(hydroxyethyl)ethylenediaminetriacetic acid (HEDTA) was added to the aqueous feed and the scrub solution to suppress fission product extraction but molybdenum and technetium were nevertheless co-extracted with the TRU actinides. A dedicated scrubbing section was thus added to the flowsheet to scrub molybdenum and technetium at pH 2-3; pH adjustment was with citric acid. The actinide stripping section was also operated at pH 3 using a solution of HEDTA, citric acid and hydroxyurea. Hydroxyurea was added as a reducing for Np(VI) and Pu(IV). At this high pH, lanthanides were retained in the organic phase by complexation with HDEHP. The lanthanides and other residual contaminants (zirconium, iron) were finally stripped from the solvent with a mixture of TEDGA and oxalic acid before the solvent is recycled [36].

This CEA-GANEX cycle has been tested with SNF at the Atalante facility (Marcoule, France) [50]. An LWR fuel was used (the aqueous raffinate from their GANEX-1 hot test described above) and the flowsheet test was performed in 48 stages of miniature mixer-settlers in a hot cell. Losses of TRU actinides were <0.5% with generally good fission product decontamination factors obtained. The exceptions were some middle lanthanide elements which contaminated the actinide product. Using their PAREX solvent extraction simulation capabilities [24], this was later shown to be due to an under-estimation of some of the fission product concentrations in the feed and simulations were run that predicted how this could be rectified in future. The CEA-GANEX was, therefore, the first process demonstration of the GANEX concept and was shown to be a viable option for the GANEX-2 cycle.

EURO-GANEX

European projects had already made substantial progress in developing processes for An(III) recovery, particularly based on applications of the diglycolamide extractants – mainly N,N,N',N'-tetra-n-octyl-diglycolamide (TODGA) [46, 63, 64]. Adapting these developments for the GANEX-2 cycle was seen as the logical place to start with early work based on a combination of TODGA and TBP [65]. However, in experiments with process concentrations of plutonium (as opposed to trace spiked solutions) precipitates were observed with TODGA and dodecyl analogue (TdDDGA) alone in diluent or with TBP, octanol and N, N -dihexyloctanamide (DHOA) as phase modifiers [66]. Addition of the malonamide DMDOHEMA, was found to provide sufficient capacity for plutonium before a conventional third phase was observed (up to 35 g/L with 0.2 M TODGA and 0.5 DMDOHEMA with extraction from 3 mol/L HNO_3); no precipitation occurred with DMDOHEMA. Screening of different TODGA:DMDOHEMA ratios settled on 0.2 M TODGA and 0.5 DMDOHEMA in an odourless kerosene diluent as the most suitable formulation. The third phase boundary was later defined as a function of nitric acid concentration showing this solvent had sufficient capacity for plutonium concentrations of ≥10 g/L for $[HNO_3] \leq 6$ mol/L [67]. Consequently, 10 g/L Pu was set as the target for future flowsheet design.

Spiked batch distribution experiments confirmed the expected efficient co-extraction of Pu(IV), Am(III) and Ln(III) [67]. Spiked batch distribution experiments also confirmed the sulphonated bistriazinyl pyridine ligand (SO_3-Ph-BTP ligand), 2,6-bis(1,2,4-triazin-3-yl)-pyridine, developed for selective stripping of An(III) from Ln(III) in the i-SANEX process [68] also worked for the EURO-GANEX solvent [53]. Further experiments with process concentrations of Pu(IV) (1-10 g/L) defined suitable acid and SO_3-Ph-BTP concentration ranges that would deliver good separation factors whilst maintaining $D_{Pu,Am}<1$ and $D_{Eu}>1$. A second hydrophilic molecule, acetohydroxamic acid (AHA), was added as this was expected to act as a complexant for Pu(IV) [66, 69] and reductant for Np(VI) [70] but it was also shown to promote stripping with the SO_3-Ph-BTP although the reasons for this effect are still unclear.

Fission product decontamination is a key challenge with any reprocessing flowsheet and the EURO-GANEX process is no exception. CDTA (trans-1,2-diaminocyclohexane-N,N,N,N'-tetraacetic acid), developed for the i-SANEX cycle, was also shown to hold back zirconium and palladium in the aqueous phase when applied to the EURO-GANEX system [71]. E.g. for 0.05 mol/L CDTA, 3 mol/L HNO_3, 17 g/L Pu, D_{Zr} and D_{Pd} decreased from 11.3 to 1.2 and 250 to 0.05 respectively whilst D_{Pu} remained sufficiently high (35). Further data on problematic fission and corrosion products were reported, specifically focusing on Fe, Sr, Tc, Mo, Ru [53]. Iron showed a steep increase in distribution ratio above 1 mol/L HNO_3 due mainly to extraction with DMDOHEMA. Strontium showed a maximum in D_{Sr} around 2 mol/L HNO_3 whereas for technetium extraction, primarily due to TODGA, D_{Tc} decreased across the HNO_3 range but remained >>1 even at 4 mol/L HNO_3. Similarly, D_{Mo} was above 1 across the HNO_3 range although there was some reduction in a HA raffinate (HAR) simulant compared with the single component solution and with CDTA. Ruthenium distribution ratios were less than one but varied with mixing time of the solutions and are likely to be affected by changes in speciation. In fact, TODGA-based flowsheet trials often report some retention of ruthenium in the organic phase [64, 72]. Ruthenium PUREX chemistry, for comparison, is known to be very complicated [73, 74].

The behaviour of neptunium in the EURO-GANEX system was given specific attention due to the known complexity of neptunium solvent extraction and redox chemistry [34, 75]. The order of extractability of the different neptunium oxidation states was shown to be Np(IV)>Np(VI)>1>Np(V) on extraction from <3 mol/L HNO_3 [76]. Of particular interest was that whilst Np(IV) and (VI) were quite stable, the Np(V) oxidation state proved to be very unstable in the organic phase with respect to disproportionation, a feature which it was realised could be exploited in flowsheet design. An increased rate of Np(V) disproportionation was similarly seen in earlier studies in TBP [77].

A flowsheet was designed and tested using a surrogate feed with realistic concentrations of plutonium (10 g/L) in the feed [52]. 16 centrifugal contactor stages of extract-scrub were followed by 12 stages of TRU actinide stripping and 4 stages of lanthanide stripping. CDTA was added to the feed (0.05 mol/L) which was 5 mol/L HNO_3 to promote neptunium disproportionation and extraction. A double strip was employed to selectively strip TRU from Ln(III) using 0.5 mol/L AHA with two different concentrations of SO_3-Ph-BTP to minimise Ln(III) stripping in low plutonium stages. Plutonium was well controlled through the flowsheet with a DF of ~14,000 but ~30% neptunium was lost to the HA raffinate and the TRU product contained ~7% of europium (used as an exemplar lanthanide). A flowsheet model developed in the CEA's PAREX simulation code was validated from this test and used to refine the flowsheet design ready for a hot test. The hot test was run at the end of the ACSEPT project at the JRC, Karlsruhe, using a feed from dissolving spent Dounreay Fast Reactor (DFR) fuels [54]. Following the GANEX-1 cycle, the EURO-GANEX cycle was run in two parts using a 16 stage miniature centrifugal contactor cascade contained in a hot cell. Changes from the surrogate test included raising the feed acidity to 5.9 mol/L HNO_3 to promote neptunium oxidation to Np(VI), reducing the scrubbing stages and simplifying the strip to a single solution (1 mol/L AHA + 0.055 mol/L SO_3-Ph-BTP in 0.5 mol/L HNO_3). The trial was very successful in demonstrating the EURO-GANEX concept – 99.9% Np, Pu and Am ions were recovered with 0.06% lanthanide contamination. The improved neptunium extraction in the initial extract-scrub was attributed to the flowsheet changes plus the nitrous acid generated from radiolysis catalysing the Np(V) oxidation most effectively [34, 78].

The subsequent SACSESS project was focused on the safety of the reference separation processes, including EURO-GANEX [30, 31]. One of the objectives for the SACSESS project was to perform a process safety review of the EURO-GANEX flowsheet under normal and potential maloperation conditions. For this purpose, a safety assessment methodology was developed based on the experience of the project collaborators across Europe and this methodology [79] was then utilised to carry out a review of the EURO-GANEX flowsheet at a SACSESS project meeting based on a workshop style approach [30]. A key maloperation identified was the loss of scrub acid from the initial extract-scrub contactor as this was likely to cause the accumulation of plutonium, americium and other species across the contactor leading to potential criticality or radiological hazards within the plant. Therefore, an experimental simulation of this maloperation was carried out in laboratory scale centrifugal contactors [80]. Following the establishment of steady state with the flowsheet under normal operating conditions, the scrub acid was reduced to 0.05 mol/L (from 0.5 mol/L). Surprisingly, plutonium accumulation was not observed, and the plutonium remained in the solvent product with almost no change to the profile. The organic phase, however, did change colour from red-brown to green and UV-vis absorption spectroscopy confirmed a change in the solvent phase speciation and that the process was reversible. This effect was proposed to be caused by hydrolysis of Pu(IV) due to the low acidity, that was then limited in its extent by the solvent shell around the hydrolysed plutonium preventing it from polymerising to form a colloid, as occurs in the aqueous phase [81]. It was concluded that the EURO-GANEX process was robust to at least this type of maloperation and, whilst wider studies are obviously needed, this is a potentially advantageous, if unexpected, feature of the system.

GANEX-2 CYCLE SCHEME 2: SELECTIVE ACTINIDE EXTRACTION

The simplest formulation of the GANEX 2nd cycle is given in Scheme 2. This involves the selective extraction of TRU actinides leaving the trivalent lanthanides as well as all other fission products in the GANEX-2 aqueous raffinate. This is only possible by judicious choice of extractants; particularly avoiding O-donor ligands such as diglycolamides that can co-extract lanthanides, but also finding extractants that have capacity to extract the larger amounts of Pu(IV) ions present. Following extraction, the actinides are then stripped group-wise from the organic phase by suitable hydrophilic O-donor ligands before the lean solvent is recycled.

THE CHALMEX PROCESS

The CHALMEX process was developed by Chalmers University of Technology (Sweden), as an alternative strategy for the GANEX 2nd cycle [55-58, 82-88]. The objective was to develop a simpler process, which could reduce the number of process steps, potentially reducing costs of a recycling plant [30]. While significantly less developed than the strategies outlined for Scheme 1, the CHALMEX process has shown promising results in its actinide/lanthanide separation characteristics.

By combining the well-known extractant TBP with 6,6’-bis(5,5,8,8-tetramethyl-5,6,7,8-tetrahydro-benzo-1,2,4-triazin-3-yl)-2,2’-bipyridine ($CyMe_4$-BTBP), the solvent can theoretically extract the actinides with oxidation states ranging from +III to +VI, without the co-extraction of lanthanides and fission products and without redox control of plutonium [55-57]. While the process chemistry of TBP is well established after decades of use in the PUREX process, the chemistry of $CyMe_4$-BTBP is less well-known. It has been found to be stable towards both hydrolysis and radiolysis, but a complete mapping of degradation products formed under process conditions is lacking. Both alpha and gamma-radiation induced degradation of $CyMe_4$-BTBP has been investigated [56]. It has been established that the ligand degrades readily when subjected to both types of radiation but extraction properties remain almost unaffected when irradiated in contact with nitric acid. It has also been suggested that the stability of the extractant towards radiolysis is dependent on the diluent having a similar shape: for cyclic extractant molecules, a cyclic diluent leads to higher radiolysis resistance, at least at low irradiation doses [89].

$CyMe_4$-BTBP is also the reference molecule for the regular (r) and 1-cycle (1c) SANEX processes and has gone through hot tests on genuine spent nuclear fuel with good results [36, 46, 47].

Phenyl trifluoromethyl sulfone (FS-13) is used as a diluent in the process. Both Russian and American research efforts have focused on its use as a diluent in the UNEX (Universal Solvent Extraction) process [90-96]. FS-13 is chemically inert and stable towards both hydrolysis and radiolysis. A major advantage of the diluent is its high density (~1.4 g/cm^3), which resolves any phase separation/inversion issues experienced in systems with more similar densities between organic and aqueous phases. Other advantageous chemical and physical properties include low aqueous solubility, low viscosity and it is non-toxic. FS-13 has a relative permittivity of approximately 30.8 F/m at 298 K [97] and high dielectric constants have been shown to beneficial for americium extraction as it increases the solubility of $CyMe_4$-BTBP and hence the distribution ratio of Am. The separation factor of Am/Eu, however, increases exponentially with decreasing relative permittivity.

The initial feasibility studies of the CHALMEX process were promising. A good separation factor of the actinides from the lanthanides was seen within only 10 minutes of contacting ($SF_{Am/Eu}$ = 160, $SF_{Pu/Eu}$ = 210, $SF_{Np/Eu}$ = 3.5). All fission products that were extracted, except samarium and zirconium, were extracted by $CyMe_4$BTBP and the most problematic fission products extracted included Ag, Cd, Mo Zr and Pd. The extraction of some corrosion products (Ni, Co, Mn) was also found to be an issue [55, 84].

To prevent the extraction of some of these fission products, different strategies were considered including pre-extraction, scrubbing and suppression. Pre-extraction is generally undesired due to the increase in final waste volume it would produce by adding another process stage. Both scrubbing and suppression are more attractive choices as they can be combined with already existing process steps. Finally, it was concluded that a combination of the masking agents bimet and mannitol added directly to the GANEX-1 raffinate successfully reduced the extraction of Mo, Zr and Pd [55, 82]. Palladium was then of concern as it is known to precipitate when in contact with a pure cyclic ketone (or rather the presence of enol impurities) [98], such as the original diluent of choice, cyclohexanone [55, 57, 82]. No such reaction is known for cyclic sulfones like FS-13. Gluco-lactone can be added to the acid scrub step to back-extract any molybdenum or zirconium [83].

The process feasibility has been demonstrated by batch scale tests [84] and the solvent has been tested for use in centrifugal contactors in single stage centrifugal contactor experiments [83]. However, to date, no counter-current flowsheet tests have been carried out.

GANEX-2 CYCLE SCHEME 3: SPLIT ACTINIDE STRIPPING

The third application of the GANEX strategy for the 2nd cycle is given in Scheme 3. This is basically a variation of Scheme 1. It involves the co-extraction of TRU actinides and the trivalent lanthanides from the GANEX-1 aqueous raffinate. The actinides are then selectively stripped from the organic phase by suitable hydrophilic ligands but, in this case, a split stripping strategy is adopted whereby firstly the multi-valent TRU ions (Np, Pu) are stripped and then the trivalent MA are stripped (Am, Cm). This gives two products that can be used for heterogeneous recycling or re-combined for homogeneous recycling. The lanthanides remain in the organic phase and are stripped in the next stage before the lean solvent is recycled. This strategy is included in this review of homogeneous recycling since it is a straight forward variation of the GANEX concept rather than a specific MA separation from PUREX HAR; options that were discussed in the preceding paper [23].

TRU-SANEX

This project has received funding from the EURATOM research and training programme 2014-2018 under grant agreement No 755171. The content of this deliverable reflects only the author's view. The European Commission is not responsible for any use that may be made of the information it contains.

Earlier papers in the development of the EURO-GANEX cycle had reported stripping of TRU actinides from the EURO-GANEX solvent with AHA and SO_3-Ph-BTP both independently and together [53, 66]. The mixture of the two reagents was the optimum combination for grouped stripping of Np-Cm. However, it was clear that, at low acidity, AHA could strip Pu(IV) and Np(IV), by complexation, and Np(VI), by reduction to Np(V), without interacting with the trivalent ions, whilst SO_3-Ph-BTP was designed to selectively strip the trivalent actinides from trivalent lanthanides. These selectivities are nicely illustrated by a comparison of reported stability constants (Table 2). This raised the interesting possibility of adapting the EURO-GANEX flowsheet to produce separate (Np,Pu) and (Am,Cm) products by separate sequential strip sections using firstly AHA and then SO_3-Ph-BTP (the AHA strip needs to be first since the SO_3-Ph-BTP will strip tetravalent as well as trivalent actinides). This variation was termed "TRU-SANEX" to highlight its hybrid nature between the GANEX and SANEX processes [99]. Results from a flowsheet test confirmed the concept with only small cross-contamination between the two products. Interestingly, <10% neptunium was lost to the aqueous raffinate which is less than the simulant EURO-GANEX test (~30%) but not as good as the hot test (<0.1%). Since the extract-scrub-section in the TRU-SANEX test was based on the hot test, this gives a rough indication of the impact of (a) the flowsheet changes and (b) radiolytically generated nitrous acid in promoting neptunium conversion to extractable Np(VI) and Np(IV) oxidation states.

Table 2: Stability constants for 1 :1 AHA lanthanide and actinide complexes (T=22-23 °C ; I = 2.0 M $NaClO_4$). All measurements made by UV-vis absorption spectrophotometry except Cm* via time resolved laser fluorescence spectroscopy (TRLFS).

Element	Oxidation state	$\log\beta_1$	Ref.
Ce	3	5.08	[100]
Pr	3	5.69	[100]
Nd	3	5.72	[100]
Sm	3	6.02	[100]
Eu	3	6.19	[101]
Gd	3	5.96	[100]
Tb	3	6.72	[101]
Dy	3	6.66	[102]
Ho	3	6.64	[102]
Er	3	6.59	[102]
Tm	3	6.7	[102]
Yb	3	7.25	[102]
Th	4	10.53	[102]
U	4	12.26	[102]
U	6	7.94	[69]
Np	4	12.83	[103]
Np	5	4.83	[103]
Pu	3	5.77	[69]
Pu	4	14.2	[69]
Am	3	5.85	[100]
Cm*	3	6.17*	[101]
Cm	3	6.05	[101]

COMPARING THE PROCESS SCHEMES

Looking at the different process schemes (Figure 2), Scheme 2 appears the simplest since it selectively extracts the actinides at the initial extract-scrub stage. However, all three schemes are based on two cycles of solvent extraction and each cycle contains extraction, scrubbing and stripping stages, spent solvent regeneration cycles and various auxiliary equipment; for example, the engineering design may include evaporators, buffer storage or conditioning tanks, reagent tanks, connecting pipework, etc. Also, the solvent extraction process is only one part of the reprocessing plant – upstream and downstream processes for fuel preparation, dissolution, product finishing and waste management must also be considered in order to make a proper evaluation of the 'simplicity' of any particular separation process. Beyond the assessment of the technologies themselves, other factors also affect the choice of separation process such as: technology readiness; safety; environmental impacts (particularly on the DGR); proliferation resistance and physical security challenges; socio-economic benefits, including public acceptability; national policies and fuel cycle scenarios [7]. Thus, evaluating the different process schemes requires consideration of many aspects which have economic implications to the viability of the flowsheet at an industrial scale. However, in the context of this article we can highlight certain features of the different processes for each scheme that enable comparisons at the technical level.

GANEX-1

The process based on the monoamide DEHiBA for selective uranium extraction has been tested twice now with SNF [51, 54]. Good results have been obtained although the slightly worse recoveries and decontamination factors in the JRC hot test, which used centrifugal contactors, point to some kinetic issues with the hydrazine scrubbing stage for technetium, neptunium and plutonium control [54]. Also, the rather low uranium saturation in the JRC hot test leads to excessive solvent and aqueous flows that should be minimised from the waste management perspective.

Nevertheless, whilst optimisation challenges remain, the concept is considered to be proven. Further physico-chemical data needed for building predictive process models are outstanding needs.

SCHEME 1 (CEA-GANEX and EURO-GANEX)

Two processes have been demonstrated with SNF – CEA-GANEX and EURO-GANEX – which confirm the technical feasibility of options that meet the challenging goals related to developing advanced reprocessing options for homogeneous recycling [36]. These two cycles are compared in Table 3. The EURO-GANEX option offers some significant advantages, notably:

- Actinide stripping in the acidic region (no need for pH adjustment)
- No phosphate wastes from the solvent management
- Compatibility with centrifugal contactors has been demonstrated at the lab scale
- No plutonium reduction

However, in its current form it also has various drawbacks:

- The sulphonated BTP reagent in the aqueous phase adds to waste volumes and is incompatible with vitrification processes for HLW immobilisation
- The combination of two extractants in the organic phase complicates solvent formulation, clean up and recycling and process simulation.
- Incomplete control of some fission products; notably molybdenum, technetium and ruthenium.

- No solvent clean up process has been developed yet for used solvent recycling.

Table 3: Comparison of key features of CEA-GANEX and EURO-GANEX cycles (data from [36, 50, 54])

	CEA-GANEX	**EURO-GANEX**
Developed by	CEA (France)	ACSEPT project (FP7)
Date of hot test	2008	2013
Fuel for hot test	LWR	DFR
Pu content in HAF	<2.5 g/L	10 g/L Pu
Equipment	Mixer-settlers	Centrifugal contactors
No. of stages	48	32
CHON?	Aqueous phase only	Organic phase only
Organic phase	DMDOHEMA + HDEHP	TODGA + DMDOHEMA
Diluent	Industrial (TPH)	Industrial (Exxsol D-80)
FP scrubbing/holdback	Citric acid (Mo,Tc)	CDTA (Zr,Pd)
Actinide strip	pH 3	0.5 mol/L HNO_3
Actinide strip agents	HEDTA + citric acid + hydroxyurea	AHA + SO_3-Ph-BTP
Pu stripping	Reduction	Complexation
Ln(III) decontamination	5% in An product	<0.06 % in An product
Np recovery	~99%	99.90%
TRL (at system level) [61]	4-5	4-5

SCHEME 2 (THE CHALMEX PROCESS)

The CHALMEX process has to date been developed at the fundamental level. Latest studies have moved into the process development side through single stage centrifugal contactor experiments and a 'flowsheet' simulation by sequential batch experiments. Clearly, the process flowsheet needs testing in a counter-current mode with a realistic simulant before it can be compared directly with the Scheme 1 options. The $CyMe_4BTBP$, although very successful in selectively extracting MA, is also known to have slow kinetics and low solubility in diluents. These issues are partially addressed by use of the FS-13 diluent but it is unclear whether this is suitable for industrial applications. CHALMEX also relies on a series of aqueous phase ligands (bimet, mannitol and gluco-lactone).

SCHEME 3 (THE TRU-SANEX PROCESS)

As has been emphasised already, this is a relatively simple adaptation of EURO-GANEX and so does not have, *per se*, pressing, unique R&D needs. However, an innovative and potentially transformative development would be if this Scheme could be extended to a "TRU-EXAm" mode; that is recovery of (Np, Pu) followed by Am alone – leaving curium in one of the waste streams.

This project has received funding from the EURATOM research and training programme 2014-2018 under grant agreement No 755171. The content of this deliverable reflects only the author's view. The European Commission is not responsible for any use that may be made of the information it contains.

OUTLOOK

The GANEX-1 cycle is necessary and has wider applicability for uranium recovery. Flowsheet optimisation, basic data generation and process simulation are obvious future directions. R&D needs for the EURO-GANEX process are also quite clear and the GENIORS project is already looking at a CHON replacement for the SO_3-Ph-BTP ligand [104, 105] and a modified DGA ligand that could replace the combined TODGA and DMDOHEMA organic phase [106]. CHALMEX would benefit from a focus on flowsheet testing and a safety review, similar to that trialled on the EURO-GANEX process in the SACSESS project [30]. All processes need solvent recycling capabilities and integration with upstream (fuel dissolution) and downstream (product finishing) stages. More in-depth safety studies, such as gas generation and thermal stability of proposed solvents, are also an essential next stage. Process modelling and simulation capabilities [107, 108] are another generic need in order to more efficiently design flowsheets and also to probe sensitivities to process upsets [109].

CONCLUSIONS

As with the heterogeneous recycling option, several solvent extraction processes addressing homogeneous recycling have been developed and demonstrated in Europe. These essentially fall into three schemes for separating the TRU actinides, all of which are preceded by a common uranium extraction cycle. The following conclusions are drawn, based on the current state of the art:

The principles of the uranium extraction (GANEX-1) cycle have been demonstrated although work is still required to optimise the process, prove the decontamination factors (particularly in short residence time centrifugal contactors) and develop a process model. Much more basic physico-chemical data are needed to support the development of a process model.

Scheme 2 appears the most complex to develop into a working process, although it is potentially the most elegant concept with the fewest number of stages. However, in its current form (the CHALMEX process) it uses a mixed organic phase, various aqueous phase complexants and a fluorinated diluent. Significant further work is required to take this option towards a process demonstration with SNF and a design that is industrially deployable.

Two promising options exist for Scheme 1, both of which have been tested with SNF and demonstrate good results. Nevertheless, questions remain around both CEA-GANEX and EURO-GANEX. For the CEA-GANEX process, testing with elevated Pu content fuels, the compatibility with centrifugal contactors and the need for a high pH strip are concerns. For the EURO-GANEX process, the replacement of the SO_3-Ph-BTP ligand with a CHON ligand, simplification of the organic phase to a single extractant and verification of DFs for some problematic fission products are key R&D directions. The big advantage of the EURO-GANEX cycle is it has been proven for actinide stripping in the acidic region.

Scheme 3 is just a variant on the EURO-GANEX cycle and, whilst further testing would be needed to confirm the DFs for this TRU-SANEX cycle, its development can be assumed to be at a similar status to the EURO-GANEX cycle. Whether a heterogeneous recycling option that was based on GANEX rather than PUREX chemistry is advantageous would depend on extraneous factors related to the deployment of advanced fuel cycles in a particular country.

For all options, integration with upstream and downstream stages and solvent management (recycling within the process and solvent destruction at end of life) are significant technology gaps. No processes yet have validated process models available for flowsheet design although some simulations have been performed.

So far, the developments discussed in this review have been pursued on the laboratory scale only. There are clearly important knowledge gaps that need to be filled before these processes would be ready for possible industrial applications. As well as those already noted, safety studies, including gas generation and impacts of maloperations; scale up; process monitoring and control technologies are certainly desirable to raise the technological readiness of the process. Beyond, technology readiness, how these processes fit into advanced, sustainable, economic and proliferation-resistant nuclear fuel cycles, supporting future low carbon generation, must be analysed [9].

TABLE OF PROCESS LIGANDS

Compound	Acronym	Name
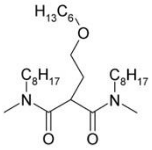	DMDOHEMA	N,N'-dimethyl-N,N'-dioctyl-2-(2-hexyloxy-ethyl)-malonamide
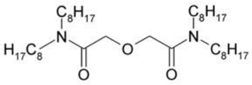	TODGA	N,N,N',N'-tetra-n-octyl diglycolamide
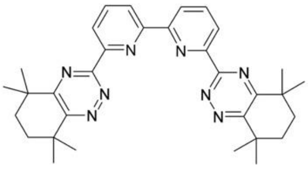	CyMe4-BTBP	6,6'-bis(5,5,8,8-tetramethyl-5,6,7,8-tetrahydro-benzo-1,2,4-triazin-3-yl)-2,2'-bipyridine
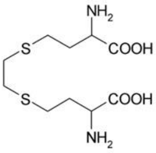	bimet	(2S,2'S)-4,4'-(ethane-1,2-diylbis(sulfanediyl))bis(2-aminobutanoic acid)
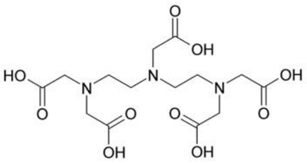	DTPA	diethylenetriaminepentaacetic acid
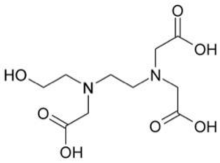	HEDTA	N-(hydroxyethyl)ethylenediaminetriacetic acid
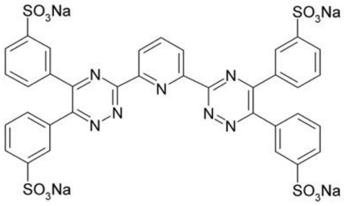	SO3-Ph-BTP	2,6-bis(5,6-di(3-sulphophenyl)-1,2,4-triazin-3-yl)-pyridine tetrasodium salt

Compound	Acronym	Name
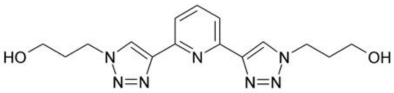	PTD	2,6-bis[1-(propan-1-ol)-1,2,3-triazol-4-yl]-pyridine
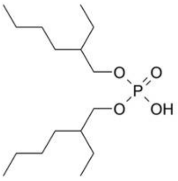	HDEHP	Di-(2-ethylhexyl)phosphoric acid
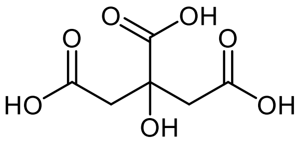	Citric acid	(2-Hydroxypropane-1,2,3-tricarboxylic acid)
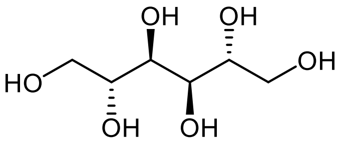	Mannitol	D-mannitol
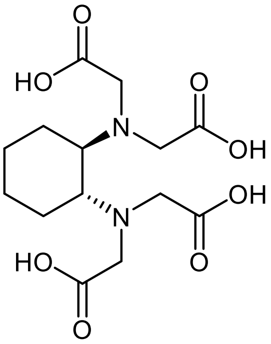	CDTA	trans-1,2-Diaminocyclohexane-N,N,N’,N’-tetraacetic acid
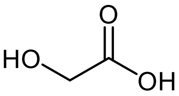	Glycolic acid	2-Hydroxyethanoic acid
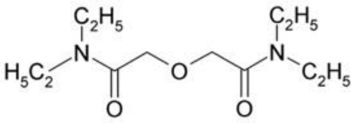	TEDGA	N,N,N’,N’-tetraethyl diglycolamide

EURO-GANEX OPTIMIZATION STUDIES – STUDIES ON MTDDGA EXTRACTANT TO REPLACE TODGA-DMDOHEMA

Andreas Wilden, Giuseppe Modolo, Bart Verlinden, A. Geist, Wim Verboom, Santa Jansone-Popova, Mike Carrott, Robin Taylor, Dan Whittaker, Billy Keywood

AIMS AND OBJECTIVES

Within the present GENIORS project the development of a new EURO-GANEX process is envisioned. The current EURO-GANEX process is based on the co-extraction of all actinides (except uranium) using a mixture of *N*,*N*,*N'*,*N'*-tetraoctyl-diglycolamide (TODGA) and *N*,*N'*-dimethyl-*N*,*N'*-dioctyl-2-hexylethoxy-malonamide (DMDOHEMA) as extractants, and selective stripping of the actinides as a group, using a mixture of 2,6-bis-(5,6-di(sulfophenyl)-1,2,4-triazin-3-yl)-pyridine (SO_3-Ph-BTP) and acetohydroxamic acid (AHA) [53, 76, 110-113]. Figure 3 shows the chemical structures of the extractants and complexants used in the former EURO-GANEX process. The EURO-GANEX process has successfully been demonstrated using genuine nuclear fuel solution [113].

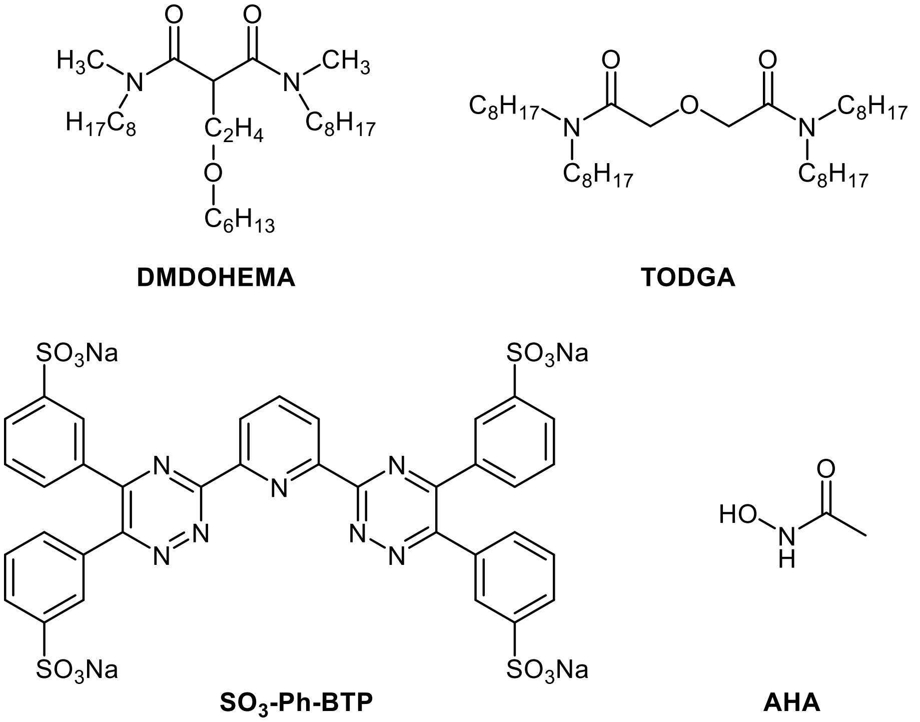

Figure 3. Chemical structures of DMDOHEMA, TODGA, SO_3-Ph-BTP, and AHA, used in the present EURO-GANEX process

Despite the successful demonstration of the process, further improvements are envisioned. The complexity of the solvent composition shall be reduced using a single extractant in a kerosene diluent, and using complexants which are composed of C, H, O, and N, exclusively (the so-called CHON principle), to reduce secondary waste and downstream target fabrication issues. For the extraction of all actinides from used nuclear fuel solutions, the diglycolamides were found to be suitable [114-116]. Diglycolamides are structurally versatile and a large number of different modifications were studied over the last decades [117]. TODGA (Figure 3) was studied most frequently, but the Pu loading capacity was found to be insufficient in kerosene diluent to be used as a single extractant in a GANEX process [110]. Malmbeck et al. recently studied a modified diglycolamide with additional methyl substituents in the backbone and increased side-chain length and found dimethyl-*N*,*N*,*N′*,*N′*-tetradecyl-diglycolamide (*cis*-mTDDGA) to be a suitable extractant for a new EURO-GANEX process, also with respect to a high Pu loading [106]. The influence of modification of the diglycolamide backbone on the extraction of trivalent metal ions was studied in detail for TODGA analogues as extractants [118-120]. It was found that the metal ion distribution ratios decrease with increasing methyl substitution of the backbone, probably due to steric interactions. Furthermore, it was found that the conformation of the double substituted Me_2-TODGA also has a huge influence on the extraction. The *cis* conformer was found to extract trivalent metal ions with up to 94-times higher distribution ratios, compared to the *trans* isomer [120]. The *cis*-mTDDGA is expected to show similarly higher distribution ratios than its *trans* isomer.

For the substitution of SO_3-Ph-BTP, 2,6-bis[1-(propan-1-ol)-1,2,3-triazol-4-yl)]pyridine (PyTri-Diol, or PTD) is under consideration. PTD was found to have high actinide selectivity and radiochemical stability [121-123] and could therefore be suitable for application as a stripping reagent in a new EURO-GANEX process. The use of PTD in a modified innovative-SANEX process is also under consideration [124]. Figure 4 shows the chemical structures of *cis*-mTDDGA and PTD, currently studied for applications in a new EURO-GANEX process.

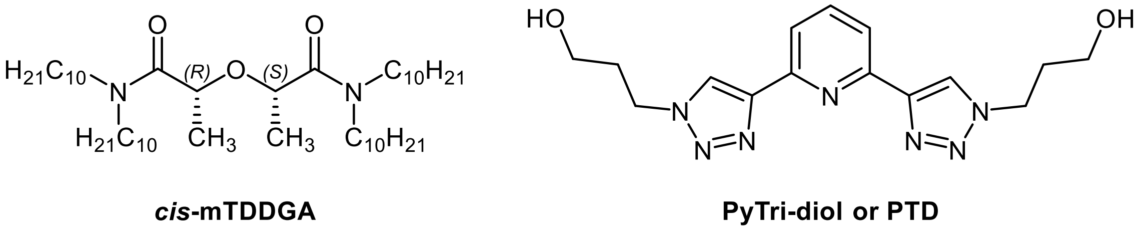

Figure 4. Chemical structures of *cis*-mTDDGA and PTD, currently studied for use in a new EURO-GANEX process

EXTRACTION EXPERIMENTS WITH MTDDGA SOLVENT

NITRIC ACID DEPENDENCY

For an increasing concentration of nitric acid, the distribution ratios of the lanthanides follow a similar trend as the distribution ratios of the actinides (Figure 5, except for Np, as its speciation is known to have a tremendous effect on its extraction, which depends on the nitric acid concentration [125] as well). At a concentration of 4 mol/L of HNO_3, the distribution ratios range from 16 for lanthanum up to 993 for holmium (Figure 6).

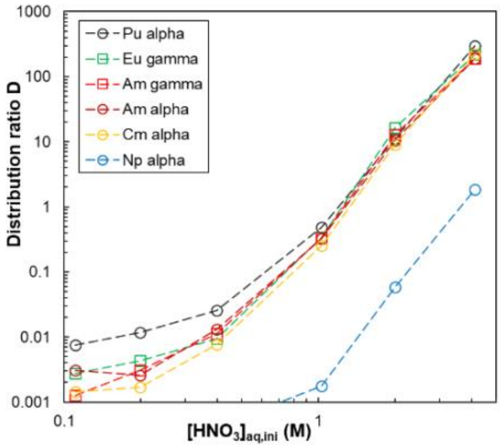

Figure 5. Distribution ratios of Np(V), Pu(IV), Am(III), Cm(III), and Eu(III) as a function of the initial nitric acid concentration. Org.: pre equilibrated 0.5 mol L^{-1} mTDDGA in Exxsol D80. Aq.: 10^{-5} mol L^{-1} Ln(III) in nitric acid, tracers: ^{237}Np, ^{239}Pu, ^{241}Am, ^{152}Eu, ^{244}Cm, 500 µL of both phases, shaking 2,500 rpm at 25°C.

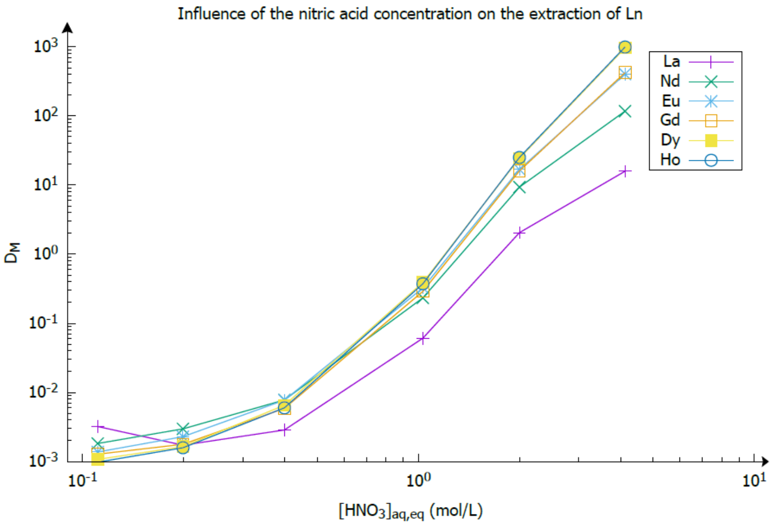

Figure 6. Extraction of Ln as a function of the nitric acid concentration of the aqueous phase. Org. 0.5 M mTDDGA in Exxsol D80, pre-equilibrated. Aq. [Ln], [Y] = 1·10^{-5} M, 1.5 kBq of ^{152}Eu, ^{241}Am, ^{244}Cm, ^{239}Pu; 0.74 kBq ^{237}Np, O/A ratio = 1, 25°C, 60 min., 2500 rpm.

KINETICS

The extraction of actinides is very fast (reaching a plateau after 15 minutes, Figure 7), except for neptunium and plutonium. It is highly probable that the initial oxidation states (+IV for Pu and +V for Np) are not stable under the extraction conditions.

Extraction of the light lanthanides reaches equilibrium after about 15 minutes, as can be seen in Figure 8. However, heavier lanthanides (e.g. holmium) show a slower extraction.

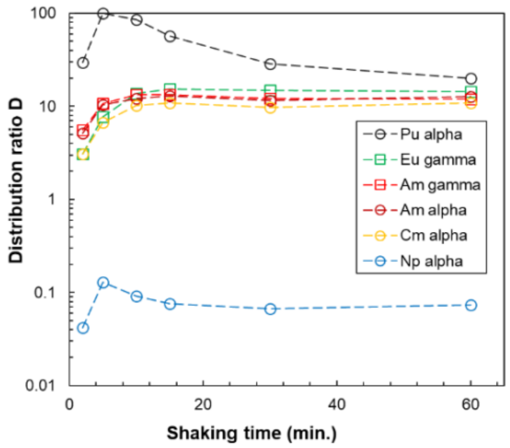

Figure 7. Distribution ratios of Np(V), Pu(IV), Am(III), Cm(III), and Eu(III) as a function of the shaking time. Org.: 0.5 mol L^{-1} mTDDGA in Exxsol D80. Aq.: 10^{-5} mol L^{-1} Ln(III) in 2 mol L^{-1} HNO_3, tracers: ^{237}Np, ^{239}Pu, ^{241}Am, ^{152}Eu, ^{244}Cm, 500 µL of both phases, shaking 2,500 rpm at 25°C.

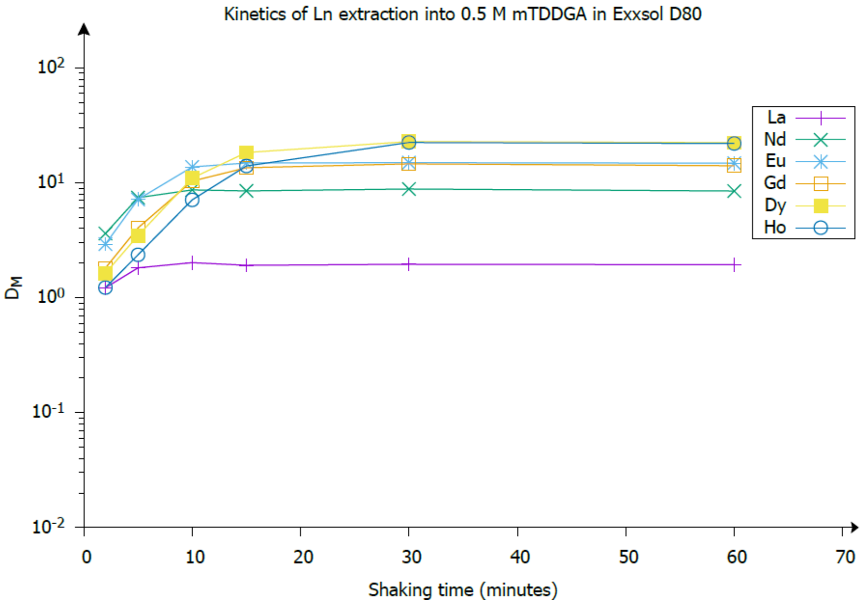

Figure 8. Kinetics of extraction of Ln with 0.5 M mTDDGA in Exxsol D80 by ICP-MS. Org. 0.5 M mTDDGA in Exxsol D80, pre-equilibrated. Aq. 2 M HNO_3, [Ln], [Y] = $1\cdot10^{-5}$ M, 1.5 kBq of ^{152}Eu, ^{241}Am, ^{244}Cm, ^{239}Pu; 0.74 kBq ^{237}Np, O/A ratio = 1, 25°C, 2500 rpm.

EXTRACTION EXPERIMENTS WITH DIFFERENT EXTRACTANT CONCENTRATIONS

The slopes of the linear fitting of the logarithm of the distribution ratio as a function of the logarithm of the concentration of the ligand indicate a 3:1 stoichiometry for the actinides and the lanthanides, which are represented in Figure 9 and Figure 10. More accurate determination of the stoichiometry of the extraction mechanism could be conducted with time resolved laser fluorescence spectroscopy (TRLFS).

This project has received funding from the EURATOM research and training programme 2014-2018 under grant agreement No 755171. The content of this deliverable reflects only the author’s view. The European Commission is not responsible for any use that may be made of the information it contains.

The calculated slopes can be found in Table 4. Since the curve flattens at higher ligand concentrations, the values of the fitting without the highest ligand concentration of 0.5 mol/L are shown in the third column. For neptunium, the fitting only starts from 0.1 mol/L mTDDGA, since distribution ratios below that were smaller than 0.001. The values for the slopes for Pu and Np extraction deviate, although this could be caused by changes in the oxidation states. For the lanthanides, slopes seem to slightly increase with their mass.

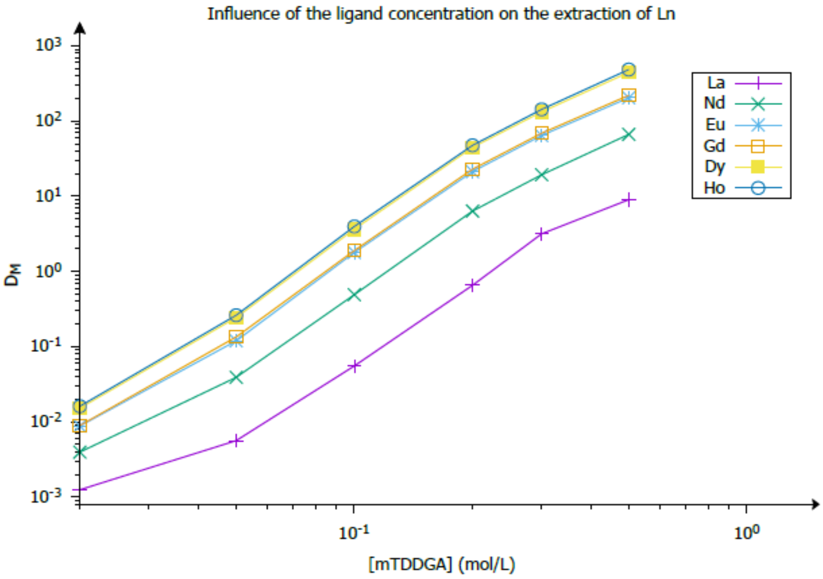

Figure 9. Extraction of Ln as a function of the ligand concentration in the organic phase. Org. mTDDGA in Exxsol D80. Aq. 4 M HNO_3, [Ln], [Y] = $1\cdot10^{-5}$ M, 1.5 kBq of ^{152}Eu, ^{241}Am, ^{244}Cm, ^{239}Pu; 0.74 kBq ^{237}Np, O/A ratio = 1, 25°C, 60 min., 2500 rpm.

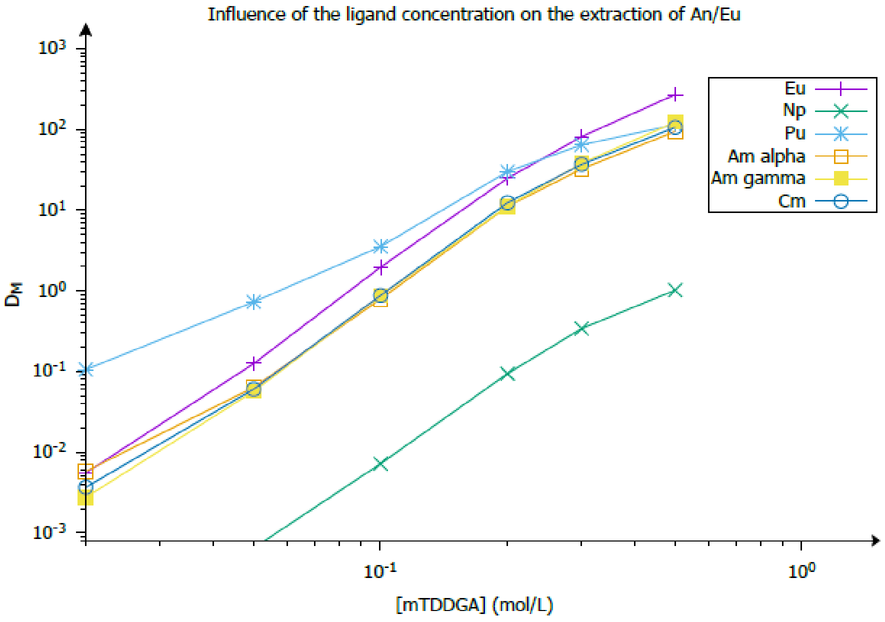

Figure 10. Extraction of radiotracers as a function of the ligand concentration in the organic phase. Org. mTDDGA in Exxsol D80. Aq. 4 mol/L HNO$_3$, [Ln], [Y] = 1·10^{-5} mol/L, 1.5 kBq of ^{152}Eu, ^{241}Am, ^{244}Cm, ^{239}Pu; 0.74 kBq ^{237}Np, O/A ratio = 1, 25°C, 60 min., 2500 rpm.

Table 4. Slopes of the linear fitting of log(D) as a function of log([ligand]).

Element	Slope	Slope ([mTDDGA] < 0.5 M)
Am (γ)	3.43	3.58
Cm	3.33	3.49
Pu	2.29	2.42
Np	3.11	3.53
Eu	3.45	3.61
La	2.94	2.95
Nd	3.15	3.23
Gd	3.25	3.39
Ho	3.31	3.44

EXTRACTION EXPERIMENTS WITH DIFFERENT DIASTEREOMERIC EXCESSES OF MTDDGA

Three different batches of mTDDGA with different diastereomeric excesses have been obtained from TWENTE (Figure 11):

1) RE1822 mixture of diastereomers (1:3.5 = *trans:cis*)
2) RE1822 lower (major) diastereomer (*cis* isomer, *RS*)
3) RE1822 upper diastereomer (*trans* isomer, *SS*)

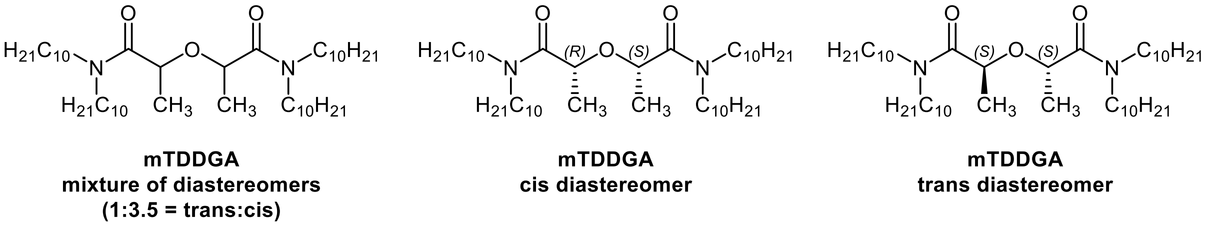

Figure 11. Chemical structures of the mTDDGA diastereomers used in the study

In a first set of experiments 0.1 mol/L of each diastereomer of mTDDGA was tested in Exxsol-D80. Exxsol-D80 was chosen as the diluent, as mTDDGA is foreseen to be used in a new GANEX process, which will probably be tested at NNL where Exxsol-D80 is the preferred diluent. A concentration of 0.1 mol/L of each mTDDGA was chosen for two reasons. First, the available amount of the pure diastereomers was low; secondly we wanted to be able to compare the results directly to the results of the extraction of the pure Me$_2$-TODGA (TWE-14) diastereomers, published recently [120].

As known from the scoping study published by Malmbeck et al. [106], we expected significant extraction only at higher nitric acid concentrations. Therefore, we used aqueous phases composed of nitric acid of different concentrations between 1-6 mol/L HNO_3 containing trace amounts of inactive metals (10^{-5} mol/L each) and spiked with radioactive tracers. The composition is shown in Table 5.

Table 5. Composition of aqueous phases

Component	Concentration	Component	Concentration	Component	Concentration
Fe	1.8E–05 mol/L	La	1.1E–05 mol/L	Tb	0.9E–05 mol/L
Sr	1.3E–05 mol/L	Ce	1.2E–05 mol/L	Dy	1.2E–05 mol/L
Zr	1.2E–05 mol/L	Pr	1.1E–05 mol/L	Ho	1.2E–05 mol/L
Mo	1.1E–05 mol/L	Nd	1.1E–05 mol/L	Er	0.9E–05 mol/L
Ru	0.9E–05 mol/L	Sm	1.1E–05 mol/L	Tm	0.9E–05 mol/L
Pd	0.7E–05 mol/L	Eu	1.2E–05 mol/L	Yb	1.0E–05 mol/L
Y	1.2E–05 mol/L	Gd	1.1E–05 mol/L	Lu	0.9E–05 mol/L
Tc-99	3.0 MBq/L	Np-237 (V)	2.2 MBq/L	Am-241	3.0 MBq/L
Eu-152	5.6 MBq/L	Pu-239	6.6 MBq/L	Cm-244	3.0 MBq/L
HNO_3	1–6 mol/L				

The phases were contacted for 30 minutes, which is expected to be sufficient to attain equilibrium. Figure 12 shows the distribution ratios of Np-237, Pu-239, and Am-241 as a function of the nitric acid concentration. For Am-241 a clear difference in the extraction is observed with the *cis* (*RS*) isomer extracting the best. The trans isomer (*SS*) extracts significantly less and for the mixture distribution ratios in between are measured (as expected). Pu extraction, however, differs, as the difference in extraction between the different diastereomers is rather small. The Np extraction is hard to get a clear picture of, as the distribution ratios are generally quite low, and Np is only extracted at the highest HNO_3 concentrations.

Figure 13 shows the distribution ratios of Am-241 and Cm-244 as a function of the nitric acid concentration. Here, the same principal trend is observed, with the *cis* (*RS*) isomer extracting the best, the *trans* isomer (*SS*) extracting significantly less and intermediate distribution ratios for the mixture. Interestingly, an inversion of selectivity is observed, similar to the same phenomenon that had been observed with the different diastereomers of Me_2-TODGA (TWE-14) [120]. The *cis* (*RS*) isomer and the mixture show a preference for Cm over Am extraction, while the *trans* isomer (*SS*) shows the opposite selectivity.

Figure 14 shows an overview of distribution ratios of all metal ions for different diastereomers of mTDDGA and nitric acid concentrations. Most metal ions show the same trends in nitric acid concentration (increasing distribution ratios with increasing nitric acid concentration) and order of diastereomers (*cis* > mixture > *trans*). The Ln extraction pattern shows a maximum for the extraction of Er, which is comparable to Me_2-TODGA (TWE-14) [120].

Regarding other fission products:

- Ru and Sr distribution ratios were low under all conditions.

- Tc extraction does not follow the trend in nitric acid concentration, which could be explained by its extraction as an anion. It follows the order of diastereomers (*cis* > mixture > *trans*).
- Fe, Pd, and Mo extraction do not follow the trends. Their distribution ratios are nearly independent of the HNO_3 concentration, and they follow a different order of diastereomers: *trans* > *cis* > mixture. Even though it could be possible that the trans isomer extracts these metal ions better, the order of diastereomers does not make much sense, as the mixture of diastereomers should show an intermediate behaviour in any case. Therefore, the Fe, Pd, and Mo extraction is currently not understood and further experiments are needed to understand their behaviours.

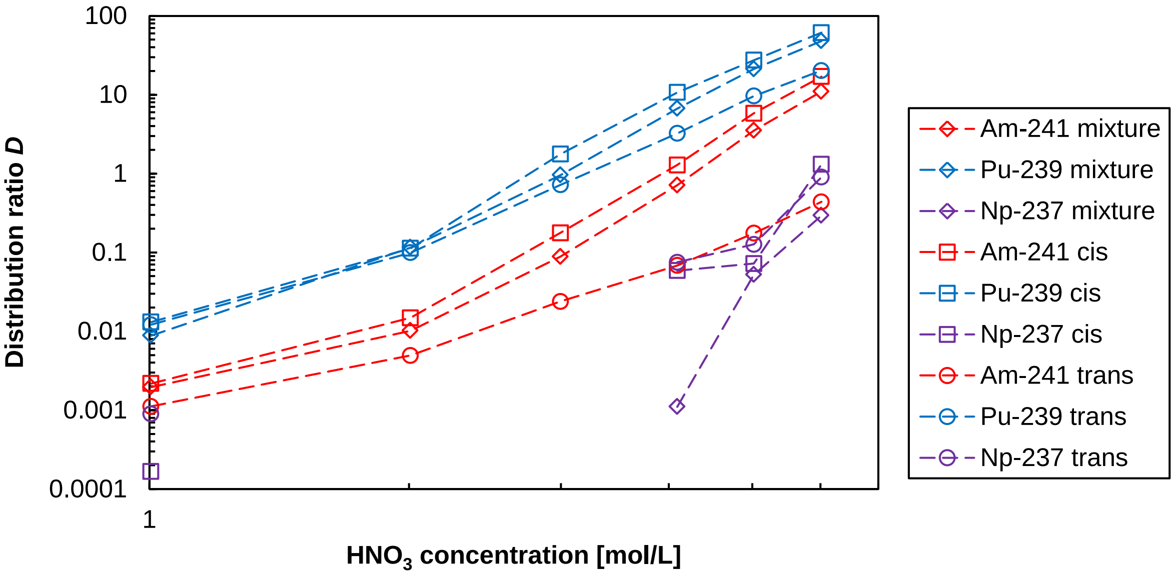

Figure 12. Distribution ratios of Np-237, Pu-239, and Am-241 as a function of the nitric acid concentration. Org.: 0.1 mol/L mTDDGA (different diastereomers) in Exxsol-D80. Aq.: 1-6 mol/L HNO_3 containing trace amounts of inactive metals (10^{-5} mol/L each) and spiked with radioactive tracers, as shown in Table 5. 22°C, 30 min. shaking time.

This project has received funding from the EURATOM research and training programme 2014-2018 under grant agreement No 755171. The content of this deliverable reflects only the author's view. The European Commission is not responsible for any use that may be made of the information it contains.

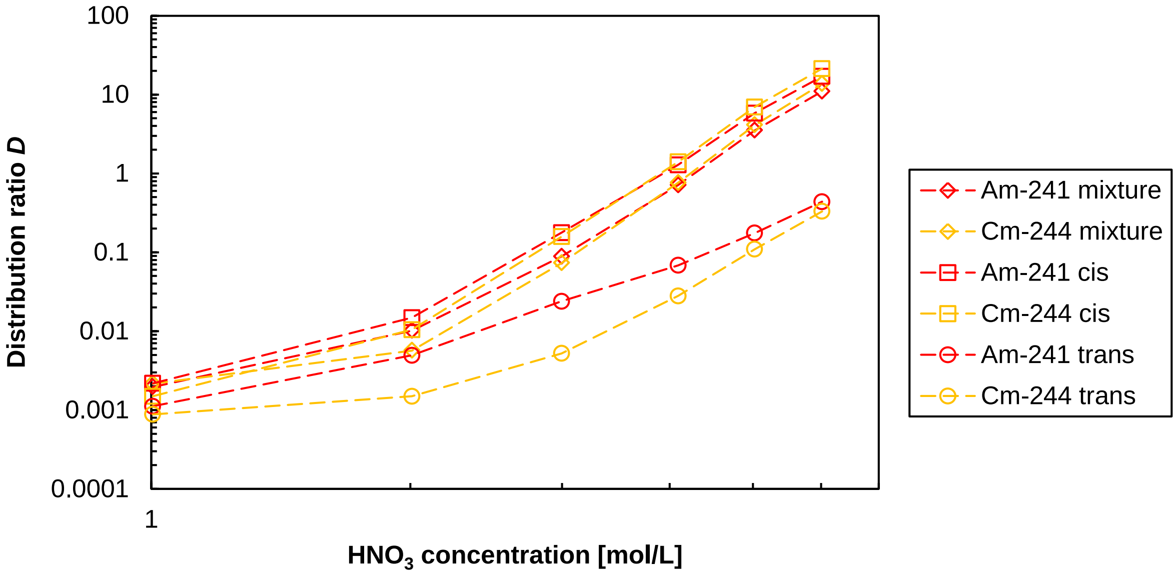

Figure 13. Distribution ratios of Am-241 and Cm-244 as a function of the nitric acid concentration. Org.: 0.1 mol/L mTDDGA (different diastereomers) in Exxsol-D80. Aq.: 1-6 mol/L HNO_3 containing trace amounts of inactive metals (10^{-5} mol/L each) and spiked with radioactive tracers, as shown in Table 5. 22°C, 30 min. shaking time.

This project has received funding from the EURATOM research and training programme 2014-2018 under grant agreement No 755171. The content of this deliverable reflects only the author's view. The European Commission is not responsible for any use that may be made of the information it contains.

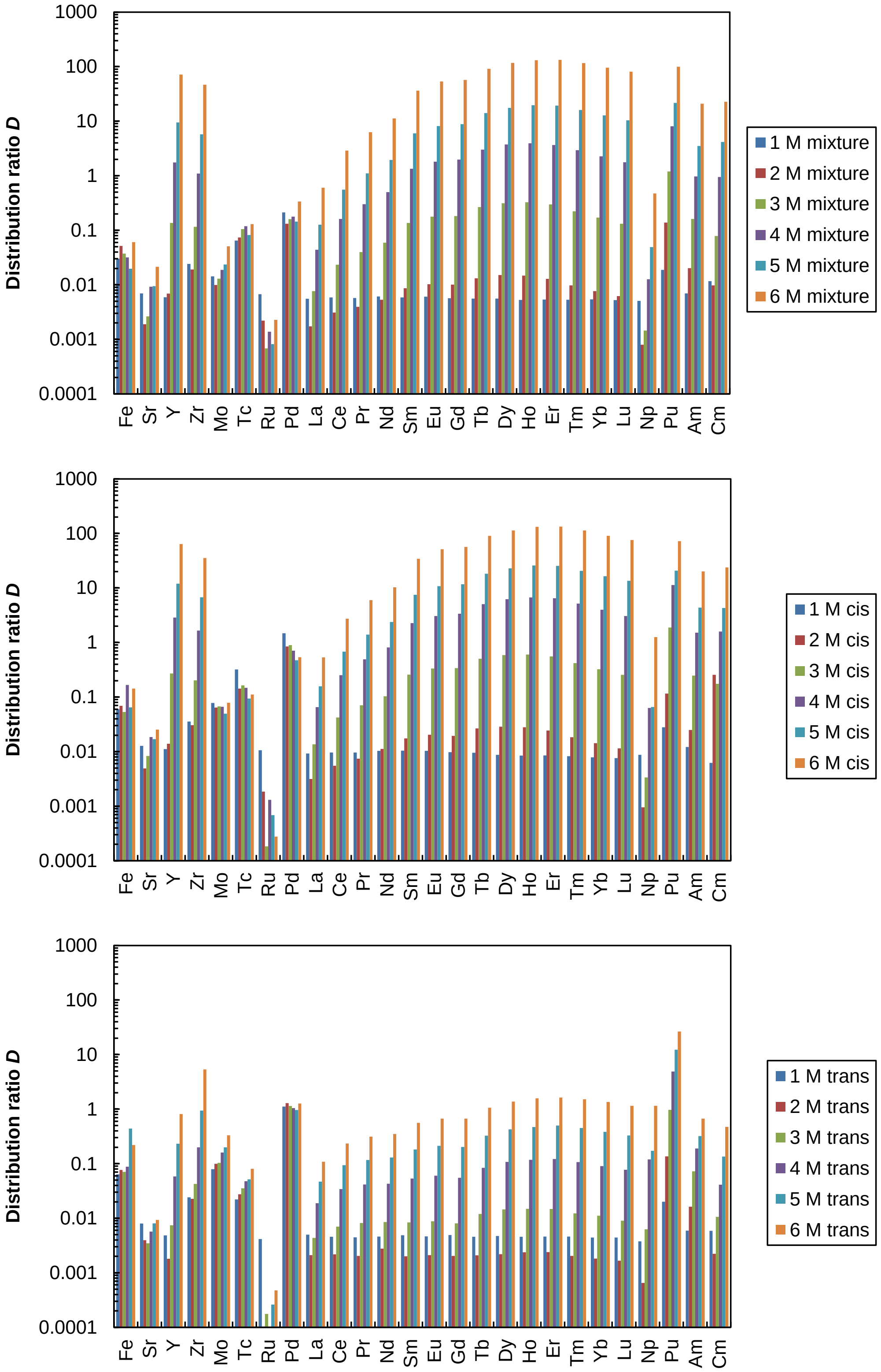

Figure 14. Distribution ratios of all metal ions for different diastereomers of mTDDGA and nitric acid concentrations. Org.: 0.1 mol/L mTDDGA (different diastereomers) in Exxsol-D80. Aq.: 1-6 mol/L HNO_3 containing trace amounts of inactive metals (10^{-5} mol/L each) and spiked with radioactive tracers, as shown in Table 5. 22°C, 30 min. shaking time

EXPERIMENTS WITH *CIS*-MTDDGA ONLY, COMPARISON OF BATCHES

Two different batches of *cis*-mTDDGA were tested, one small batch obtained from TWENTE University (Enschede, The Netherlands) and another larger batch obtained from Oak Ridge National Laboratory (Oak Ridge, USA), which is intended to be used for loop irradiation tests within the GENIORS project. The diastereomeric excess (*de*) of the Oak Ridge batch was ca. 30:1 *cis* over *trans* (93.5% *de*). PTD was obtained from University of Parma (Parma, Italy). During the virtual project meeting on 8 August 2020, conditions for the loop irradiation tests were discussed. Due to the relatively large volumes needed in the loop tests and the limited amount of *cis*-mTDDGA available, it was decided to test concentrations of 0.3 or 0.4 mol/L *cis*-mTDDGA, with a preference for 0.4 mol/L. The diluent was decided to be *n*-dodecane. This solvent composition differs from the previously tested 0.5 mol/L *cis*-mTDDGA in Exxsol-D80. NNL showed that 0.3 or 0.4 mol/L *cis*-mTDDGA would still enable a Pu loading of ≥40 g/L. A Pu loading of ca. 40 g/L is more than required in the EURO-GANEX process (>10 g L^{-1}) and similar to the loading capacity of the current formulation with 0.2 mol/L TODGA and 0.5 mol/L DMDOHEMA [67].

Figure 15 and Figure 16 show the distribution ratios for actinides and all fission and corrosion products tested. Am^{3+}, Cm^{3+} and Pu^{4+} were well extracted with high distribution ratios. The variation in the distribution ratios comparing different analytical techniques was rather high, but it is thought that this is due to the high distribution values and related experimental uncertainties. The maximum in extractability within the Ln series (+Y) was observed for Ho, which is the same as observed for *cis*-Me_2-TODGA.[120] The least extractable lanthanide ion is La^{3+}. A co-extraction of Sr, Zr, and Pd was observed, without showing a distinct nitric acid dependency. We believe that the co-extraction of Zr and Pd can be avoided using CDTA in the extraction stage, although this still must be shown. Fe and Mo distribution ratios were < 1, and Ru distribution ratios even < 0.01. These metal ions should not be problematic.

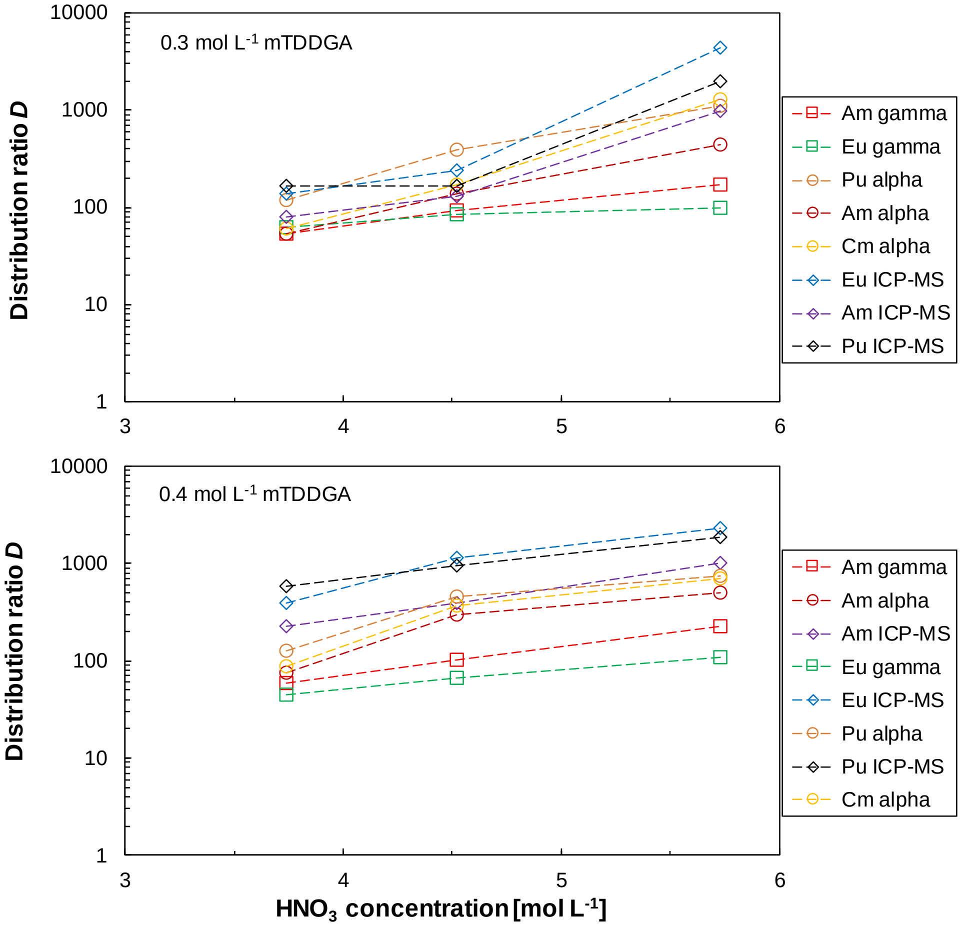

Figure 15. Distribution ratios *D* as a function of the HNO_3 concentration for 0.3 (top) and 0.4 (bottom) mol/L *cis*-mTDDGA (Twente). Org.: 0.3 or 0.4 mol/L *cis*-mTDDGA (Twente) in *n*-dodecane. Aq.: 10^{-5} mol/L Ln and FP in HNO_3, spiked with ^{152}Eu, ^{239}Pu, ^{241}Am, and ^{244}Cm. 22°C, 2,220 rpm, 60 min

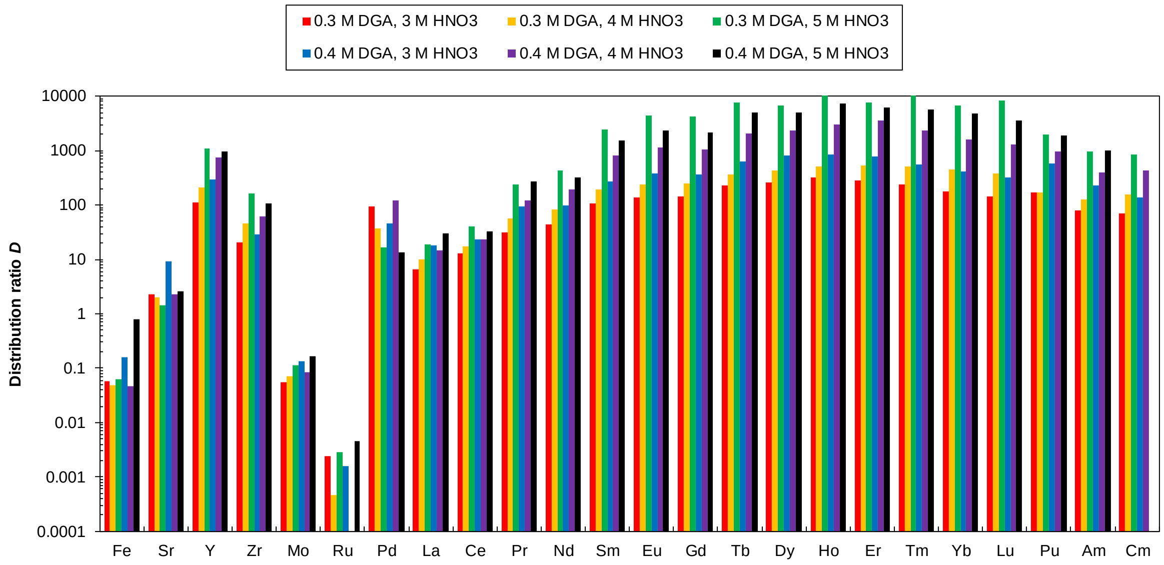

Figure 16. Distribution ratios *D* of actinides, lanthanides, and fission products as a function of *cis*-mTDDGA (TWENTE) and HNO_3 concentration (ICP-MS measurement). Experimental details see Figure 15 caption.

Figure 17 shows the Am distribution ratios *D* as a function of the HNO_3 concentration for the extraction with different concentrations and batches of *cis*-mTDDGA. The shaking time was different for different experimental series between 15 – 60 min, but we believe that 15 min is enough to reach the equilibrium. Therefore, all data are equilibrium data. The results show good comparison between the different batches of *cis*-mTDDGA, although the number of data points measured under identical conditions is limited. The new *cis*-mTDDGA batch obtained from Oak Ridge showed very comparable extraction results in comparison to the batch obtained from TWENTE. Data scattered more for Eu and Pu in the directly comparable high HNO_3 concentration range, due to the high *D* values and associated uncertainties.

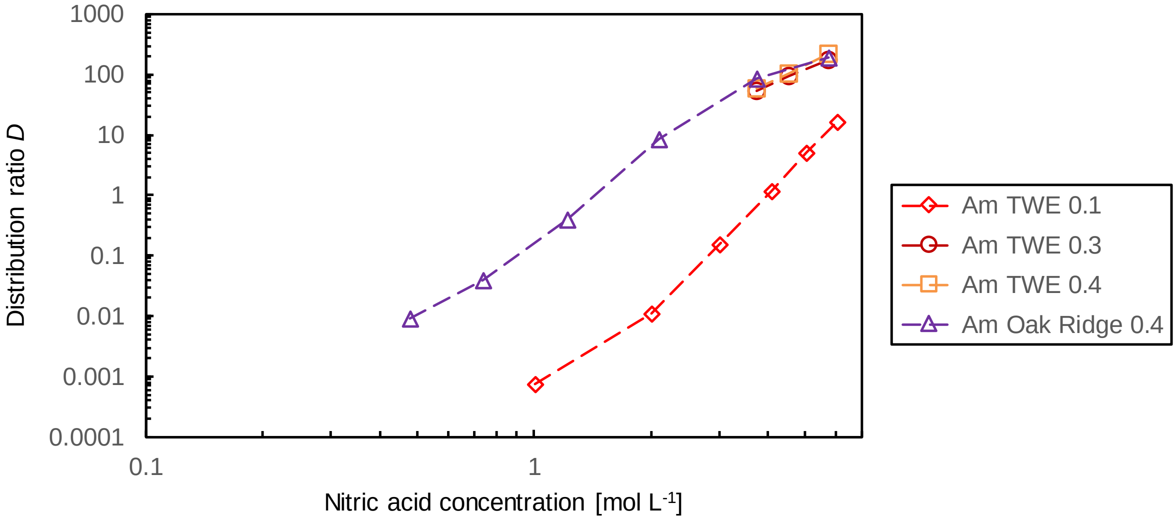

Figure 17. Americium distribution ratios *D* as a function of the HNO_3 concentration for the extraction with different concentrations and batches of *cis*-mTDDGA. Org.: *cis*-mTDDGA (TWENTE or Oak Ridge) in *n*-dodecane. Aq.: 10^{-5} mol/L Ln and FP in HNO_3, spiked with ^{152}Eu, ^{239}Pu, ^{241}Am, and ^{244}Cm. 22°C, 2,220 rpm, 15-60 min

Figure 18 shows increasing distribution ratios as a function of the HNO_3 concentration for 0.4 mol/L *cis*-mTDDGA (Oak Ridge), and Figure 19 shows an overview of all metal ions. Interestingly, the maximum in extractability within the Ln series (+Y) is shifted to Eu for the Oak Ridge *cis*-mTDDGA batch, while the TWENTE batch showed a maximum at Ho. The reason for that shift is unclear. The least extractable of the light lanthanides is still La. A slight co-extraction of Sr and stronger co-extraction of Zr was observed showing increasing *D* values with increasing HNO_3 concentrations. Pd showed *D* values of 2-7 without showing a distinct nitric acid dependency. Fe and Mo distribution ratios were < 1, and Ru distribution ratios even < 0.01. These metal ions should not be problematic.

Figure 20 shows the extraction of nitric acid by 0.4 mol/L *cis*-mTDDGA (Oak Ridge). The data are roughly comparable with nitric acid extraction data measured by KIT, although not directly comparable due to differences in the experimental conditions. The HNO_3 distribution ratio is ca. 0.1.

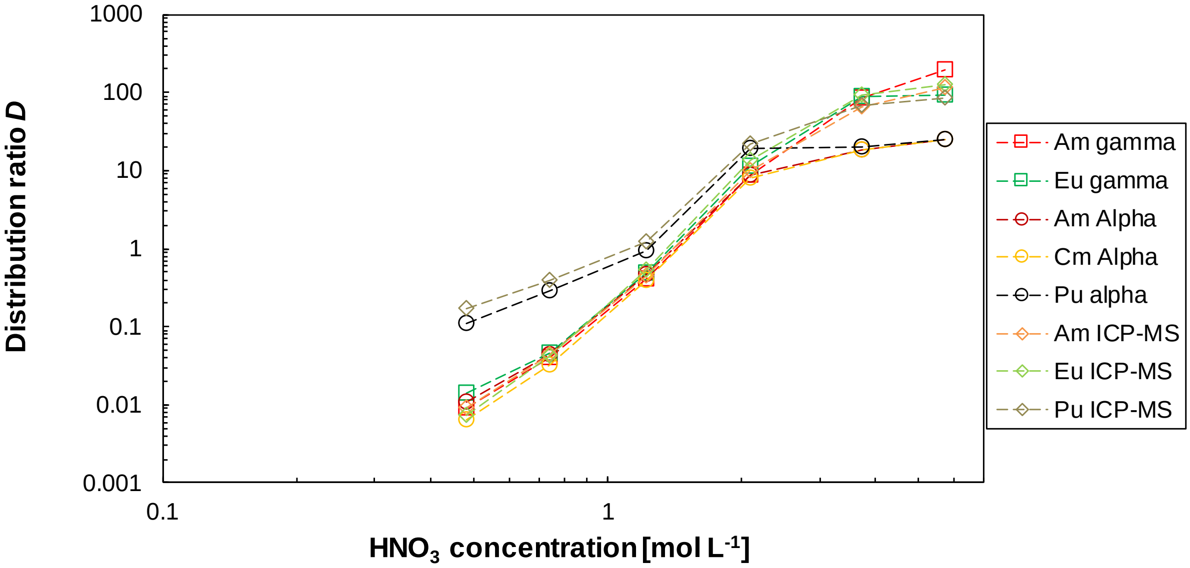

Figure 18. Distribution ratios *D* as a function of the HNO_3 concentration for 0.4 mol/L *cis*-mTDDGA (Oak Ridge). Org.: 0.4 mol/L *cis*-mTDDGA (Oak Ridge) in *n*-dodecane. Aq.: 10^{-5} mol/L Ln and FP in HNO_3, spiked with ^{152}Eu, ^{239}Pu, ^{241}Am, and ^{244}Cm. 22°C, 2,220 rpm, 15 min

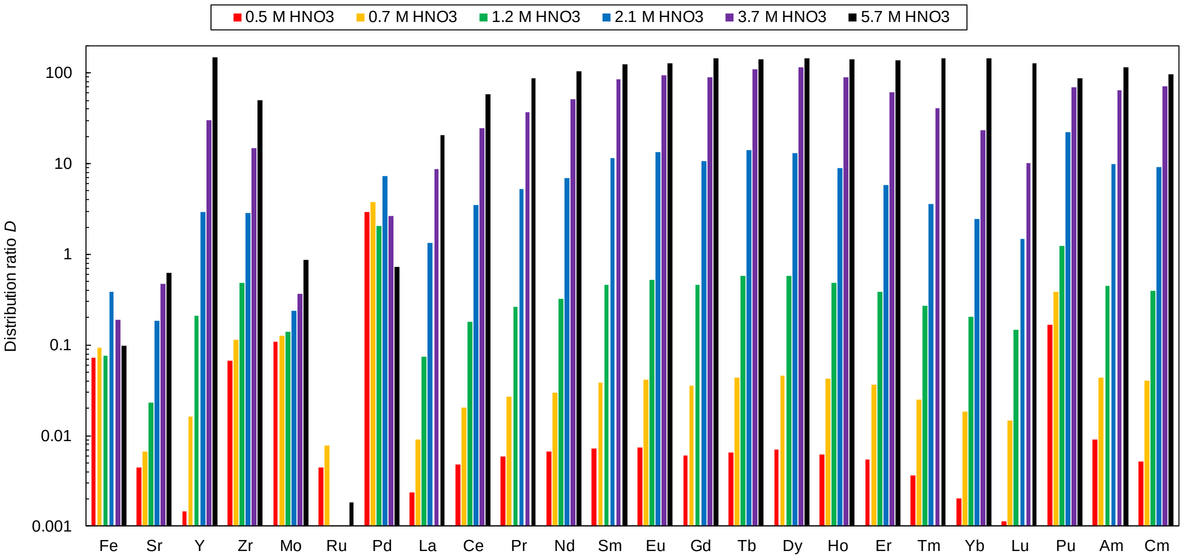

Figure 19. Distribution ratios *D* as a function of the HNO_3 concentration for extraction with 0.4 mol/L *cis*-mTDDGA (Oak Ridge). Experimental details see Figure 18 caption.

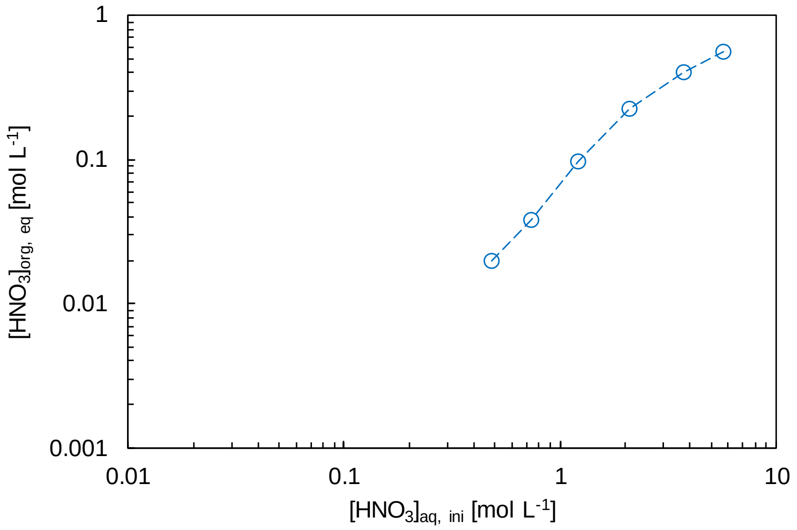

Figure 20. Organic nitric acid concentration as a function of the initial HNO_3 concentration for the extraction with 0.4 mol/L *cis*-mTDDGA (Oak Ridge). Experimental details see Figure 18 caption.

AM(III) AND LN(III) EXTRACTION WITH MTDDGA

Distribution ratios for An(III) and Ln(III) were acquired with mTDDGA (TWENTE, *cis:trans* ≈ 95:5) dissolved in kerosene as function of the initial nitric acid concentration (Figure 21). Compared to TODGA in kerosene + 5 vol.% 1-octanol, distribution data were found to be rather low, requiring higher nitric acid concentrations to extract Am(III) and Ln(III). This trend had also been observed for methylated and dimethylated TODGA [126]. mTDDGA synthesized at KIT (INE) shows a diastereomeric composition of 50:50. The fact that only the *cis* diastereomer extracts is reflected in the distribution ratios in Table 6.

Distribution ratios for the TWENTE compound are larger by a factor 5, which is in good agreement with the relative concentrations of the (better extracting) *cis* diastereomer being 1.9. Applying the concentration dependency observed for TODGA in TPH/1-octanol (slope ≈ 2.7), a factor of 5.7 is expected.

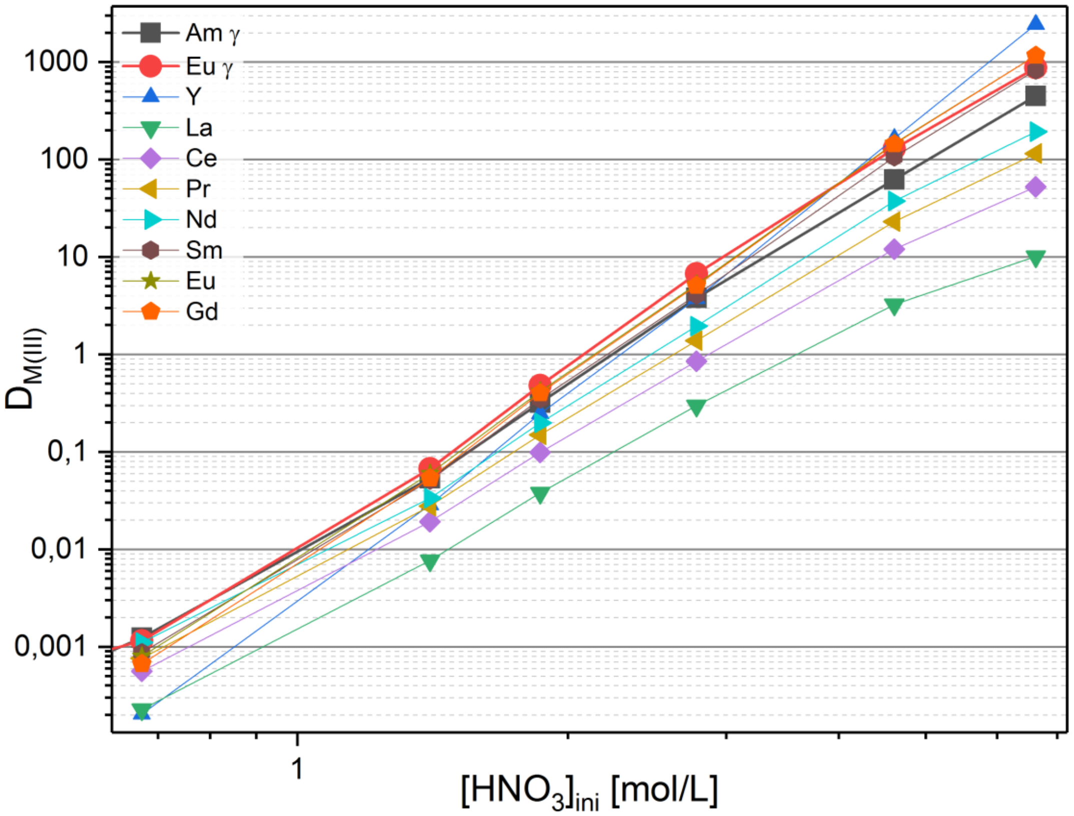

Figure 21. Distribution data for the extraction of metal ions from HNO_3 into mTDDGA in kerosene. Organic phase: 0.2 mol/L. Aqueous phase: [^{241}Am]] = [^{154}Eu] = 1 kBq. [Ln] = 6 mg/L, *T* = 293 K. *O/A* = 1

Table 6. Extraction of Am(III) and Eu(III) from HNO_3 into mTDDGA in kerosene. Organic phase, 0.1 mol/L mTDDGA. Aqueous phase, ^{241}Am(III) and ^{154}Eu(III) = (1 kBq/mL each) In 3 mol/L HNO_3. *T* = 293 K. *O/A* = 1

	TWENTE **(*cis:trans* ≈ 95:5)**	**KIT-INE** **(*cis:trans* ≈ 50:50)**	D_{TWE}/D_{KIT}
D_{Am}	0.54	0.11	4.9
D_{Eu}	1.1	0.20	5.5
$SF_{Eu/Am}$	2.0	1.8	

NP(IV) EXTRACTION INTO MTDDGA

Studies were commenced into neptunium behaviour with mTDDGA since Np is known to have a complex chemistry in solvent extraction processes due to having three accessible oxidation states that are inter-convertible and exhibit varying extractabilities [34, 75, 76]. It is intended to replicate previous studies on TODGA/DMDOHEMA [76] but so far this work has only considered the +4 oxidation state.

Briefly, a 2 g/L Np stock solution in 2 mol/L HNO_3 was electrochemically conditioned to Np(IV) and aliquots of this conditioned Np stock solution diluted with nitric acid to obtain solutions of ~0.2 g/L Np(IV) at a range of nitric acid concentrations (0.25-6 mol/L). The aqueous phase was then contacted with 0.5 mol/L mTDDGA at S/A = 1 and T=22 °C for approximately 15 minutes before phase separation. Np concentrations in aqueous and organic phases were determined by gamma spectroscopy using Np-237 gamma peak at 85 keV and a correction applied for the contribution from the Pa-233 daughter.

Results are shown in Figure 22. $D_{Np(IV)}$ shows a similar trend to the EURO-GANEX solvent. Increasing $D_{Np(IV)}$ with increasing acidity but $D_{Np(IV)}$ values are significantly lower in mTDDGA than observed for the corresponding acidity with either the EURO-GANEX solvent or its separate constituents (0.2 mol/L TODGA and 0.5 mol/L DMDOHEMA). A high result was observed for 5 mol/L that may indicate a maximum extractability but this needs to be confirmed. Of greater concern is that $D_{Np(IV)}$ is < 1 at 0.5 mol/L HNO_3 and in the original EURO-GANEX solvent $D_{Np(VI)} < D_{Np(IV)}$ so assuming that the same trend is observed for 0.5 mol/L mTDDGA then modification of the scrub acidity would be needed to maintain complete extraction of Np with Pu and other minor actinides in the initial extract-scrub stage.

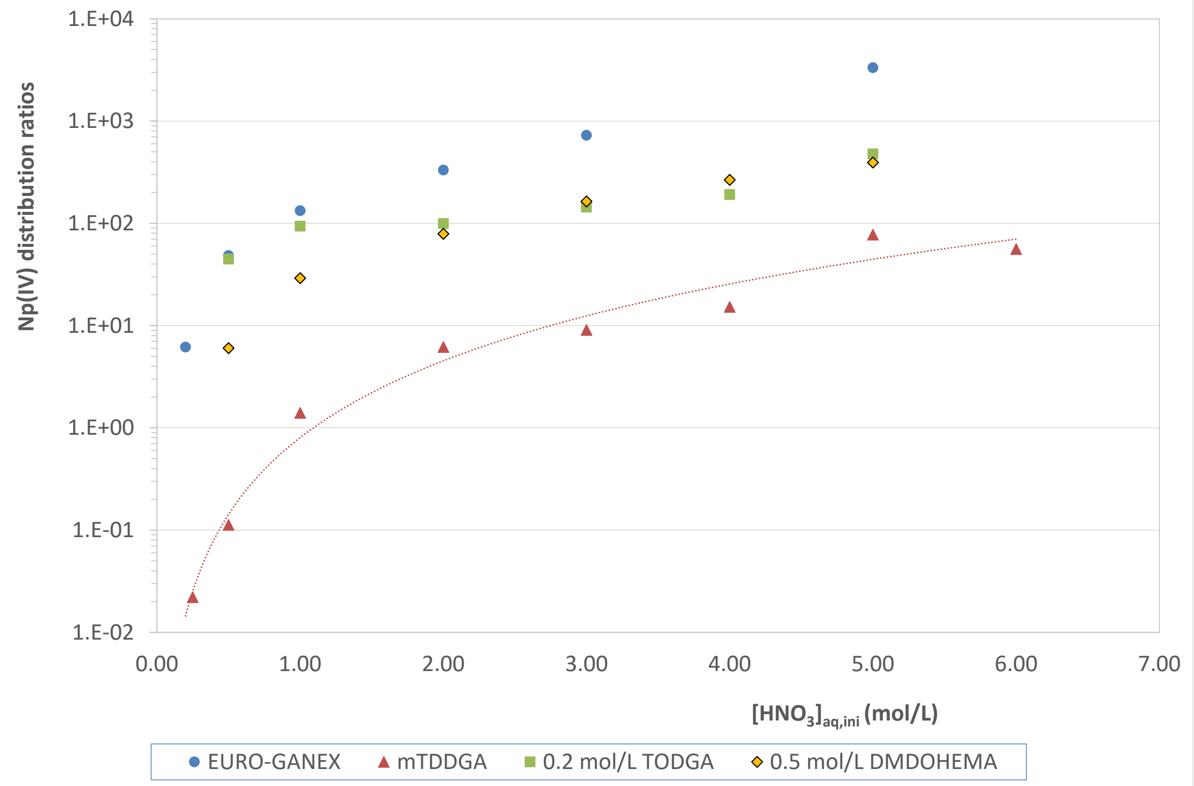

Figure 22: Np(IV) distribution data for mTDDGA compared to previous data on EURO-GANEX extractants

MTDDGA PU(IV) LOADING EXPERIMENTS

In support of the development of an improved EURO-GANEX process, preliminary Pu(IV) loading studies of two DGA based solvents were performed: a solvent comprising 0.5 mol/L TODGA in di-isopropyl benzene [127] and a solvent comprising 0.5 mol/L cis-mTDDGA in Exxsol D80 [128]. The results are reported in the Deliverable Report, GENIORS D3.3, Status on TODGA organic phase loading.

Further data were obtained at NNL and are reported here – see Figure 23 and Table 7. A series of batch tests were performed to assess the effect of mTDDGA concentration, nitric acid concentration and Pu loading upon third phase formation with conditions set as [mTDDGA] = 0.1 to 0.5 mol/L; [Pu(IV)] = 0 to 60 g/L; [HNO_3]: 1 to 7 mol/L, at ambient temperature (≈22 °C) and S/A ratio of 1. Aqueous solutions were prepared by dilution of the concentrated laboratory stock of Pu(IV) nitrate and nitric acid to obtain the desired concentration. 0.5 mL of the aqueous phase was contacted with an equal volume of mTDDGA in OK for 15 minutes. Samples were allowed to settle and the presence or absence of 3rd phase was recorded. Unless stated, all batch tests were performed with the *cis* isomer of mTDDGA obtained from Technocomm Ltd. In 0.3 mol/L (and above) mTDDGA, the high Pu loading produced a very dark, viscous organic phase that made it difficult to observe the presence of a third phase at the aqueous / organic interface and this may introduce some uncertainties to the values recorded.

It was found that for 0.1 mol/L mTDDGA the 3rd phase boundary is quite consistent at around 9 g/L, at least for nitric acid concentrations above 4 mol/L. Surprising results were obtained below 4 mol/L as the 3rd phase boundary appeared to rise and then fall again at 1 mol/L with 3rd phase observed as low as 2.5 g/L Pu. Interestingly, the *trans* isomer gave the same capacity at 5 mol/L HNO_3. For 0.5 mol/L mTDDGA, no third phase formation was seen even up to 55 g/L Pu at 4-5 mol/L HNO_3.

Table 8 calculates the apparent ratios of mTDDGA to Pu(IV) that correspond to these concentrations. Data at 4-7 mol/L HNO_3 for 0.1 mol/L m-TDDGA are consistent with ~2.5 mTDDGAs per Pu at third phase formation (TPF). This decreases to ~2 at 3 mol/L and less at 2 mol/L HNO_3. At 1 mol/L HNO_3, the value is >9.6. For 0.3 mol/L and 0.5 mol/L, at 5 mol/L HNO_3, the apparent solvation number is probably less than 2.

These data agree with the previous report (D3.3) where no third phase was found for solutions up to 48 g/L Pu in 5 mol/L HNO_3 with 0.5 mol/L *cis*-mTDDGA in Exxsol D-80 (98% *cis* isomer). It was noted that the published work observed a precipitate with 48 g/L Pu solution in 5 mol/L HNO_3 but this was ascribed to their use of the n-dodecane diluent rather than the mixed branched alkane Exxsol-D80 diluent [106].

In summary, it appears that m-TDDGA has very good capacity for Pu(IV) above 2 mol/L HNO_3 and can form complexes of 2:1 mTDDGA:Pu stoichiometry or possibly higher. From this perspective it is a very promising extractant to replace the TODGA/DMDOHEMA solvent used in EURO-GANEX but the apparent low capacity for Pu below 2 mol/L HNO_3 is now of significant concern. Interestingly, a single experiment with *trans*-mTDDGA gave identical results perhaps implying differing behaviour between tetravalent plutonium and trivalent americium ions with mTDDGA isomers.

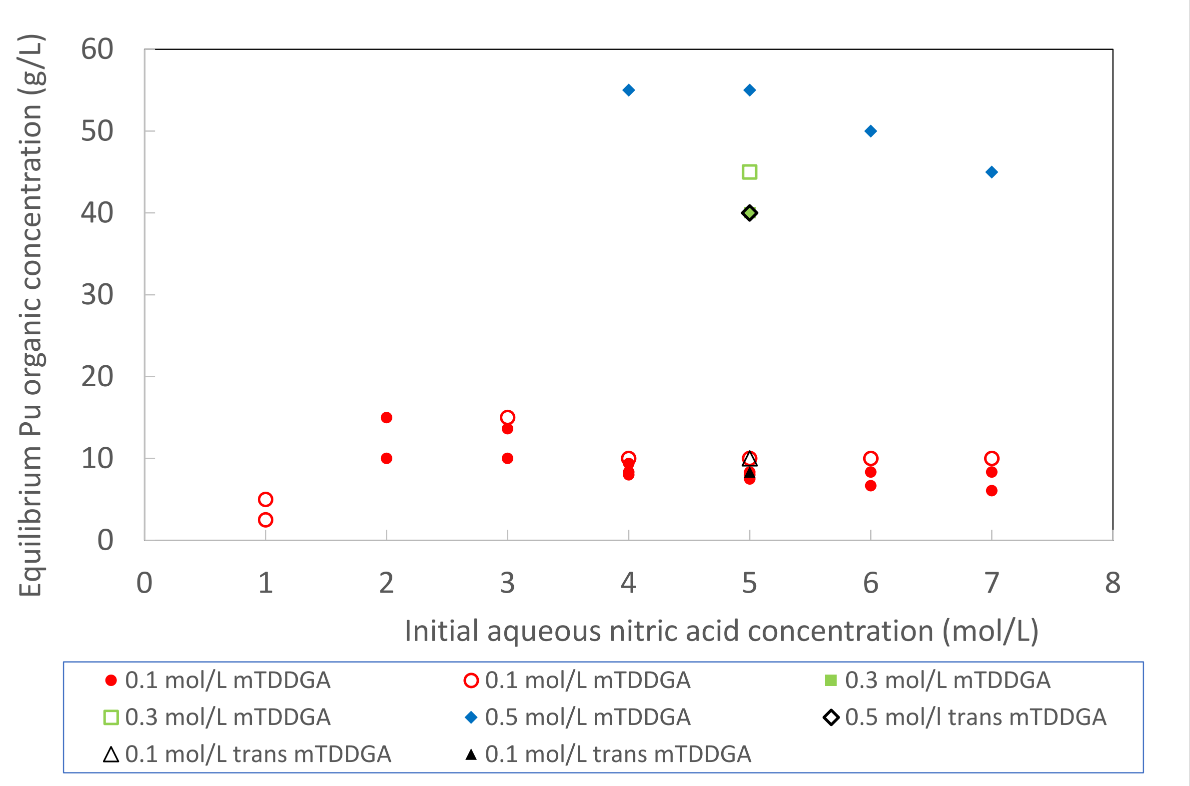

Figure 23: Third phase formation with plutonium in the m-TDDGA solvent system

Table 7: Pu(IV) concentrations (g/L) for data in Figure 23, (i.e. highest value before TPF, lowest value with TPF)

Initial $[HNO_3]_{aq}$ (mol/L)	Range of [Pu]org (g/L) before TPF		
	0.1 mol/L	0.3 mol/L	0.5 mol/L
1	<2.5		
2	>15		
3	13.6, 15		
4	9.4, 10		>55
5	8.3, 10	40. 45	>55
6	8.3, 10		>50
7	8.3, 10		>45

Table 8: Apparent solvation numbers (number of TODGA ligands per Pu(IV)) for data in Figure 23, (i.e. highest value before TPF, lowest value with TPF)

Initial $[HNO_3]_{aq}$ (mol/L)	Range of [Pu]org (g/L) before TPF		
	0.1 mol/L	0.3 mol/L	0.5 mol/L
1	>9.6		
2	<1.6		
3	1.6,1.8		
4	2.9, 2.4		<2.2

5	2.9, 2.4	1.8, 1.6	<2.2
6	2.9, 2.4		<2.4
7	2.9, 2.4		<2.7

STRIPPING EXPERIMENTS WITH MTDDGA AND PTD

EXPERIMENTS WITH CIS-MTDDGA AND PTD

In a first series of extraction experiments a fixed PTD concentration of 0.04 mol/L was chosen and the extraction with 0.4 mol/L *cis*-mTDDGA was tested as a function of the HNO_3 concentration. Figure 24 shows the Am and Eu distribution ratios in comparison with a series of extractions without PTD addition. The *D* values increased with increasing HNO_3 concentration. The Am/Eu selectivity was not much increased by the addition of PTD. In the range of 0.5 – 1.2 mol/L HNO_3 slightly lower *D* values were measured for the experiments with added PTD compared to the one without PTD addition. The separation factor $SF_{Eu/Am}$ did not exceed a value of 5.

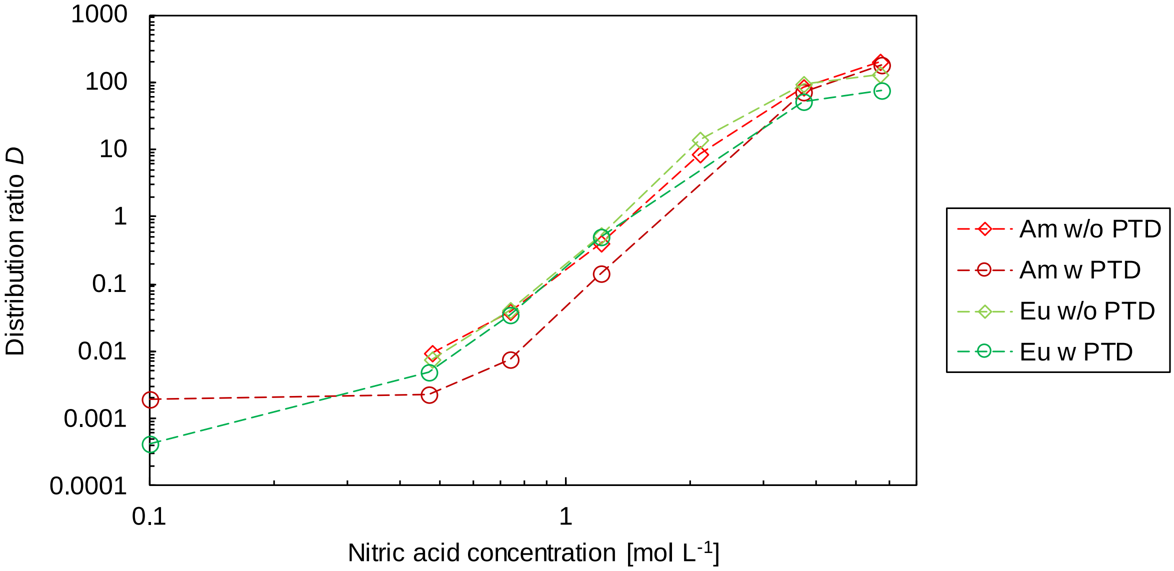

Figure 24. Distribution ratios *D* as a function of the HNO_3 concentration for the extraction with 0.4 mol/L *cis*-mTDDGA (Oak Ridge) with and without addition of 0.04 mol/L PTD. Org.: 0.4 mol/L *cis*-mTDDGA (Oak Ridge) in *n*-dodecane. Aq.: 10^{-5} mol/L Ln and FP in HNO_3, with and without addition of 0.04 mol/L PTD, spiked with ^{152}Eu, ^{239}Pu, ^{241}Am, and ^{244}Cm. 22°C, 2,220 rpm, 15 min

Figure 25 shows increasing distribution ratios of Am, Eu, Cm, and Pu as a function of the HNO_3 concentration for 0.4 mol/L *cis*-mTDDGA (Oak Ridge) with addition of 0.04 mol/L PTD, and Figure 26 shows an overview of all metal ions. The maximum in extractability within the Ln series (+Y) varies much for the different nitric acid concentrations, and no clear trend can be recognized. The least extractable of the light lanthanides (La to Gd) is still La. Increasing co-extraction of Sr, Zr and Mo was observed with increasing HNO_3 concentrations. Pd and Fe showed *D* values of ca. 0.1 without showing a distinct nitric acid dependency. Ru distribution ratios were < 0.01. Figure 27 shows the extraction of nitric acid by 0.4 mol/L *cis*-mTDDGA (Oak Ridge) with addition of 0.04 mol/L PTD. The nitric acid extraction is practically identical to the one without addition of PTD shown in Figure 20.

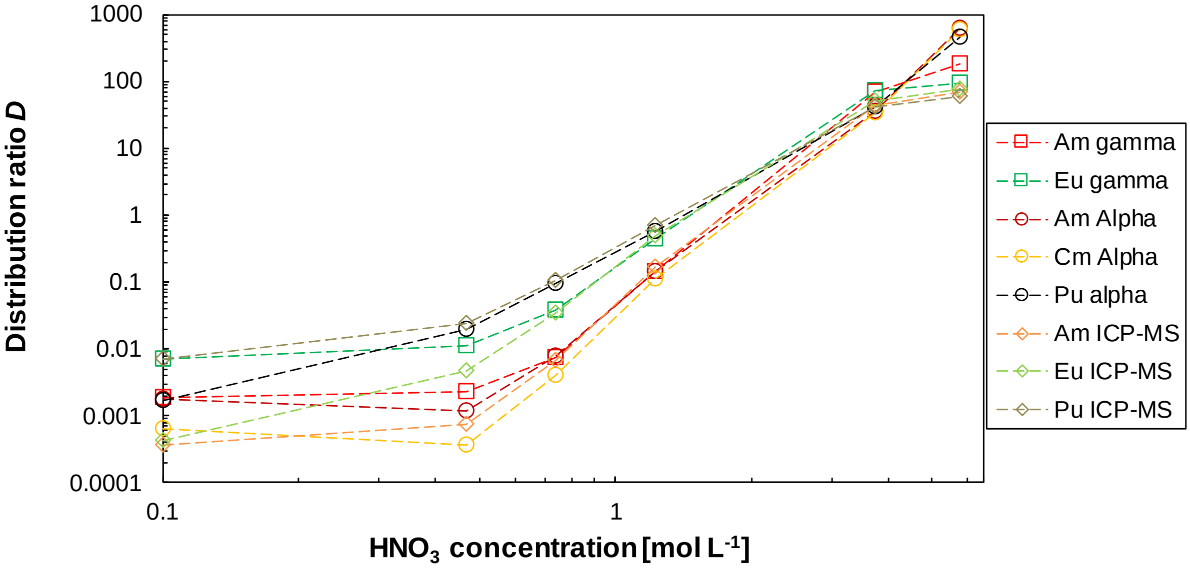

Figure 25. Distribution ratios *D* as a function of the HNO_3 concentration for the extraction with 0.4 mol/L *cis*-mTDDGA (Oak Ridge) with addition of 0.04 mol/L PTD. Org.: 0.4 mol/L *cis*-mTDDGA (Oak Ridge) in *n*-dodecane. Aq.: 10^{-5} mol/L Ln and FP in HNO_3, 0.04 mol/L PTD, spiked with ^{152}Eu, ^{239}Pu, ^{241}Am, and ^{244}Cm. 22°C, 2,220 rpm, 15 min.

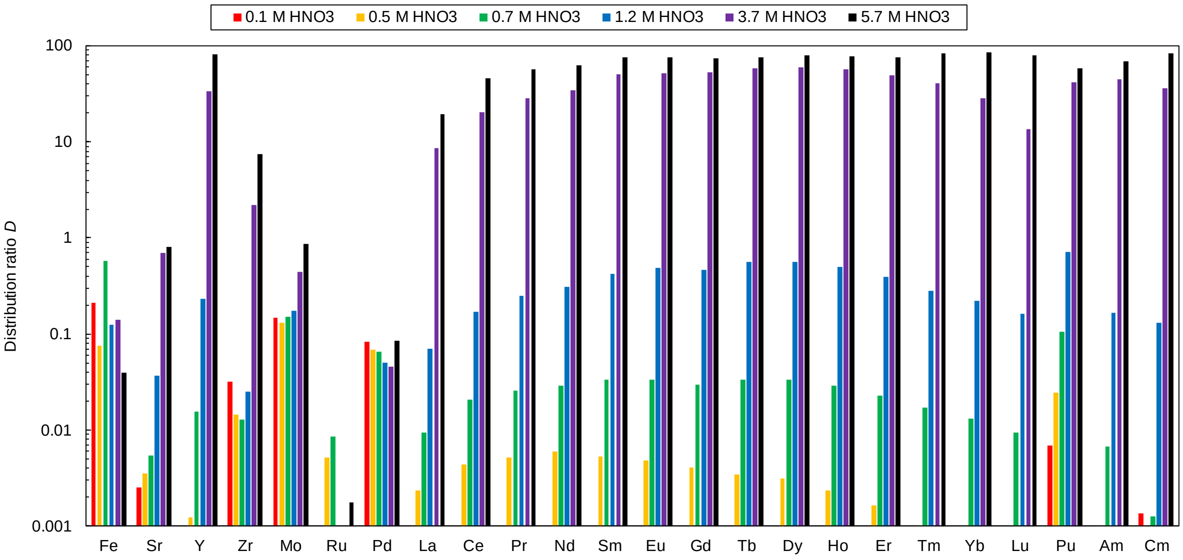

Figure 26. Distribution ratios *D* as a function of the HNO_3 concentration for the extraction with 0.4 mol/L *cis*-mTDDGA (Oak Ridge) with addition of 0.04 mol/L PTD. Experimental details see Figure 25 caption.

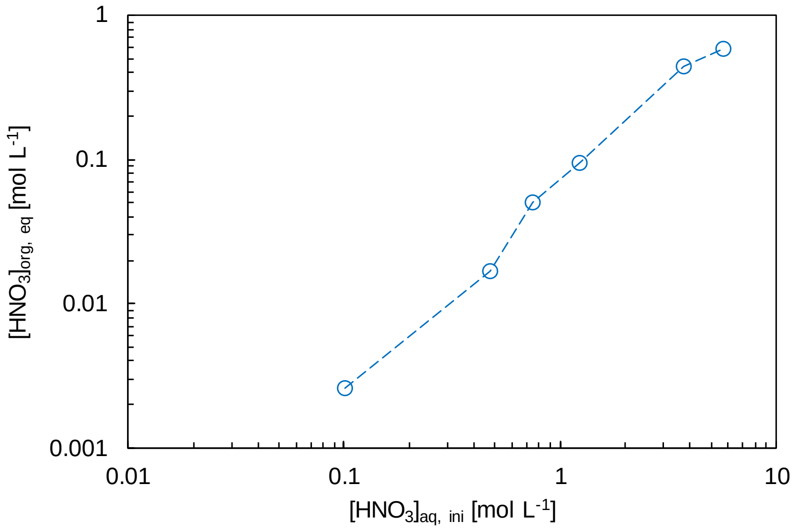

Figure 27. Organic nitric acid concentration as a function of the initial HNO_3 concentration for the extraction with 0.4 mol/L *cis*-mTDDGA (Oak Ridge) with addition of 0.04 mol/L PTD. Experimental details see Figure 25 caption.

In the next series, the PTD concentration was varied between 0 – 0.4 mol/L PTD at 2.1 mol/L HNO_3 and extraction with 0.4 mol/L *cis*-mTDDGA. The results in Figure 28 and Figure 29 show decreasing distribution ratios for all metal ions with increasing PTD concentration. The trivalent actinides Am and Cm were affected the most, resulting in increasing $SF_{Eu/Am}$ (≤ 23) and $SF_{Pu/Am}$ (≤ 14) separation factors. The Am/Cm selectivity remained unchanged with $SF_{Am/Cm}$ ca. 1.5. Figure 29 shows the *D* values for Am and the light lanthanides (La to Gd) as a function of the PTD concentration. The separation of Am from the lanthanides is governed by the least extractable La. Am *D* values fall below the La *D* values at PTD concentration > 0.2 mol/L, but with a low $SF_{La/Am}$ of 1.4. The best separation ($SF_{La/Am}$ = 4.8) was achieved at 0.4 mol/L PTD, but with a La *D* value of 0.56.

Figure 30 shows the distribution ratios for all investigated metal ions. Again, the maximum in extractability within the Ln series (+Y) is shifted to Eu, also for the experiment with addition of PTD. Zr and Pd distribution ratios also decrease strongly with increasing PTD concentration, while little to no effect was observed for Fe, Sr, and Mo. Ru distribution ratios were generally very low.

HNO_3 extraction was relatively constant with *D* values of ca. 0.1, but an overall decreasing HNO_3 concentration was observed. This is probably caused by partial protonation of PTD, consuming some ca. half the amount (in mol) HNO_3 per mol PTD.

The same PTD concentration range (0 – 0.4 mol/L) was also tested at 3.7 mol/L HNO_3 and extraction with 0.4 mol/L *cis*-mTDDGA. Figure 31 shows that distribution ratios were generally higher compared to the extraction from 2.1 mol/L HNO_3, as expected for the higher nitric acid concentration. At any PTD concentration, Am *D* values were ≥ 10 and no separation from La was achieved. The use of higher than 2 mol/L HNO_3 is therefore not usable for the selective Am stripping.

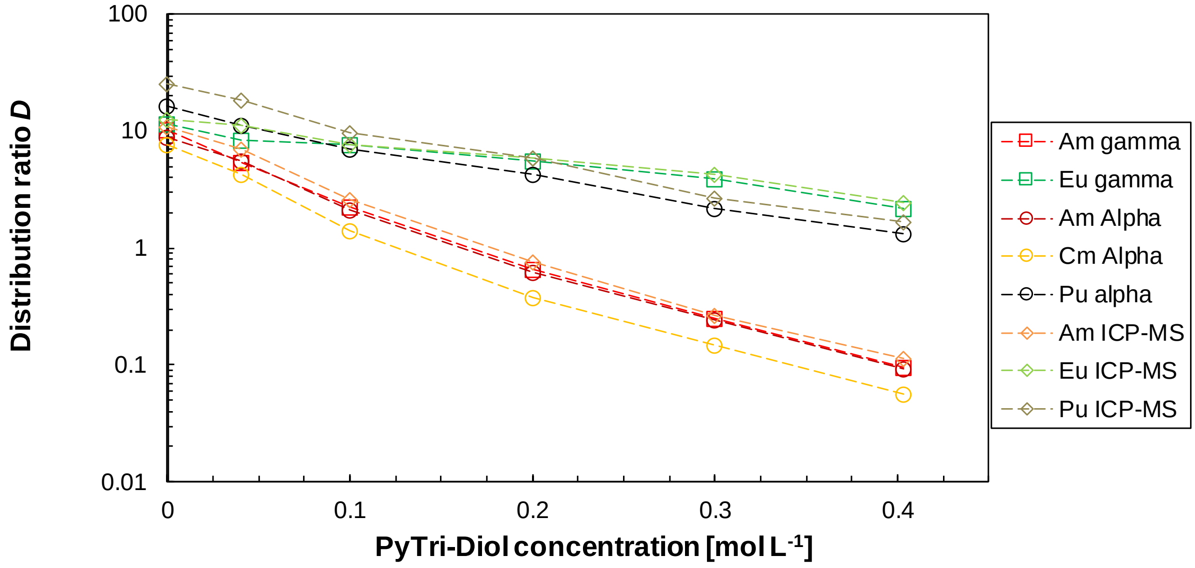

Figure 28. Distribution ratios *D* as a function of the PTD concentration for extraction with 0.4 mol/L *cis*-mTDDGA (Oak Ridge) from 2.1 mol/L HNO_3. Org.: 0.4 mol/L *cis*-mTDDGA (Oak Ridge) in *n*-dodecane. Aq.: 10^{-5} mol/L Ln and FP in 2.1 mol/L HNO_3, spiked with ^{152}Eu, ^{239}Pu, ^{241}Am, and ^{244}Cm. 22°C, 2,220 rpm, 15 min.

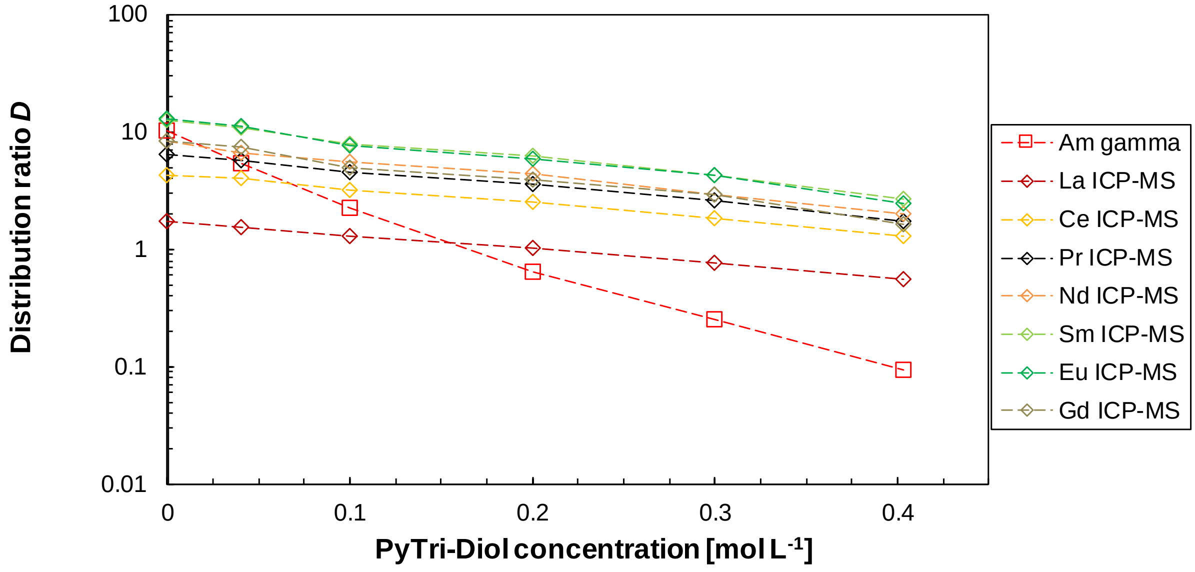

Figure 29. Distribution ratios *D* as a function of the PTD concentration for extraction with 0.4 mol/L *cis*-mTDDGA (Oak Ridge) from 2.1 mol/L HNO_3. Experimental details see Figure 28 caption.

This project has received funding from the EURATOM research and training programme 2014-2018 under grant agreement No 755171. The content of this deliverable reflects only the author's view. The European Commission is not responsible for any use that may be made of the information it contains.

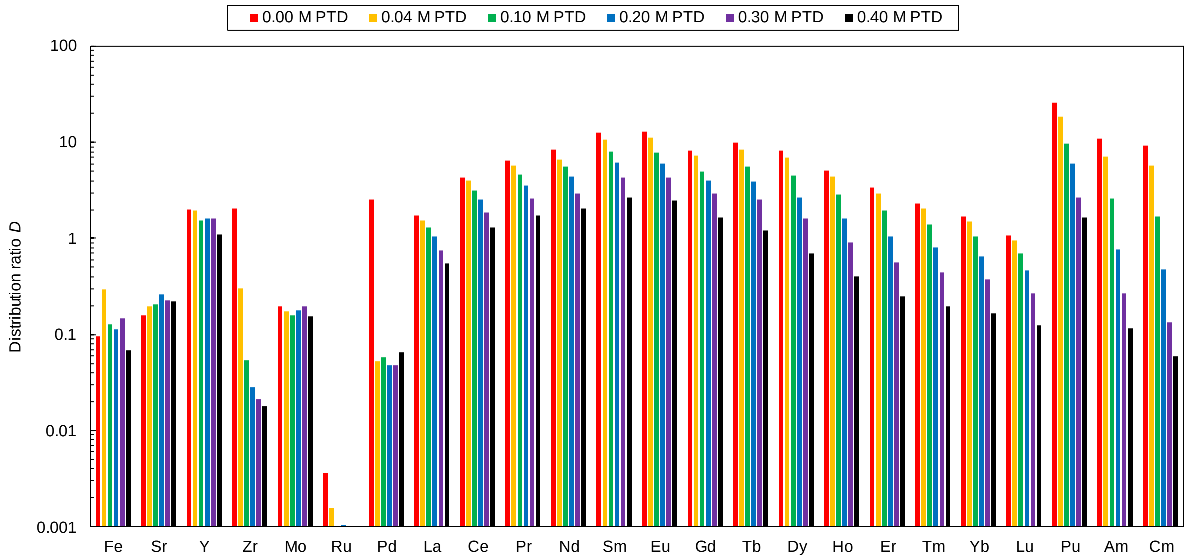

Figure 30. Distribution ratios *D* as a function of the PTD concentration for extraction with 0.4 mol/L *cis*-mTDDGA (Oak Ridge) from 2.1 mol/L HNO_3. Experimental details see Figure 28 caption

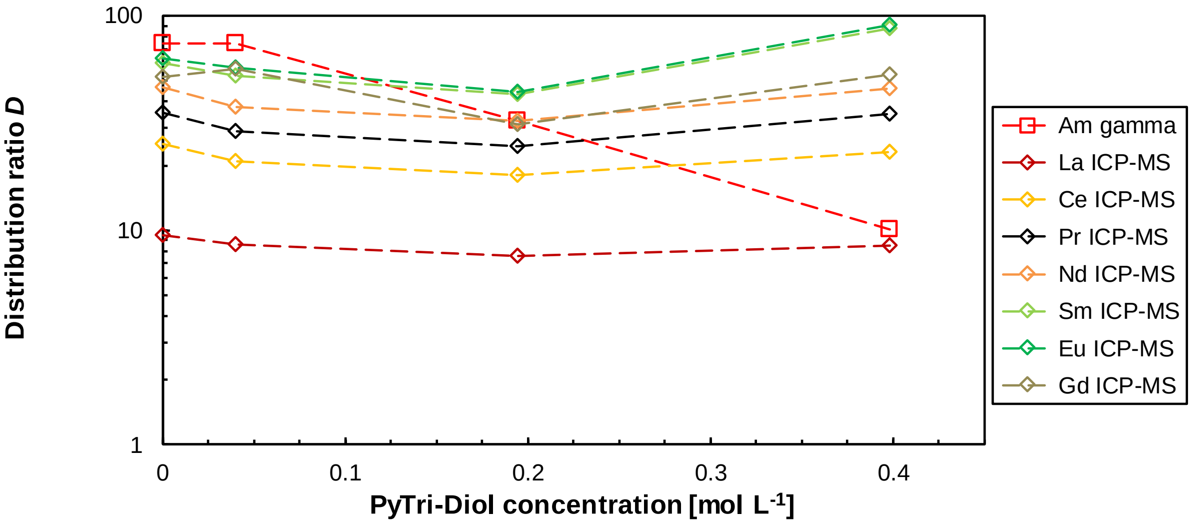

Figure 31. Distribution ratios *D* as a function of the PTD concentration for extraction with 0.4 mol/L *cis*-mTDDGA (Oak Ridge) from 3.7 mol/L HNO_3. Org.: 0.4 mol/L *cis*-mTDDGA (Oak Ridge) in *n*-dodecane. Aq.: 10^{-5} mol/L Ln and FP in 3.7 mol/L HNO_3, spiked with ^{152}Eu, ^{239}Pu, ^{241}Am, and ^{244}Cm. 22°C, 2,220 rpm, 15 min.

Maybe, the use of a stronger extractant will be necessary, e.g. an analogue of TWE-21 with four decyl side chains. This would also reduce the need for the tedious diastereomeric separation. Such a proposed extractant is Me-TDDGA, shown in Figure 32.

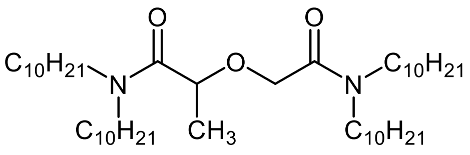

Me-TDDGA

Figure 32. Chemical structure of the proposed new extractant Me-TDDGA.

This project has received funding from the EURATOM research and training programme 2014-2018 under grant agreement No 755171.

EURO-GANEX OPTIMISATION STUDIES – TODGA-DMDOHEMA SYSTEM

M. Carrott, R. Taylor, D. Whittaker, B. Keywood, A. Geist

TECHNETIUM BEHAVIOUR

INTRODUCTION

Technetium is known to be a problematic element to separate in the original EURO-GANEX system as it was previously shown to exhibit high distribution ratios across the nitric acid range [53]. Tc is also a problem element in the PUREX process [18] and here the co-extraction with zirconium, uranium and plutonium is an exacerbating factor. In EURO-GANEX, zirconium extraction is suppressed by the use of CDTA in the primary extract-scrub section and uranium is not present – having been removed in the GANEX-1 cycle [54]. However, plutonium is present at higher concentrations and this may deleteriously impact on the achievable decontamination from technetium. Therefore, new data has been acquired to improve our understanding of Tc behaviour in the EURO-GANEX process.

TECHNETIUM DISTRIBUTION MEASUREMENTS

Batch distribution experiments were carried out to study the extraction of technetium into the EURO-GANEX solvent from HNO_3 in the absence and presence of process level concentrations of Pu. Briefly, a Pu stock solution was concentrated down to ~20 mL of ~250-300 g/L Pu) and analysed by the Ce(IV) method. A 50 g/L Tc-99 stock solution in 1 mol/L nitric acid was diluted in the glovebox to give 10 mL of a working solution containing ~5 g/L Tc-99. Using an in-house capability for Tc-99m generation, the commercially supplied generator was eluted to obtain a Tc-99m stock solution (up to 2GBq) for the batch experiments. Aliquots of this stock solution were taken to give 10 mL of a working solution with a concentration of ~2 MBq/mL. Initial aqueous phases (2 mL) were then prepared for each extraction experiment by mixing aliquots of the working solutions, deionised water and nitric acid solutions to obtain the desired nitric acid (1-10 mol/L), Pu (0-50 g/L) and Tc (up to 250 mg/L) concentrations with Tc-99m tracer (up to 100 kBq/mL) to aid analysis. A solvent of 0.2 mol/L TODGA / 0.5 mol/L DMDOHEMA in odourless kerosene was prepared by standard methods.

A series of small scale batch extraction experiments (<4 mL per vial at an S/A ratio of 1, ambient glove box temperature of ≈22 °C) were then performed to assess the co-extraction of Tc-99 with Pu in the EURO-GANEX system. Aqueous and solvent phases were mixed using a vortex mixer (up to 15 minutes mixing time) followed by settling (with centrifugation in some cases), separation of phases and sampling for analysis by gamma spectroscopy. Acidity determinations used auto-titration of acid-base in a KF media. Selected samples were also submitted for total alpha / alpha spectroscopy.

Figure 33 illustrates the distribution of Tc-99 between aqueous nitric acid and the EURO-GANEX solvent. It is seen that there is good agreement with previous literature data reported in ref. [53] for ≥0.5 mol/L HNO_3. D_{Tc} is above 1 across the full acidity range implying it will be extractable in the process. However, the new data deviate from previous measurements at <0.5 mol/L HNO_3 and start to decrease. In the presence of plutonium it is seen from Figure 34 that there is an increase in D_{Tc} across the acidity range and no sign of a maximum in the data at least for $[HNO_3] \geq 0.5$ mol/L. Some additional data points in the low acidity range are planned to check the trends below this point. The effect of plutonium concentration on D_{Tc} is clearly seen in Figure 35, where D_{Tc} is plotted against initial aqueous plutonium concentration from 2-20 g/L. The increase, which is neatly described by a second order polynomial, is indicative of the co-extraction of Pu and Tc, where it is most likely anionic TcO_4^- replaces a nitrate anion in the extracted complex, as occurs with tributyl phosphate [18]. At no point in any of the batch tests was $D_{Tc} < 1$ implying that technetium will be carried through the EURO-GANEX cycle into the final stage. However, given the maximum in D_{Tc} observed (no Pu present) in Figure 34, further data at <<0.1 mol/L HNO_3, possibly with the aqueous phase TEDGA complexant (or glycolic acid) present, would be useful to see if Tc can be stripped with the lanthanides in the final stripping section.

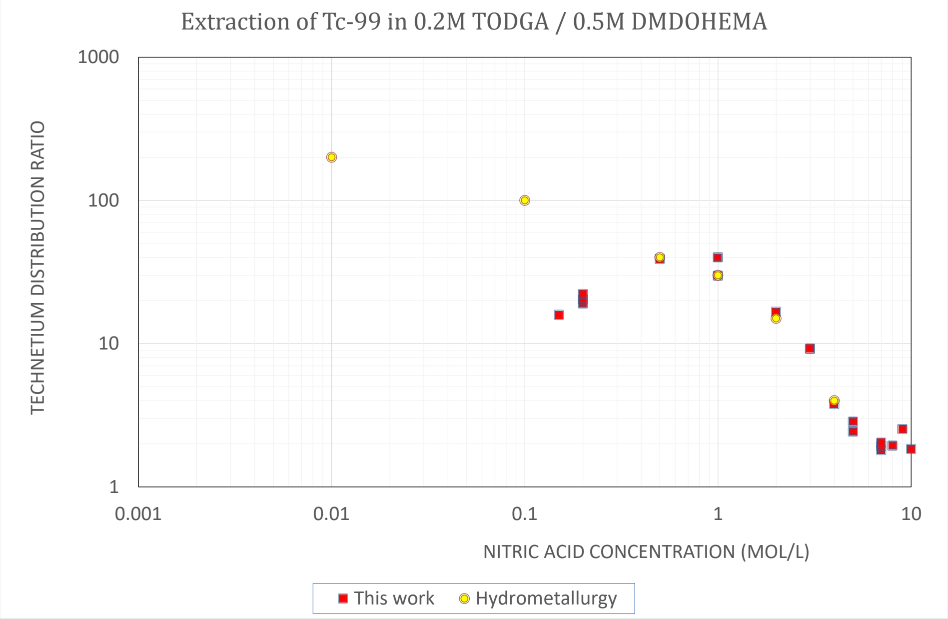

Figure 33: Extraction of technetium into the EURO-GANEX solvent versus initial aqueous nitric acid concentration and comparison with data from ref. [53]

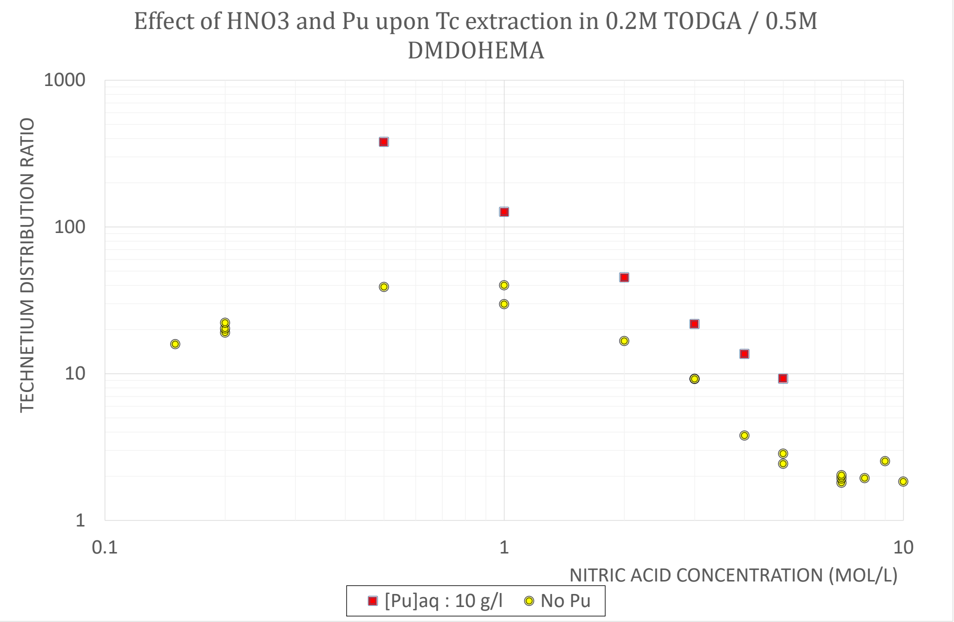

Figure 34: Extraction of technetium into the EURO-GANEX solvent versus initial aqueous nitric acid concentration in the absence and presence of 10 g/L plutonium concentration (initial aqueous concentration)

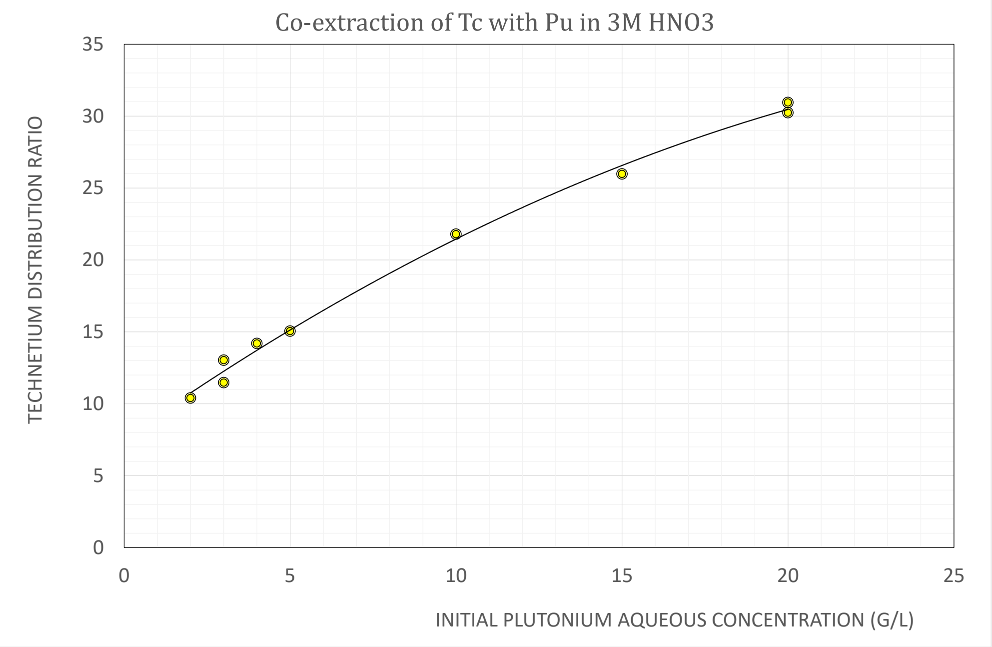

Figure 35: Extraction of technetium into the EURO-GANEX solvent from 3 mol/L nitric acid versus initial aqueous plutonium concentration (line is a 2nd order polynomial fitting)

STUDIES ON PTD FOR PU(IV) AND AM(III) STRIPPING FROM A TODGA/DMDOHEMA SOLVENT

This project has received funding from the EURATOM research and training programme 2014-2018 under grant agreement No 755171. The content of this deliverable reflects only the author's view. The European Commission is not responsible for any use that may be made of the information it contains.

DATA AT TRACE CONCENTRATIONS

PTD was tested as an alternative for the non-CHON SO_3-Ph-BTP to selectively back-extract actinides from a loaded EURO-GANEX organic phase. Organic phases were 0.2 mol/L TODGA and 0.5 mol/L DMDOHEMA in Exxsol D80. Aqueous phases contained 0.04–0.12 mol/L PTD in 0.05–1 mol/L nitric acid. Distribution ratios for Y(III), all Ln(III) (except Pm(III)), Pu(IV) and Am(III) at a PTD concentration of 0.08 mol/L are shown in Figure 36. Distribution ratios for La(III), Ho(III), Pu(IV) and Am(III) at different PTD concentrations are given in Figure 37. Pu(IV) and Am(III) show distribution ratios below one for $[HNO_3]$ > 0.41 – 0.6 mol/L with Pu(IV) having slightly greater distribution ratios than Am(III). Y(III) is extracted for $[HNO_3]$ > 0.06–0.09 mol/L (with increasing PTD concentration). Ln(III) are extracted for $[HNO_3]$ > 0.12–0.2 mol/L (with increasing PTD concentration). Light lanthanides (La, Ce) show the lowest distribution ratios at high $[HNO_3]$; however, at low $[HNO_3]$ the heavy lanthanides (Ho – Lu, with Ho being the lowest) are extracted the least.

With a PTD concentration of 0.08 mol/L, Pu(IV) and Am(III) are separated from Ln(III) with a An/Ln selectivity of 20–100 in a nitric acid concentration range of 0.2–0.5 mol/L. PTD shows promise as a CHON stripping agent for the EURO-GANEX process for selectively stripping actinides from a loaded TODGA/DMDOHEMA solvent thus potentially replacing the undesirable but effective SO_3-Ph-BTP ligand. Further studies involving nominal Pu(IV) concentrations are required to evaluate whether PTD can replace SO_3-Ph-BTP in a EURO-GANEX process.

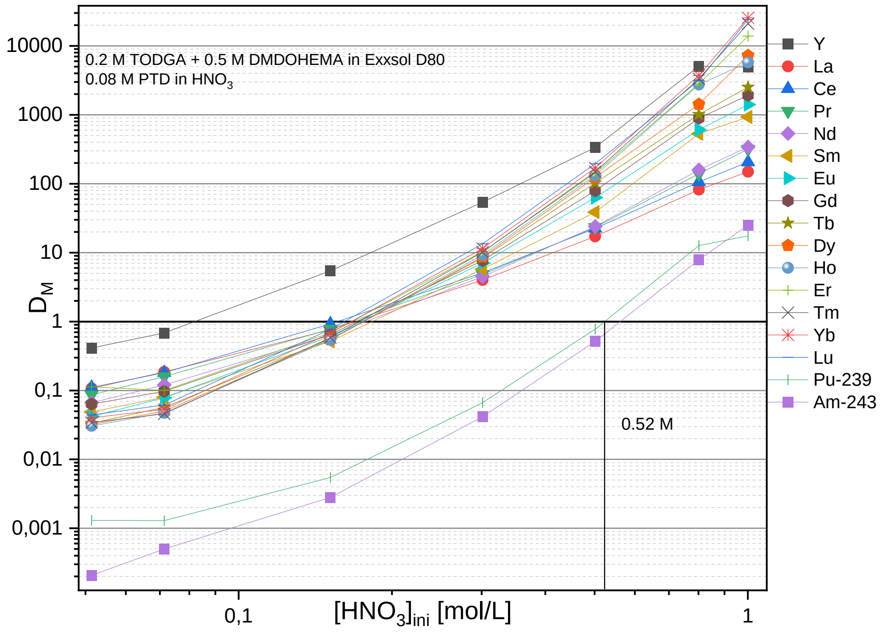

Figure 36. Distribution ratios for Y(III), Ln(III), Pu(IV) and Am(III) in the TODGA/DMDOHEMA/PTD system as a function of the nitric acid concentration. Organic phase, 0.2 mol/L TODGA + 0.5 mol/L DMDOHEMA in Exxsol D80. Aqueous phase, 0.08 mol/L PTD in 0.05 – 1 mol/L HNO_3. A/O = 1, T = 293 K; t = 30 min.

This project has received funding from the EURATOM research and training programme 2014-2018 under grant agreement No 755171. The content of this deliverable reflects only the author’s view. The European Commission is not responsible for any use that may be made of the information it contains.

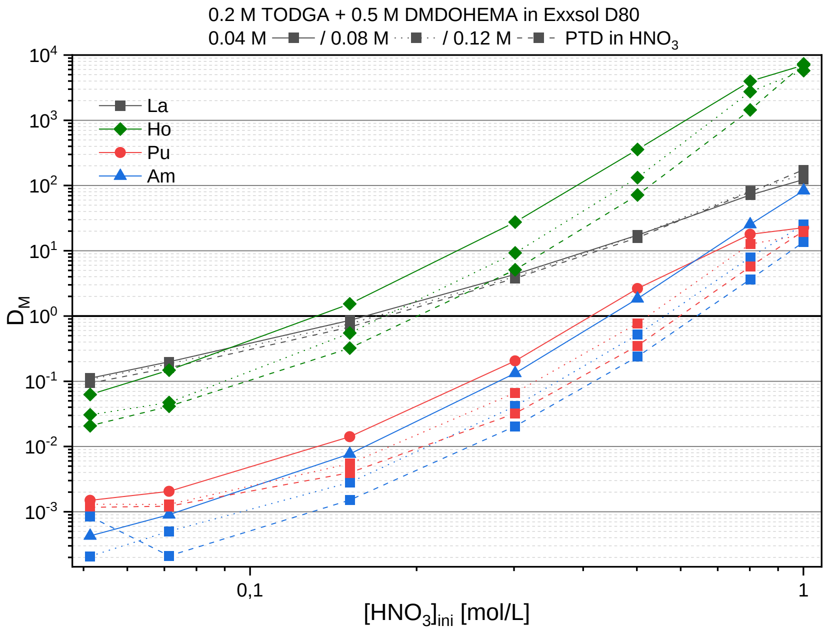

Figure 37. Distribution ratios for La(III), Ho(III), Pu(IV) and Am(III) in the TODGA/DMDOHEMA/PTD system as a function of the nitric acid and PTD concentrations. Organic phase, 0.2 mol/L TODGA + 0.5 mol/L DMDOHEMA in Exxsol D80. Aqueous phase, 0.04–0.12 mol/L PTD in 0.05–1 mol/L HNO_3. *A/O* = 1, *T* = 293 K; *t* = 30 min

FURTHER STRIPPING DATA AT PROCESS CONCENTRATIONS OF PU

Experiments at NNL focused on establishing the efficiency of PTD stripping for key elements under process conditions (realistic concentrations of Pu, similar to past work for the EURO-GANEX development [53]).

Briefly, all stripping experiments were performed using a loaded organic phase prepared by contacting the EURO-GANEX solvent with an equivalent volume of aqueous phase containing Pu in 3.5 mol/L HNO_3 to obtain the desired solvent loading. The Pu loaded solvent was scrubbed 3 times with 0.5 mol/L HNO_3 to reduce the acidity of the organic phase prior to the strip section (as would be the case in flowsheet applications). The aqueous strip solution was prepared by combining aliquots of individual stock solutions of nitric acid, PTD and AHA to achieve the required composition. The Pu loaded solvent was then contacted with aqueous stripping solution at an S/A ratio of 1:1 and temperature of 22 °C for approximately 20 minutes. The phases were then centrifuged to separate them and samples of aqueous and solvent phases were taken, diluted and analysed by gamma spectroscopy to determine Am-241, Eu-152 and Pu-241 in each phase for the calculation of distribution ratios and mass balances. Results are illustrated in Figures 38-41.

As expected, (Figure 38), distribution ratios for Pu, Am and Eu increase with [HNO_3] leading to a corresponding reduction in the SF for Eu/Am at higher acidities. At the lower acidities (0.02 to 0.1 mol/L) it was not possible to measure the low Pu concentration in the organic phase at the count times used (this is being repeated using longer count times). So, at present, it is only possible to state that D_{Pu} at these acidities will be < 0.05. However, whilst Pu stripping is quite effective, at acidities greater than ca. 0.4 mol/L HNO_3 D_{Am} exceeds 1.

With varying PTD concentration (Figure 39) there is very little change in D_{Eu} with increasing [PTD] whilst D_{Am} decreases with increasing [PTD] as expected and there is a corresponding increase in $SF_{Eu/Am}$ with PTD concentration. As this series of experiments was in 0.5 mol/L HNO_3 D_{Am} remained >1 even at 0.1 mol/L PTD. There is also a slight decrease in D_{Pu} with [PTD] which implies some degree of complexation with Pu. Results suggest [PTD] in the range of 0.08M – 0.1M would be suitable for selective stripping of Am with Pu providing the acidity is reduced.

Experiments were also done with varying AHA concentration (Figure 40). Without AHA present it is seen that D_{Pu} was >70, which confirms that AHA is required for stripping of Pu. With increasing AHA concentration there is a corresponding decrease in D_{Pu} as expected. However, there is also a corresponding increase in D_{Am} and a reduction in $SF_{(Eu/Am)}$. Whether this is due to an aqueous phase interaction with Pu and PTD that reduces the concentration available for the stripping of Am or formation of mixed complexes that promote americium extraction is not clear but the effect is that the $SF_{(Eu/Am)}$ drops from ~130 with no AHA present to ~30 with 0.5 mol/L AHA in solution.

From Figure 41, with increasing [Pu] a small increase in D_{Am} is observed that results in a concomitant decrease in $SF_{Eu/Am}$. Again, this seems to imply that there is a degree of Pu complexation with PTD in the aqueous phase that subsequently affects the stripping of Am and separation from lanthanides, i.e. implying that the Pu(IV)-PTD complex is stronger than the Am(III)-PTD complex.

In summary, batch tests have been completed to evaluate use of PTD as a stripping agent for Am (and by analogy Cm) in presence of flowsheet levels of Pu. Results indicate that PTD is suitable, in conjunction with AHA, for selective stripping of Am with Pu and Np and separation from the lanthanides but the operational window is perhaps rather narrow. Although PTD does not appear to be effective in stripping Pu from the organic phase (perhaps due to kinetic constraints), the results suggest that a complex may be formed in the aqueous phase between Pu and PTD which affects the SF for Eu/Am. Measurement of aqueous phase stability constants would be informative in this regard. As expected, the stripping of Am/Pu and selective separation from Ln is sensitive to [HNO_3], [AHA] and [PTD] and based on these initial tests it is proposed that suitable strip conditions for the EURO-GANEX flowsheet using a PTD based strip would be [HNO_3] = 0.1 to 0.2 mol/L; [PTD] = 0.08 to 0.1 mol/L; [AHA] = 1 mol/L. However, results above covering the full lanthanide series suggest that there may be problems with extraction of some lanthanides at these acidities. Neptunium behaviour also needs to be addressed and some of the mass balances were slightly low in the present series of experiments and confirmatory data should be accumulated.

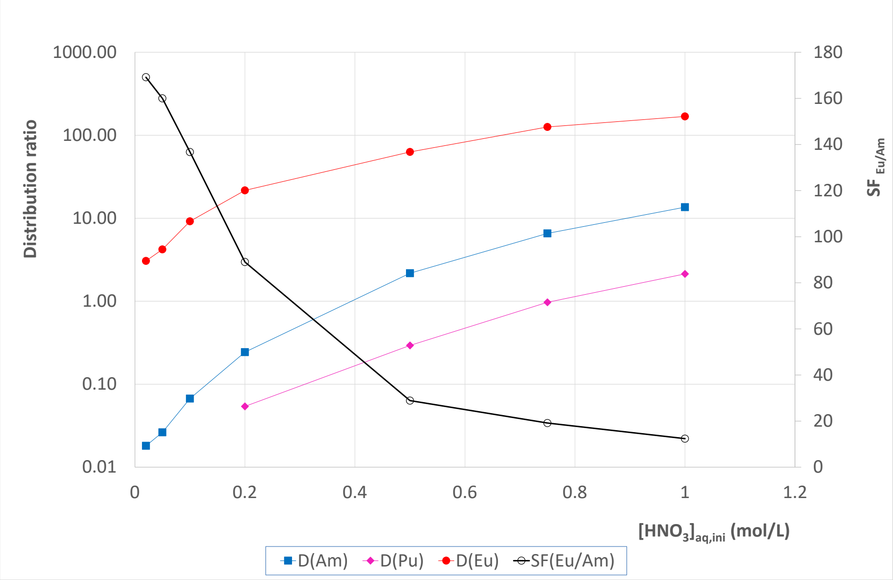

Figure 38: Distribution ratios (Pu, Am, Eu) and separation factor (SF) for europium over americium for PTD stripping from the EURO-GANEX solvent phase : effect of HNO_3 ([Pu] = 10 g/L, [PTD] = 0.08 mol/L, [AHA] = 1 mol/L)

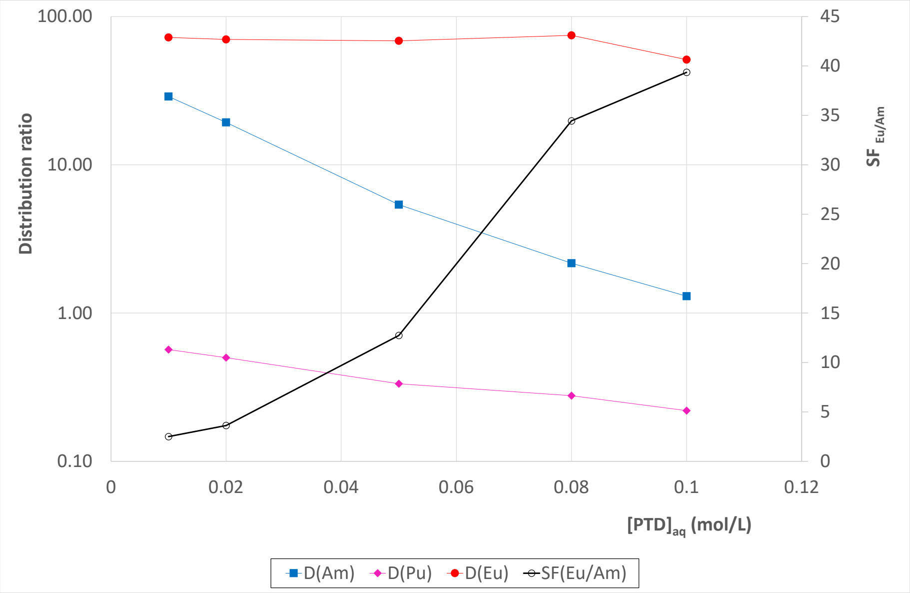

Figure 39: Distribution ratios (Pu, Am, Eu) and separation factor (SF) for europium over americium for PTD stripping from the EURO-GANEX solvent phase : effect of PTD ([Pu] = 10 g/L, $[HNO_3]$ = 0.5 mol/L, [AHA] = 1 mol/L)

This project has received funding from the EURATOM research and training programme 2014-2018 under grant agreement No 755171. The content of this deliverable reflects only the author’s view. The European Commission is not responsible for any use that may be made of the information it contains.

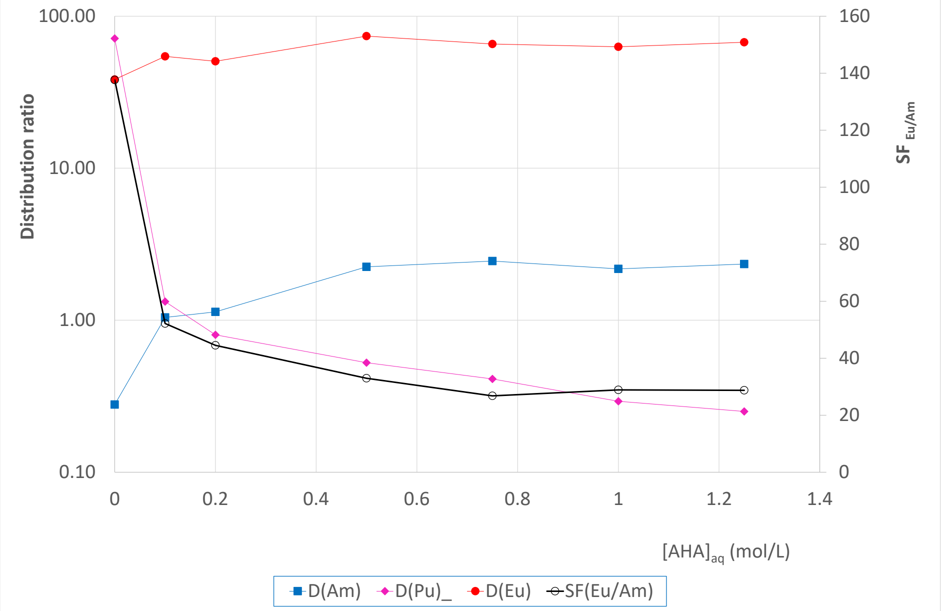

Figure 40: Distribution ratios (Pu, Am, Eu) and separation factor (SF) for europium over americium for PTD stripping from the EURO-GANEX solvent phase : effect of AHA ([Pu] = 10 g/L, [HNO_3] = 0.5 mol/L, [PTD] = 0.08 mol/L)

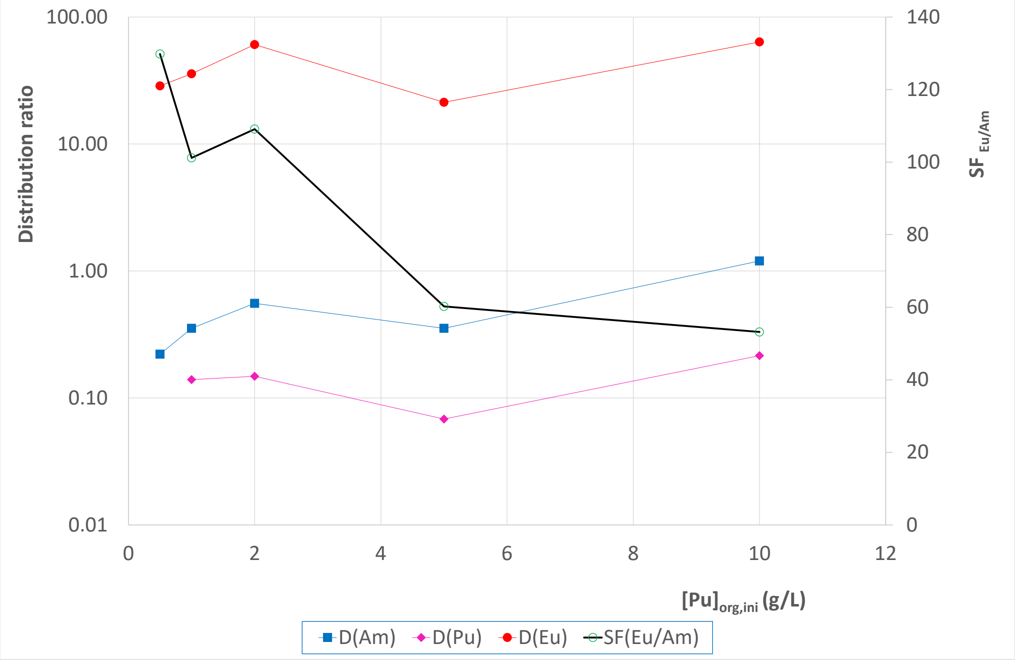

Figure 41: Distribution ratios (Pu, Am, Eu) and separation factor (SF) for europium over americium for PTD stripping from the EURO-GANEX solvent phase : effect of [Pu] ([AHA] = 1 mol/L, [HNO_3] = 0.5 mol/L, [PTD] = 0.08 mol/L)

This project has received funding from the EURATOM research and training programme 2014-2018 under grant agreement No 755171. The content of this deliverable reflects only the author's view. The European Commission is not responsible for any use that may be made of the information it contains.

CHALMEX OPTIMISATION STUDIES

Thea Lyseid Authen, Christian Ekberg, Andreas Wilden, Giuseppe Modolo

As a second potential candidate for a new GANEX process, the CHALMEX FS-13 process was studied in collaboration with CHALMERS. The process uses a mixture of $CyMe_4BTBP$ and TBP in the diluent FS-13. The chemical structures are shown in Figure 42.

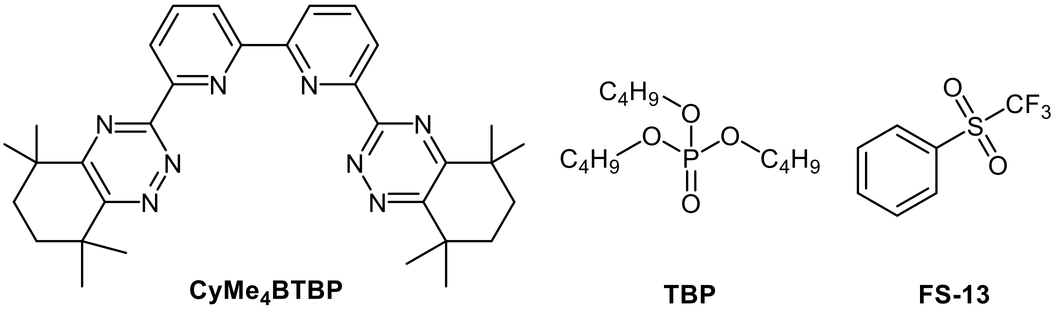

Figure 42. Chemical structures of $CyMe_4BTBP$, TBP, and FS-13 used as solvent in the CHALMEX FS-13 process

SOLVENT OPTIMISATION

INTRODUCTION

Batch test optimisation studies of solvent composition and process flexibility of the CHALMEX FS-13 solvent were studied. The results were published in Solvent Extr. Ion Exch. journal[84]. The abstract from this paper is cited below:

> *“Studies have been performed with the purpose of determining the optimal solvent composition of a Chalmers grouped actinide extraction (CHALMEX) solvent for the selective coextraction of transuranic elements in a novel Grouped ActiNide EXtraction (GANEX) process. The solvent is composed of 6,6’-bis(5,5,8,8-tetramethyl-5,6,7,8-tetrahydro-benzo-[1,2,4]-triazin-3-yl)-[2,2’]-bipyridine (CyMe*$_4$*-BTBP) and tri-n-butyl phosphate (TBP) in phenyl trifluoromethyl sulfone (FS-13). The performance of the system has been shown to significantly depend on the ratios of the two extracting agents and the diluent to one another. Furthermore, the performance of the determined optimal solvent (10 mM CyMe*$_4$*-BTBP in 30% v/v TBP and 70% v/v FS-13) on various simulated PUREX raffinate solutions was tested. It was found that the solvent extracts all transuranic elements with high efficiency and good selectivity with regard to most other elements (fission products/activation products) present in the simulated PUREX raffinate solutions. Moreover, the solvent was found to extract a significant amount of acid. Palladium, silver, and cadmium were co-extracted along with the TRU-radionuclides, which has also been observed in other similar CHALMEX systems. The extraction of plutonium and uranium was preserved for all tested simulated PUREX raffinate solutions compared to experiments using trace amounts.”*

VARYING EXTRACTANT CONCENTRATIONS

The extraction of plutonium and the MA have been studied as a function of extractant concentrations and the results for varying TBP volume fraction is presented in Figure 43. The range of TBP ratios correspond to concentrations 0 M to 1.79 M. It is seen that the extraction of americium, plutonium and europium all increase with increasing TBP fractions. As both Am and Eu are extracted by CyMe$_4$-BTBP and not TBP, this is believed to be due to an increasing solubility of the Am/Eu complexes in the TBP/FS-13 mixture. Increasing the TBP ratio of the solvent decreases the overall charge density of the solvent, which has been reported to increase the solubility of Am/Eu-CyMe$_4$-BTBP complexes [129].

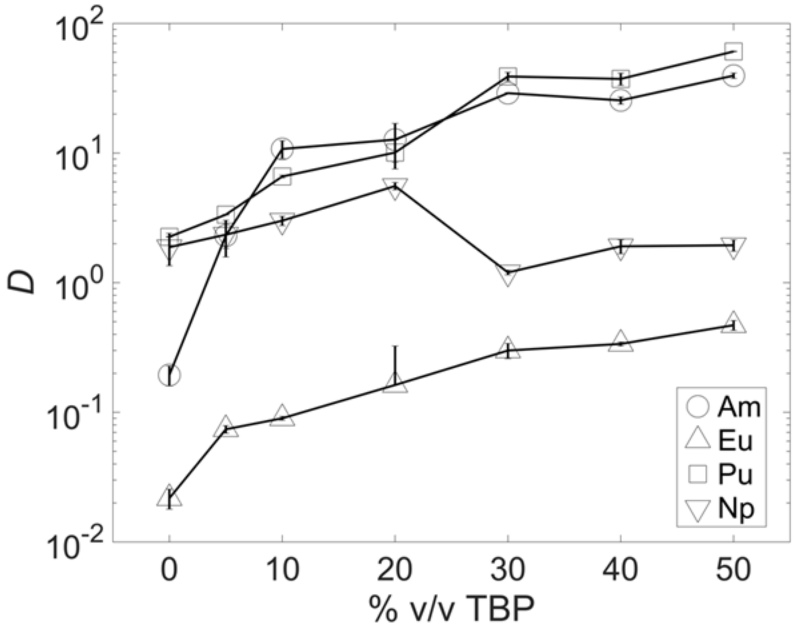

Figure 43. The extraction of Am, Eu, Pu and Np as a function of %v/v TBP content in the solvent. The aqueous phase was 4M HNO3 spiked with the radionuclides (note that Figures 43-50 are redrawn from references [84, 85])

Np(V,VI) did not show a clear trend as a function of the TBP ratio in the solvent, with increasing D-values until 20% v/v TBP after which a significant drop in D-value is observed. This is in contrary to what would be expected from PUREX chemistry. The drop in D-value is believed to be due to a change in neptunium oxidation state as it is known that the pentavalent oxidation state is less extractable by TBP compared to the tetra- and hexavalent oxidation states. Both the P=O group on TBP and TBP's by- and degradation products are known reducing agents and could be responsible for a reduction of Np(VI) to Np(V).

The actinide and europium extraction as a function of CyMe$_4$-BTBP concentration in different TBP/FS-13 ratios was investigated, as presented in Figure 44. In all systems, an increase in CyMe$_4$-BTBP concentration resulted in higher D-values for all investigated radiotracers. At increasing TBP concentrations, however, the D(Eu) value surpasses that of D(Np) at lower CyMe$_4$-BTBP concentrations. A slope analysis for the TBP extraction was performed for the distribution data as seen in Table 9, by plotting the log(D) vs the logarithm of the extractant concentration. The slope analysis was performed in the low extractant concentration region to gain the most accurate results.

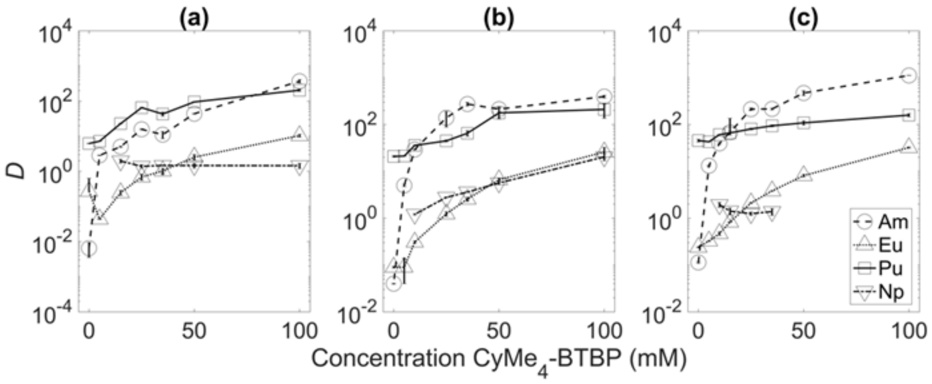

Figure 44. Distribution ratios for Pu, Np, Am and Eu as a function of the CyMe$_4$-BTBP concentration in (a) 15% v/v TBP and 85% v/v FS-13; (b) 30% v/v TBP and 70% v/v FS-13 and 50% v/v TBP and 50% v/v FS-13. The aqueous phase was 4 mol/L HNO_3 with added radiotracers (note that Figures 43-50 are redrawn from references [84, 85])

In the PUREX process, TBP is known to extract plutonium in a 2:1 complex. In the CHALMEX system, however, a lower slope of 1.27 was found, suggesting a 1:1 complex. This may suggest a parallel adduct formation with nitric acid, as reported by Ochkin et al. [130]. A 1:1 complex is also formed between TBP and americium, and that between TBP and europium, which agrees with earlier published results by our group [131]. The slope of 0.62 for Np extraction by TBP suggests a predominant oxidation state of +5, which is the least extractable by TBP.

Table 9. The slope for americium, europium, plutonium and neptunium extracted by 10 mM CyMe$_4$-BTBP and varying ratios of TBP/FS-13 from nitric acid media [84, 85]

	Am	Eu	Pu	Np
Slope (TBP)	1.12	0.83	1.27	0.62

Slope analysis for the extraction of actinides by CyMe$_4$-BTBP has earlier been published by our group for systems with 30% v/v TBP [86]. We showed that americium, curium, and europium are all extracted as 2:1 complexes with CyMe$_4$-BTBP, while plutonium is extracted as a 1:1 complex. Here, we see that in systems with lower TBP fractions (15% v/v), the same complex formation is seen with slopes of 2.20, 1.82, and 1.08 for americium, europium, and plutonium, respectively (Table 10). At 50% v/v TBP, however, a decrease in CyMe$_4$-BTBP:TBP ratio is seen for americium, europium, and plutonium, with slopes of 1.49, 1.59, and 0.42 respectively. This can be explained by the higher concentration of TBP, which also extracts these elements. However, it is more likely that the reduced slope is due to the complete extraction of the radiotracers at such high concentrations. In contrast to earlier reported neptunium trends, neptunium is found to be independent of the CyMe$_4$-BTBP concentration here, once again suggesting either Np(IV) or Np(VI) as the main oxidation state.

Table 10. The slope for americium, europium, plutonium and neptunium extracted by varying concentrations of CyMe4-BTBP with either 15% v/v TBP or 50% v/v TBP.

	Am	Eu	Pu	Np
Slope (15% v/v TBP)	2.20	1.82	1.08	-0.13
Slope (50% v/v TBP)	1.49	1.59	0.42	-0.09

NITRIC ACID DEPENDENCY AND EXTRACTION

The CHALMEX FS-13 solvent is dependent on acid extraction as it increases the CyMe$_4$-BTBP solubility in FS-13 [87]. This effect is possibly due to protonation of the CyMe$_4$-BTBP. This is beneficial for the dissolution of CyMe$_4$-BTBP due to the polar nature of the diluent. The distribution ratios of the actinides and europium as a function of acid concentration are shown in Figure 45. The minor actinide extraction is found to increase with the nitric acid concentration, up to 2.5 mol/L HNO_3. This is most likely due to two factors: the increased solubility of CyMe$_4$-BTBP in the organic phase and the increased nitrate concentration in the aqueous phase.

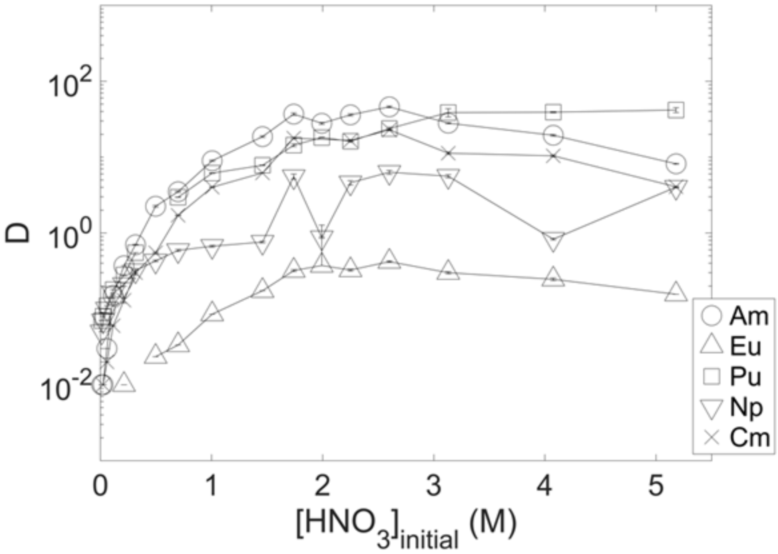

Figure 45. The distribution ratios of plutonium and the minor actinides as a function of nitric acid concentration (note that Figures 43-50 are redrawn from references [84, 85])

The americium distribution ratio presented in Figure 45 increases up to 2.5 mol/L HNO_3, and at subsequently higher acid concentrations, the americium distribution ratio decreases. This suggests that the americium extraction is in competition with acid extraction. Competition with other metals is unlikely as all elements were only present in trace concentrations (10^{-5} mol/L). Curium, having the same electro-negativity as americium, shows the same distribution ratio trend as americium.

Europium extraction also shows similar trends to americium, although its distribution ratio never passes 0.4 in value. The remaining lanthanides were excluded from the results, as the distribution ratios were below 0.01 at all nitric acid concentrations. This agrees with the extraction trends reported by Geist et al. [44] that europium, of all the lanthanides, is the most extracted by CyMe$_4$-BTBP. Neptunium distribution ratios show a less conclusive trend as a function of initial acid concentration compared to americium and curium. This is believed to be due to the speciation of the different neptunium stock solutions used in the experiments. Due to availability, two different neptunium stock solutions were used to determine the dependency of neptunium extraction on acid concentration. The speciation of both stock solutions was controlled and found to be Np(V) by UV-VIS spectrometry, but the clear increase in distribution ratio for the second Np stock solution is believed to be due to the presence of Np(VI). Np(VI) is highly extractable by TBP, which is clearly seen in Figure 45 [67]. Furthermore, neptunium redox chemistry is highly complex and is affected by many factors. The nitric acid concentration plays a significant role, but so does the absorbed dose of the solutions, and various radiolysis products and radicals formed during spent nuclear fuel reprocessing. The speciation of neptunium is therefore very challenging to control in a process [132, 133].

Fission product extraction as a function of nitric acid concentration was investigated to establish an understanding of the extraction mechanism. All relevant elements (fission, corrosion and activation products) were included in the experiments, but only the results for elements of concern are shown in Figure 46. As can be seen above 0.5 mol/L HNO_3, the distribution ratios increase for all investigated elements at higher nitric acid concentrations except for silver which has a consistent D-value> 100. This is probably due to the higher availability of NO_3^- for complex formation. At nitric acid concentrations below 0.5 mol/L HNO_3, the D-values of all elements except Ag are very low, probably due to the low solubility of CyMe$_4$-BTBP.

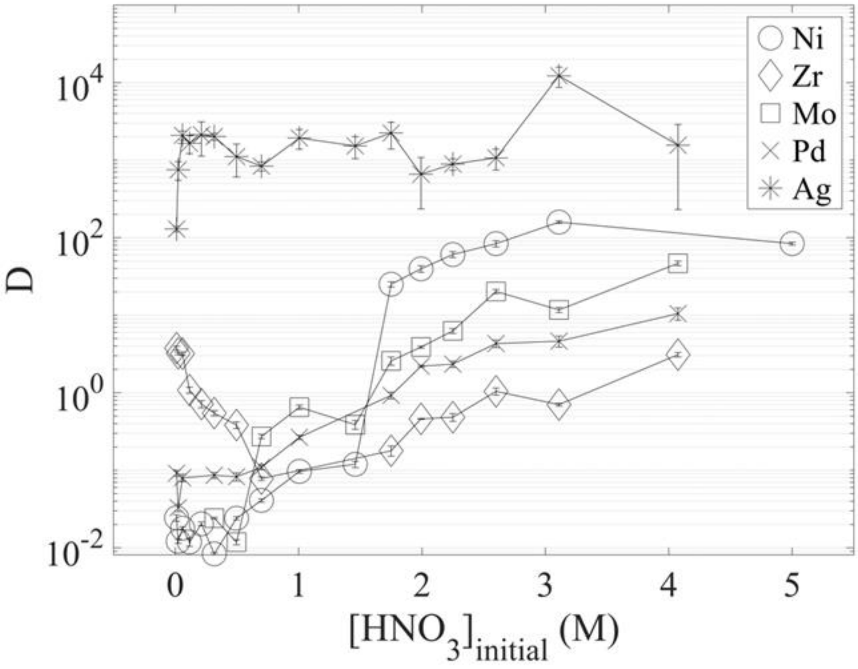

Figure 46: The distribution ratios of selected fission products as a function of nitric acid concentration (note that Figures 43-50 are redrawn from references [84, 85])

It is acknowledged by a range of studies that TBP extracts a significant amount of acid [17, 130, 134-136]. Acid is also extracted to a significant degree by the CHALMEX solvent, as seen in Figure 47. Although acid extraction by CyMe$_4$-BTBP is not unlikely due to its four N-donors, the concentration of the extractant in the CHALMEX solvent 10 mmol/L) suggests that the main extraction is rather due to extraction by the TBP molecule. It is also seen that the solvent extraction becomes saturated by HNO_3 at an acid concentration of 4 mol/L.

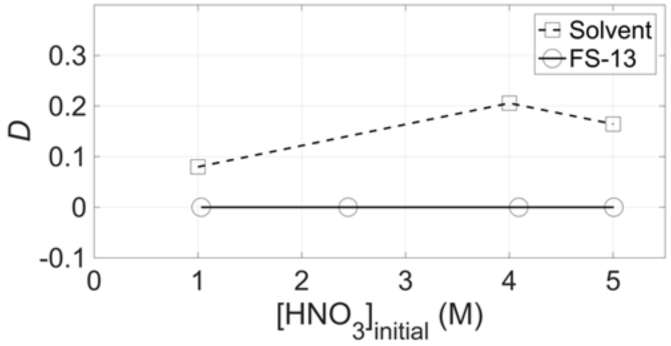

Figure 47: The distribution ratio (D) of HNO_3 extraction by pre-equilibrated CHALMEX solvent as a function of initial nitric acid concentration (note that Figures 43-50 are redrawn from references [84, 85])

FLOWSHEET DEVELOPMENT

INTRODUCTION

A flowsheet for a promising solvent composition for the CHALMEX FS-13 process was developed and tested in batch mode. The results were published in Solvent Extr. Ion Exch. journal [85]. The abstract from this paper is cited below:

> *"The Chalmers grouped actinide extraction (CHALMEX) process is focused on the co-separation of actinides from all other elements in spent nuclear fuel solution, with the ultimate purpose of transmuting the actinides into shorter-lived and less radiotoxic elements. Based on solvent extraction equilibrium distribution data of actinides and fission products, a preliminary flowsheet was developed and tested in batch mode. The flowsheet consists of one extraction step with the CHALMEX FS-13 solvent (25 mM CyMe$_4$-BTBP in 30% v/v TBP and 70% v/v FS-13), using hydrophilic masking agents (20 mM bimet and 0.2 M mannitol) in the aqueous phase for the complexation of troublesome fission products. Two nitric acid scrub steps (0.5 M HNO_3) were efficient in removing co-extracted acid, all molybdenum and the majority of silver. Two stripping stages (0.5 M glycolic acid at pH 4) were efficient in recovery of the actinides from the organic phase. The need for a solvent clean-up stage for the removal of nickel, cadmium, iron and the remaining silver from the organic phase was demonstrated. Based on the distribution data, it was calculated that a 99.9% recovery of americium is possible using only 3 ideal extraction stages, 3 ideal scrubbing stages and 2 ideal stripping stages."*

BATCH MODE FLOWSHEET RESULTS

A batch flowsheet test was performed using 1 extraction stage, 2 scrubbing stages and 2 stripping stages. In the extraction stage, the solvent (25 mmol/L CyMe$_4$-BTBP, 30% v/v TBP and 70% v/v FS-13) was contacted with a simulated PUREX raffinate with added actinide and europium radiotracers. The aqueous phase also contained bimet and mannitol as masking agents to prevent co-extraction of fission products. The scrubbing solution was 0.5 mol/L HNO_3 and the stripping solution 0.5 mol/L glycolic acid ($C_2H_3O_4$) adjusted to pH using NaOH.

Overall, the distribution ratios for the actinides remained high during both the extraction stage and the scrubbing stages, as seen in Figure 48. The stripping stages were also very efficient in back-extracting the actinides with D-values < 0.1 for all of them. The most concerning aspect of the flowsheet was the low D-values of Np in the scrubbing stages causing a significant loss. This was unexpected as literature shows that in 0.5 mol/L HNO_3, Np exists with mole fractions above 0.65 for Np(VI) and less than 0.35 for Np(V) [137]. Both Np(IV) and Np(VI) have been shown to remain in the organic phase during such scrubbing conditions in similar systems, while Np(V) is readily back-extracted and has low distribution ratios at low acid concentrations [34, 76].

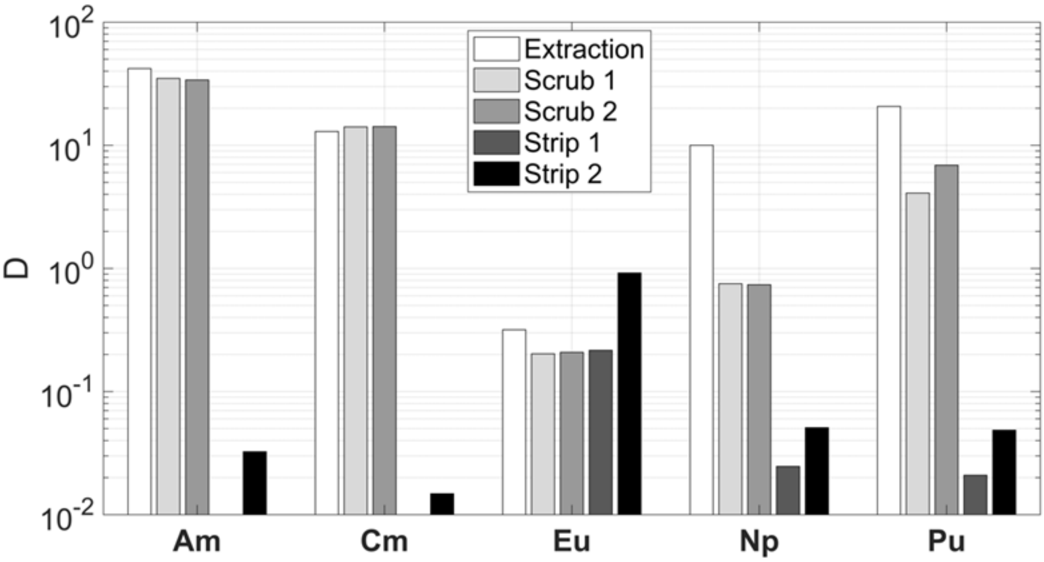

Figure 48. The D-values of the actinides and europium for the different process stages in the batch flowsheet test (note that Figures 43-50 are redrawn from references [84, 85])

Although several fission products were extracted with D>0.1, it can be seen from Table 11 that the fission products that were not scrubbed by 0.5 mol/L HNO_3 remained in the organic phase also after the stripping stages. This means that a good actinide/fission product separation is achieved in the CHALMEX process.

Table 11. The distribution ratios for all fission products with D>0.1 and the titrated pH of each process stage after contacting.

Process stage	pH	Fe	Ni	Cu	Mo	Ag	Cd	Sn
Extraction	-0.5	0.1	>100	1.0	2.2	0.2	41.8	0.2
Scrub 1	0.2	24	13	0.84	0.004	0.5	23.6	0.3
Scrub 2	0.3	52	>100	1.0	0.3	0.5	15.5	0.4
Strip 1	0.4	29	94	9.0	5.9	2.0	>100	7.6

Strip 2	0.8	42	4.1	1.9	>100	0.8	>100	3.1

Calculations on ideal numbers of stages were based on the distribution data in the batch flowsheet test. The calculations were based on a counter current contacting scheme, and the results were promising with 3 extraction stages, 3 scrubbing stages and 1 stripping stage a 99.9% recovery of americium is possible, as illustrated in Figure 49. As previously mentioned, there was also a very low degree of contamination.

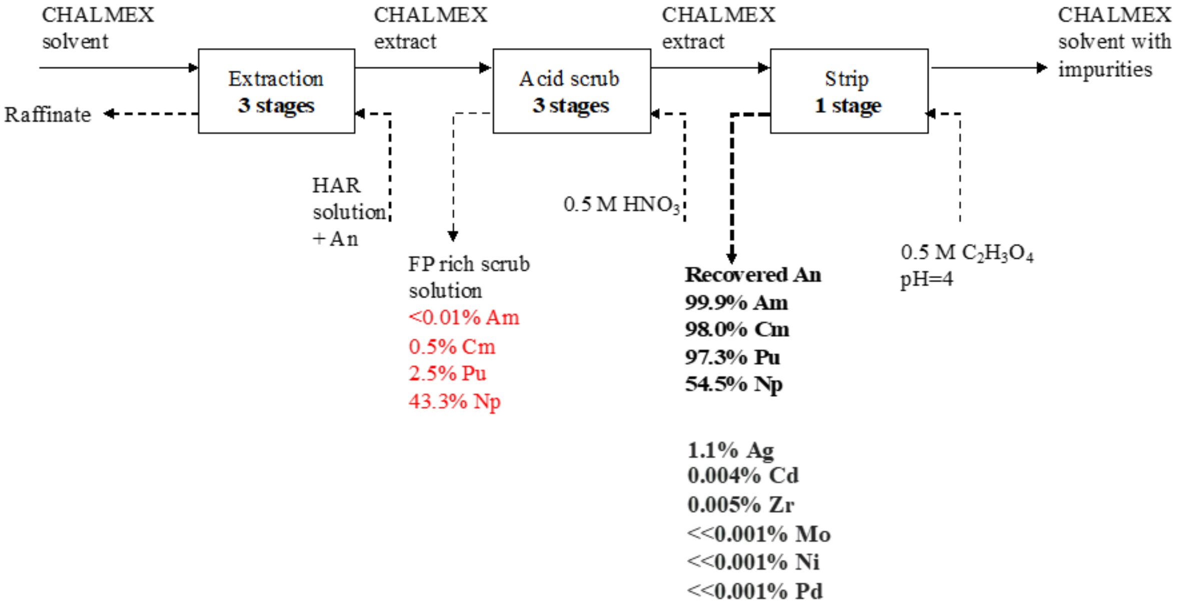

Figure 49. A process flow diagram for the CHALMEX process, calculated based on batch distribution data and a counter-current contacting scheme. The illustration shows the %recovered actinides and losses to the scrubbing solution, as well as fission product impurities for the recovered actinide stream (note that Figures 43-50 are redrawn from references [84, 85])

SINGLE CENTRIFUGAL CONTACTOR TEST OF THE CHALMEX FS-13 PROCESS

Earlier cyclohexanone-based diluents for the CHALMEX process were abandoned for, amongst other reasons, phase separation issues in centrifugal contactors. A single centrifugal contactor test of the current FS-13 solvent was performed to evaluate the new diluent performance under more process like conditions and to assess the suitability of this type of contactor for the scaled-up operation of the CHALMEX process.

Tests on the first CHALMEX solvent, in which cyclohexanone was used as a diluent, reported phase separation issues due to the similar densities of the loaded organic phase and the aqueous phase [138]. Unsurprisingly, lower flow rates yielded higher distribution ratios as seen in Figure 50. The distribution ratios for Am and Cm were also low (D<1), due to the low concentration of CyMe$_4$-BTBP (10 mmol/L) and the high concentration of metal in the aqueous phase. The elements extracted by the kinetically faster TBP (Np, U and Pu) showed D>1 for all flow rates. In contrast to the earlier cyclohexanone-solvent, no phase separation issues were observed, neither was loading of the solvent by iron.

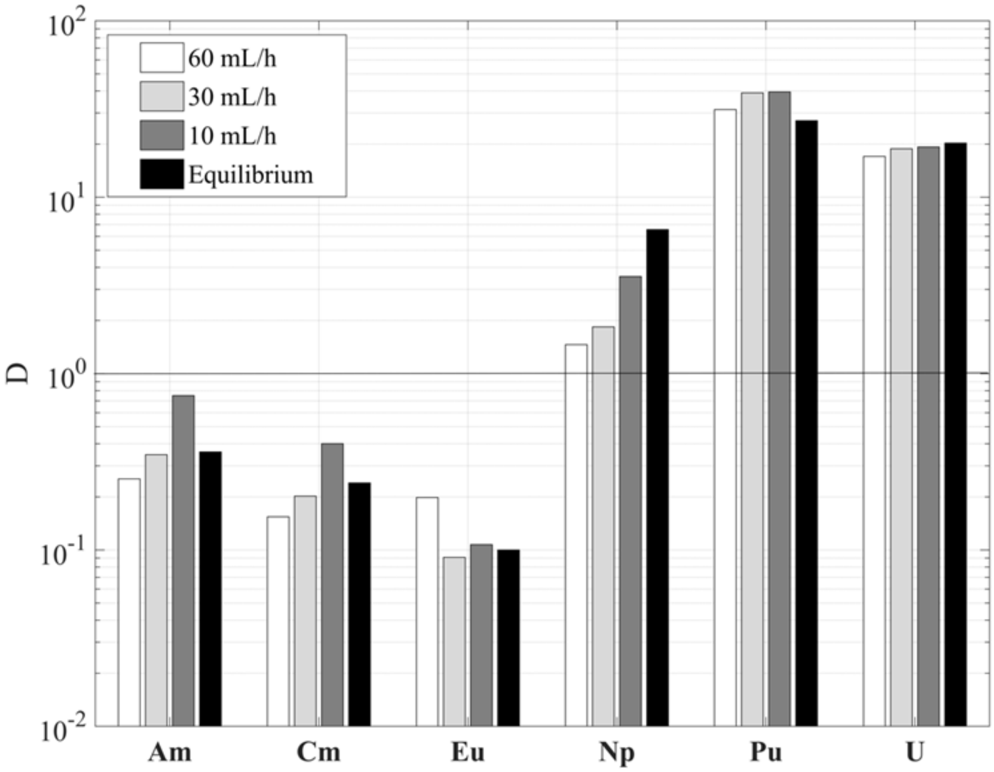

Figure 50. The D-values of the actinides extracted by 10 mmol/L CyMe$_4$-BTBP in 30% v/v TBP in 70% v/v FS-13 in a single centrifugal contactor operated at different speeds, extracting from a simulated PUREX process raffinate (note that Figures 43-50 are redrawn from references [84, 85])

CONCLUSIONS AND OUTLOOK

Substantial progress has been made in analysing the potential improvements for the EURO-GANEX process that were identified at the start of the GENIORS project, namely:

- Replacing the two-component organic phase with a single extractant – mTDDGA (in an aliphatic diluent), and
- Replacing the aqueous phase ligand SO_3-Ph-BTP with CHON-compliant PTD

Work to date suggests that:

- At process acidities mTDDGA shows good D_{An} and D_{Ln} suitable for co-extraction with no obvious kinetic problems. Extraction of trivalent ions is primarily via the *cis* isomer but Pu(IV) extraction showed little difference between *cis* and *trans* isomers. Fission product decontamination appears promising with D_{Ru}<0.01 and $D_{Fe,Sr\&Mo}$ <1 whilst Zr, Pd extractions are still likely to be suppressed by CDTA. Pu loading capacities are good for ≥2 mol/L HNO_3 (>50 g/L Pu for 0.5 mol/L mTDDGA) but appeared to be very low at 1 mol/L HNO_3. Selective stripping of actinides from lanthanides also appeared to be rather ineffective with mTDDGA as the organic phase. Further data are needed on (i) Pu loading at low acidity and (ii) PTD stripping as these issues may rule out the application of mTDDGA in the EURO-GANEX process.
- In the standard EURO-GANEX system, PTD appears to have potential to replace the sulphonated BTP ligand although there is perhaps quite a small operating window ([HNO_3], [PTD]) in which it will be effective. Further data are needed at process level concentrations of actinides/lanthanides but it appears PTD can be quite confidently now carried forward into flowsheet testing.

In addition, further data were accumulated on Tc behaviour in the present EURO-GANEX system in the absence and presence of process level concentrations of Pu. These data confirmed it would be difficult to strip Tc (D>1) at any acidity in the presence of Pu (there is significant co-extraction) or even at high acidity (in the absence of Pu). However, in a departure from previous data, D_{Tc} appeared to fall below 0.5 mol/L HNO_3 which suggests Tc will be carried through the process up to the final lanthanide strip section where it may be possible to backwash Tc with the lanthanides. Further studies are needed to confirm the co-stripping of Tc with lanthanides at very low acidity.

Significant progress has also been made to demonstrate the CHALMEX concept for the GANEX-2 cycle. In particular, the replacement of the diluent with FS-13 diluent has been shown to be very effective in many respects. Single stage contactor tests have been completed and a pseudo-flowsheet test using sequential batch-wise extractions has been carried out. Calculations suggest that CHALMEX should be effective at actinide recoveries with a small number of stages. The recent work makes a significant step forward towards the prospects of flowsheet design and testing of the CHALMEX concept in counter-current centrifugal contactor cascades.

REFERENCES

Uncategorized References

[1] Management of spent nuclear fuel and its waste, The European Academies' Science Advisory Council (EASAC), Brussels, 2014, pp. 1-40.

[2] Eurostat Electricity production, consumption and market overview, in.

[3] World Nuclear Association Nuclear Power in the European Union, in.

[4] Inventory of radioactive waste and spent fuel present in the Community's territory and the future prospect, 2019.

[5] Electricity generation statistics - first results, 2020.

[6] Nuclear Technology Review, 2019, GC(63)/INF/2, International Atomic Energy Agency, Vienna, 2019, pp. 1-49.

[7] G.V.d. Eynde, S. Pedoux, R. Trtilek, L. Fritz, C. Evans, G. Mathonnière, J.V.d. Werf, P. Lucibello, K. Suzuki, T. Sano, S. Takeda, H.-o. Nam, A. Khasperskaya, T. Rakitskaya, E. Zhurbenko, B. Dixon, W. McCaughey, A. Gonzalez-Espartero, S.B.y. León, D. Henderson, W.I. Ko, H. Goto, Strategies and Considerations for the Back End of the Fuel Cycle, NEA 7469, OECD-NEA, 2021, pp. 1-72.

[8] M. Kazimi, E.J. Moniz, C.W. Forsberg, S. ansolabehere, J.M. deutch, M.J. driscoll, M.W. Golay, A.c. Kadak, J.e. Parsons, M. regalbuto, G. apostolakis, P. hejzlar, E. Shwageraus, The Future of the Nuclear Fuel Cycle: An Interdisciplinary MIT Study, ISBN 978-0-9828008-4-3, Massachusetts Institute of Technology, Cambridge, USA, 2011, pp. 1-258.

[9] E.D. Collins, G.D. DelCul, B.B. Spencer, R.T. Jubin, C. Maher, I.-T. Kim, H. Lee, Y.S. Fedorov, V.F. Saprykin, V.I. Beznosyuk, A.B. Kolyadin, P. Baron, M. Miguirditchian, C. Sorel, Y. Morita, R. Taylor, A. Khaperskaya, C. Hill, R. Malmbeck, J. Law, G. de Angelis, L. Boucher, X. Xeres, E. Mendes, T. Inoue, J.P. Glatz, M. Kormilitsyn, J. Uhlíř, V. Ignatiev, J. Serp, S. Delpech, State-of-the-art report on the progress of nuclear fuel cycle chemistry, NEA No, 7267, OECD-NEA, Paris, France, 2018, pp. 1-300.

[10] C. Behar, Energy for the future: Generation IV fast reactors and the closed fuel cycle, Nuclear Future, 10 (2014) 23-25.

[11] C. Poinssot, S. Bourg, N. Ouvrier, N. Combernoux, C. Rostaing, M. Vargas-Gonzalez, J. Bruno, Assessment of the environmental footprint of nuclear energy systems. Comparison between closed and open fuel cycles, Energy, 69 (2014) 199-211.

[12] R. Wigeland, T. Taiwo, H. Ludewig, M. Todosow, W. Halsey, J. Gehin, R. Jubin, J. Buelt, S. Stockinger, N.K. Jenni, B. Oakley, Nuclear Fuel Cycle Evaluation and Screening – Final Report FCRD-FCO-2014-000106, INL/EXT-14-31465 Fuel Cycle Research and Development, United States Department of Energy, Idaho National Laboratory, 2014, pp. 1-51.

[13] P.K. Dey, M. Giroux, A. Khaperskaya, J. Laidler, A. Machiels, M. Masson, F. Storrer, G. Uchiyama, Participants, S. Bakhtyar, A. Bohe, A. Bychkov, O. Godun, T. Inoue, D. Jackson, I.H. Jung, L. Koch, V. Kormilitsyn, J. Law, M. Maurin, C. Ospina-Esperon, A. Osipenko, X. Sheng, R. Tulackova, Spent Fuel Reprocessing Options, IAEA-TECDOC-1587, International Atomic Energy Agency, Vienna, 2008, pp. 1-151.

[14] Orano La Hague, on the cutting edge of used fuel recycling, Orano.

[15] J. Benedicic, Life without reprocessing – the end of an era, Nuclear Future, 13 (2017) 34-39.

[16] I.S. Denniss, A.P. Jeapes, Reprocessing irradiated fuel, in: P.D. Wilson (Ed.) The Nuclear Fuel Cycle, Oxford Science Publications, Oxford, 1996.

[17] R.S. Herbst, P. Baron, M. Nilsson, Standard and advanced separation: PUREX processes for nuclear fuel reprocessing, in: K.L. Nash, Lumetta, G. J. (Ed.) Advanced separation techniques for nuclear fuel reprocessing and radioactive waste treatment, Woodhouse Publishing Ltd., Oxford, 2011, pp. 141-175.

[18] R. Taylor, The Chemical Basis for Separating Recycling Materials by Hydro-Processes, in, 2021.

[19] J. Serp, C. Poinssot, S. Bourg, Assessment of the Anticipated Environmental Footprint of Future Nuclear Energy Systems. Evidence of the Beneficial Effect of Extensive Recycling, Energies, 10 (2017).

[20] K. Nishihara, S. Nakayama, Y. Morita, H. Oigawa, T. Iwasaki, Impact of Partitioning and Transmutation on LWR High-Level Waste Disposal, Journal of Nuclear Science and Technology, 45 (2008) 84-97.

[21] K. Nishihara, H. Oigawa, S. Nakayama, K. Ono, H. Shiotani, Impact of Partitioning and Transmutation on High-Level Waste Disposal for the Fast Breeder Reactor Fuel Cycle, Journal of Nuclear Science and Technology, 47 (2010) 1101-1117.

[22] Homogeneous versus heterogeneous recycling of transuranics in fast nuclear reactors, NEA No. 7077, Paris, 2012.

[23] A. Geist, J.-M. Adnet, S. Bourg, C. Ekberg, H. Galán, P. Guilbaud, M. Miguirditchian, G. Modolo, C. Rhodes, R. Taylor, An overview of solvent extraction processes developed in Europe for advanced nuclear fuel recycling, part 1 — heterogeneous recycling, Separation Science and Technology, (2020) 1-16.

[24] M.E. Lecomte, Treatment and recycling of spent nuclear fuel: actinide partitioning - application to waste management CEA Saclay, Paris, 2008, pp.

[25] C. Madic, M. Lecomte, P. Baron, B. Boullis, Separation of long-lived radionuclides from high active nuclear waste, Comptes Rendus Physique, 3 (2002) 797-811.

[26] C. Madic, M.J. Hudson, J.-O. Liljenzin, J.-P. Glatz, R. Nannicini, A. Facchini, Z. Kolarik, R. Odoj, New Partitioning Techniques for Minor Actinides. Final Report, EUR 19149, Luxembourg, 2000.

[27] C. Madic, F. Testard, M.J. Hudson, J.-O. Liljenzin, B. Christiansen, M. Ferrando, A. Facchini, A. Geist, G. Modolo, A.G. Espartero, J. De Mendoza, PARTNEW—New Solvent Extraction Processes for Minor Actinides. Final Report, CEA-R-6066, France, 2004.

[28] C. Madic, N. Ouvrier, EUROPART: EUROpean research program for the PARTitioning of minor actinides from high active wastes arising from the reprocessing of spent nuclear fuels, Radiochimica Acta, 96 (2008) 183-185.

[29] S. Bourg, C. Hill, C. Caravaca, C. Rhodes, C. Ekberg, R. Taylor, A. Geist, G. Modolo, L. Cassayre, R. Malmbeck, M. Harrison, G. de Angelis, A. Espartero, S. Bouvet, N. Ouvrier, ACSEPT--Partitioning technologies and actinide science: Towards pilot facilities in Europe, Nuclear Engineering and Design, 241 (2011) 3427-3435.

[30] S. Bourg, P. Guilbaud, E. Mendes, C. Ekberg, M. Gibilaro, P. Soucek, G. Modolo, A. Geist, E. Boo, B. Duplantier, C. Rhodes, R. Taylor, M. Harrison, L. Flint, K. Bell, C. Sharrad, B. Hanson, SACSESS: Final Report, SACSESS – R01.3 – rev 0, CEA, France, 2016, pp. 1-35.

[31] A. Geist, R. Taylor, C. Ekberg, P. Guilbaud, G. Modolo, S. Bourg, The SACSESS Hydrometallurgy Domain — An Overview, Procedia Chemistry, 21 (2016) 218-222.

[32] S. Bourg, A. Geist, J. Narbutt, SACSESS – the EURATOM FP7 project on actinide separation from spent nuclear fuels, Nukleonika, 60 (2015) 809-814.

[33] S. Bourg, A. Geist, J.-M. Adnet, C. Rhodes, B.C. Hanson, Partitioning and transmutation strategy R&D for nuclear spent fuel: the SACSESS and GENIORS projects, EPJ Nuclear Sci. Technol., 6 (2020) 35.

[34] R.J. Taylor, C.R. Gregson, M.J. Carrott, C. Mason, M.J. Sarsfield, Progress towards the Full Recovery of Neptunium in an Advanced PUREX Process, Solvent Extraction and Ion Exchange, 31 (2013) 442-462.

[35] R.G. Lewin, M.T. Harrison, 15 - International developments in electrorefining technologies for pyrochemical processing of spent nuclear fuels, in: R. Taylor (Ed.) Reprocessing and Recycling of Spent Nuclear Fuel, Woodhead Publishing, Oxford, 2015, pp. 373-413.

[36] G. Modolo, A. Geist, M. Miguirditchian, 10 - Minor actinide separations in the reprocessing of spent nuclear fuels: recent advances in Europe, in: R. Taylor (Ed.) Reprocessing and Recycling of Spent Nuclear Fuel, Woodhead Publishing, Oxford, 2015, pp. 245-287.

[37] J.-P. Glatz, R. Malmbeck, P. Souček, B. Claux, R. Meier, M. Ougier, T. Murakami, 26 - Development of Pyrochemical Separation Processes for Recovery of Actinides from Spent Nuclear Fuel in Molten LiCl-KCl, in: F. Lantelme, H. Groult (Eds.) Molten Salts Chemistry, Elsevier, Oxford, 2013, pp. 541-560.

[38] C.E. Till, Y.I. Chang, Plentiful energy: the story of the Integral Fast Reactor, CreateSpace, Amazon, 2011.

[39] T. Koyama, 10 - Nuclear engineering for pyrochemical treatment of spent nuclear fuels, in: K.L. Nash, G.J. Lumetta (Eds.) Advanced Separation Techniques for Nuclear Fuel Reprocessing and Radioactive Waste Treatment, Woodhead Publishing, Oxford, 2011, pp. 269-310.

[40] T. Koyama, M. Iizuka, 18 - Pyrochemical fuel cycle technologies for processing of spent nuclear fuels: Developments in Japan, in: R. Taylor (Ed.) Reprocessing and Recycling of Spent Nuclear Fuel, Woodhead Publishing, Oxford, 2015, pp. 457-519.

[41] H. Lee, 16 - Oxide electroreduction and other processes for pyrochemical processing of spent nuclear fuels: Developments in Korea, in: R. Taylor (Ed.) Reprocessing and Recycling of Spent Nuclear Fuel, Woodhead Publishing, Oxford, 2015, pp. 415-436.

[42] P. Souček, R. Malmbeck, 17 - Pyrochemical processes for recovery of actinides from spent nuclear fuels, in: R. Taylor (Ed.) Reprocessing and Recycling of Spent Nuclear Fuel, Woodhead Publishing, Oxford, 2015, pp. 437-456.

[43] K. Minato, 22 - Development of closed nuclear fuel cycles in Japan, in: R. Taylor (Ed.) Reprocessing and Recycling of Spent Nuclear Fuel, Woodhead Publishing, Oxford, 2015, pp. 565-578.

[44] A. Geist, C. Hill, G. Modolo, M.R.S.J. Foreman, M. Weigl, K. Gompper, M.J. Hudson, 6,6'-Bis(5,5,8,8-tetramethyl-5,6,7,8-tetrahydro-benzo[1,2,4]triazin-3-yl) [2,2']bipyridine, an Effective Extracting Agent for the Separation of Americium(III) and Curium(III) from the Lanthanides, Solvent Extraction and Ion Exchange, 24 (2006) 463-483.

[45] P.J. Panak, A. Geist, Complexation and Extraction of Trivalent Actinides and Lanthanides by Triazinylpyridine N-Donor Ligands, Chemical Reviews, 113 (2013) 1199-1236.

[46] G. Modolo, A. Wilden, A. Geist, D. Magnusson, R. Malmbeck, A review of the demonstration of innovative solvent extraction processes for the recovery of trivalent minor actinides from PUREX raffinate, Radiochimica Acta, 100 (2012) 715-725.

[47] G. Modolo, A. Wilden, P. Kaufholz, D. Bosbach, A. Geist, Development and demonstration of innovative partitioning processes (i-SANEX and 1-cycle SANEX) for actinide partitioning, Progress in Nuclear Energy, 72 (2014) 107-114.

[48] R. Taylor, S. Bourg, J.-P. Glatz, G. Modolo, Development of actinide separation processes for future nuclear fuel cycles in Europe, Nuclear Future, 11 (2015) 38-43.

[49] M. Miguirditchian, L. Chareyre, X. Hérès, C. Hill, P. Baron, M. Masson, GANEX: Adaptation of the DIAMEX-SANEX Process for the Group Actinide Separation, in: Proc. GLOBAL 2007, Advanced Nuclear Fuel Cycles and Systems, American Nuclear Society, Boise, Idaho, 2007, pp. 550-552.

[50] M. Miguirditchian, H. Roussel, L. Chareyre, P. Baron, HA demonstration in the Atalante facility of the GANEX 2nd cycle for the grouped TRU extraction, in: GLOBAL 2009, American Nuclear Society, Paris, France, 2009, pp. 9378.

[51] M. Miguirditchian, C. Sorel, B. Camès, I. Bisel, P. Baron, Extraction of uranium (VI by N,N-di(2-ethylhexyl)isobutyramide (DEHIBA): from the batch experimental data to the countercurrent process, in: B.A. Moyer (Ed.) Solvent extraction: fundamentals to industrial applications. Proceedings ISEC 2008 International Solvent Extraction conference, Can. Inst. Min. Metall. Pet., Montreal, Canada, 2008, pp. 721-726.

[52] M. Carrott, K. Bell, J. Brown, A. Geist, C. Gregson, X. Hères, C. Maher, R. Malmbeck, C. Mason, G. Modolo, U. Müllich, M. Sarsfield, A. Wilden, R. Taylor, Development of a new flowsheet for co-separating the transuranic actinides: the “EURO-GANEX” process, Solvent Extraction and Ion Exchange, 32 (2014) 447-467.

[53] M. Carrott, A. Geist, X. Hères, S. Lange, R. Malmbeck, M. Miguirditchian, G. Modolo, A. Wilden, R. Taylor, Distribution of plutonium, americium and interfering fission products between nitric acid and a mixed organic phase of TODGA and DMDOHEMA in kerosene, and implications for the design of the “EURO-GANEX” process, Hydrometallurgy, 152 (2015) 139-148.

[54] R. Malmbeck, D. Magnusson, S. Bourg, M. Carrott, A. Geist, X. Hérès, M. Miguirditchian, G. Modolo, U. Müllich, C. Sorel, R. Taylor, A. Wilden, Homogenous recycling of transuranium elements from irradiated fast reactor fuel by the EURO-GANEX solvent extraction process, Radiochimica Acta, 107 (2019) 917-929.

[55] E. Aneheim, C. Ekberg, M.R.S.J. Foreman, A TBP/BTBP-Based GANEX Separation Process – Part 3: Fission Product Handling, Solvent Extraction and Ion Exchange, 31 (2013) 237-252.

[56] E. Aneheim, C. Ekberg, A. Fermvik, M.R.S.J. Foreman, B. Grűner, Z. Hájková, M. Kvičalová, A TBP/BTBP-based GANEX Separation Process—Part 2: Ageing, Hydrolytic, and Radiolytic Stability, Solvent Extraction and Ion Exchange, 29 (2011) 157-175.

[57] E. Aneheim, C. Ekberg, A. Fermvik, M.R.S.J. Foreman, T. Retegan, G. Skarnemark, A TBP/BTBP-based GANEX Separation Process. Part 1: Feasibility, Solvent Extraction and Ion Exchange, 28 (2010) 437-458.

[58] J. Halleröd, C. Ekberg, E. Aneheim, Phenyl trifluoromethyl sulfone as diluent in a grouped actinide extraction process: extraction properties of the solvent components TBP and CyMe4-BTBP, Journal of Radioanalytical and Nuclear Chemistry, 307 (2016) 1711-1715.

[59] P.N. Pathak, R. Veeraraghavan, D.R. Prabhu, G.R. Mahajan, V.K. Manchanda, Separation Studies of Uranium and Thorium Using Di-2-Ethylhexyl Isobutyramide (D2EHIBA), Separation Science and Technology, 34 (1999) 2601-2614.

[60] N. Condamines, C. Musikas, The extraction by N,N-dialkylamides. II. Extraction of actinide cations, Solvent Extraction and Ion Exchange, 10 (1992) 69-100.

[61] P. Baron, S.M. Cornet, E.D. Collins, G. DeAngelis, G. Del Cul, Y. Fedorov, J.P. Glatz, V. Ignatiev, T. Inoue, A. Khaperskaya, I.T. Kim, M. Kormilitsyn, T. Koyama, J.D. Law, H.S. Lee, K. Minato, Y. Morita, J. Uhlíř, D. Warin, R.J. Taylor, A review of separation processes proposed for advanced fuel cycles based on technology readiness level assessments, Progress in Nuclear Energy, 117 (2019) 103091.

[62] P. Baron, National Programmes in Chemical Partitioning: A Status Report, 5245, Nuclear Energy Agency, Organisation for Economic Cooperation and Development, Paris, 2010, pp. 1-120.

[63] G. Modolo, H. Asp, C. Schreinemachers, H. Vijgen, Development of a TODGA based Process for Partitioning of Actinides from a PUREX Raffinate Part I: Batch Extraction Optimization Studies and Stability Tests, Solvent Extraction and Ion Exchange, 25 (2007) 703-721.

[64] G. Modolo, H. Asp, H. Vijgen, R. Malmbeck, D. Magnusson, C. Sorel, Demonstration of a TODGA-Based Continuous Counter-Current Extraction Process for the Partitioning of Actinides from a Simulated PUREX Raffinate, Part II: Centrifugal Contactor Runs, Solvent Extraction and Ion Exchange, 26 (2008) 62-76.

[65] J. Brown, M.J. Carrott, O.D. Fox, C.J. Maher, C. Mason, F. McLachlan, M.J. Sarsfield, R.J. Taylor, D.A. Woodhead, Screening of TODGA/TBP/OK solvent mixtures for the grouped extraction of actinides, IOP Conference Series: Materials Science and Engineering, 9 (2010) 012075.

[66] J. Brown, F. McLachlan, M.J. Sarsfield, R.J. Taylor, G. Modolo, A. Wilden, Plutonium loading of prospective grouped actinide extraction (GANEX) solvent systems based on diglycolamide extractants, Solvent Extraction and Ion Exchange, 30 (2012) 127-141.

[67] K. Bell, C. Carpentier, M. Carrott, A. Geist, C. Gregson, X. Hérès, D. Magnusson, R. Malmbeck, F. McLachlan, G. Modolo, U. Müllich, M. Sypula, R. Taylor, A. Wilden, Progress Towards the Development of a New GANEX Process, Proc. Chem., 7 (2012) 392-397.

[68] A. Geist, U. Müllich, D. Magnusson, P. Kaden, G. Modolo, A. Wilden, T. Zevaco, Actinide(III)/Lanthanide(III) Separation Via Selective Aqueous Complexation of Actinides(III) using a Hydrophilic 2,6-Bis(1,2,4-Triazin-3-Yl)-Pyridine in Nitric Acid, Solvent Extraction and Ion Exchange, 30 (2012) 433-444.

[69] M.J. Carrott, Fox, O. D., Maher, C. J., Mason, C., Taylor, R. J., Sinkov, S. I., Choppin, G. R., Solvent Extraction Behavior of Plutonium (IV) Ions in the Presence of Simple Hydroxamic Acids, Solvent Extraction and Ion Exchange, 25 (2007) 723-745.

[70] M.J. Carrot, C.R. Gregson, R.J. Taylor, Neptunium extraction and stability in the GANEX solvent: 0.2 M TODGA / 0.5 M DMDOHEMA / kerosene, Solvent Extraction and Ion Exchange, 31 (2013) 463-482

[71] M. Sypula, A. Wilden, C. Schreinemachers, R. Malmbeck, A. Geist, R. Taylor, G. Modolo, Use of polyaminocarboxylic acids as hydrophilic masking agents for fission products in actinide partitioning processes, Solvent Extraction and Ion Exchange, 3 (2013) 748-764.

[72] D. Magnusson, B. Christiansen, J.-P. Glatz, R. Malmbeck, G. Modolo, D. Serrano-Purroy, C. Sorel, Demonstration of a TODGA based Extraction Process for the Partitioning of Minor Actinides from a PUREX Raffinate -- Part III: Centrifugal Contactor Run using Genuine Fuel Solution, Solvent Extraction and Ion Exchange, 27 (2009) 26-35.

[73] P. Moeyaert, M. Miguirditchian, M. Masson, B. Dinh, X. Hérès, S. De Sio, C. Sorel, Experimental and modelling study of ruthenium extraction with tri-n-butylphosphate in the purex process, Chemical Engineering Science, 158 (2017) 580-586.

[74] D.J. Pruett, Extraction chemistry of fission products, in: W.W. Schulz, L.L. Burger, J.D. Navratil (Eds.) Science and Technology of Tributyl Phosphate, CRC Press, Boca Raton, 1990, pp. 81-122.

[75] V.A. Drake, Extraction chemistry of neptunium, in: W.W. Schulz, L.L. Burger, J.D. Navratil, K.P. Bender (Eds.) Science and technology of tributyl phosphate, CRC Press Inc., Boca Raton, Florida, 1990, pp. 123-146.

[76] M.J. Carrott, C.R. Gregson, R.J. Taylor, Neptunium extraction and stability in the GANEX solvent (0.2 M TODGA / 0.5 M DMDOHEMA / kerosene), Solvent Extr. Ion Exch., 31 (2013) 463-482.

[77] M.J. Sarsfield, Taylor, R. J., Maher, C. J., Neptunium(V) disproportionation and cation–cation interactions in TBP/kerosene solvent, Radiochimica Acta, 95 (2007) 677-682.

[78] J.P. Moulin, Oxidation – reduction kinetics of neptunium in nitric acid solution, CEA-R-4912, Fontenay-aux-Roses, France, 1978.

[79] L. Flint, Production of SACSESS combined safety methodology: Delivery of the SACSESS combined safety assessment methodology, Report D3.1.1b, National Nuclear Laboratory, Preston, 2014.

[80] M.J. Carrott, C.J. Maher, C. Mason, M.J. Sarsfield, D. Whittaker, R.J. Taylor, Experimental test of a process upset in the EURO-GANEX process, Separation Science and Technology, in preparation (2021).

[81] D.W. Ockenden, G.A. Welch, 653. The preparation and properties of some plutonium compounds. Part V. Colloidal quadrivalent plutonium, Journal of the Chemical Society (Resumed), (1956) 3358-3363.

[82] E. Aneheim, C. Ekberg, M.R.S. Foreman, Aqueous complexation of palladium to prevent precipitation and extraction in a group actinide extraction system, Hydrometallurgy, 115-116 (2012) 71-76.

[83] T.L. Authen, CHALMEX FS-13 investigations for process implementation, in: Department of Chemistry and Chemical Engineering Chalmers University of Technology, Gothenburg, Sweden, 2020, pp. 62.

[84] T.L. Authen, A. Wilden, J. Halleröd, D. Schneider, F. Kreft, G. Modolo, C. Ekberg, Batch Tests for Optimisation of Solvent Composition and Process flexibility of the CHALMEX FS-13 Process, Solvent Extr. Ion Exch., 39 (2021) 1-17.

[85] T.L. Authen, A. Wilden, D. Schneider, F. Kreft, G. Modolo, M.R.S. Foreman, C. Ekberg, Batch flowsheet test for a GANEX-type process: the CHALMEX FS-13 process, Solvent Extr. Ion Exch., DOI:10.1080/07366299.2021.1890372 (2021).

[86] J. Halleröd, C. Ekberg, T. Authen, L. Bertolo, M. Lin, B. Grüner, J. Švehla, C. Wagner, A. Geist, P. Panak, E. Aneheim, On the Basic Extraction Properties of a Phenyl Trifluoromethyl Sulfone-Based GANEX System Containing CyMe4-BTBP and TBP, Solvent Extraction and Ion Exchange, 36 (2018) 360-372.

[87] J. Halleröd, C. Ekberg, I. Kajan, E. Aneheim, Solubility Thermodynamics of $CyMe_4$-BTBP in Various Diluents Mixed with TBP, Journal of Solution Chemistry, 47 (2018) 1021-1036.

[88] J. Halleröd, C. Ekberg, E. Löfström-Engdahl, E. Aneheim, Development of the Chalmers Grouped Actinide Extraction Process, Nukleonika, 60 (2015) 829-835.

[89] T. Retegan, C. Ekberg, S. Englund, A. Fermvik, M.R.S. Foreman, G. Skarnemark, The behaviour of organic solvents containing C5-BTBP and CyMe4-BTBP at low irradiation doses, Radiochimica Acta, 95 (2007) 637-642.

[90] R.S. Herbst, J.D. Law, T.A. Todd, V.N. Romanovskiy, I.V. Smirnov, V.A. Babain, V.N. Esimantovskiy, B.N. Zaitsev, Development Of The Universal Extraction (Unex) Process For The Simultaneous Recovery Of Cs, Sr, And Actinides From Acidic Radioactive Wastes, Separation Science and Technology, 38 (2003) 2685-2708.

[91] S. Kumar, M. Muthukumar, P.K. Sinha, U. Kamachi Mudali, R. Natarajan, PVT properties of UNEX/HCCD-PEG diluent phenyl trifluoromethyl sulfone (FS-13) and experimental measurement of vapour pressure in 283.15–363.15 K range, Journal of Radioanalytical and Nuclear Chemistry, 289 (2011) 247-249.

[92] J.D. Law, R.S. Herbst, T.A. Todd, V.N. Romanovskiy, V.A. Babain, V.M. Esimantovskiy, I.V. Smirnov, B.N. Zaitsev, THE UNIVERSAL SOLVENT EXTRACTION (UNEX) PROCESS. II. FLOWSHEET DEVELOPMENT AND DEMONSTRATION OF THE UNEX PROCESS FOR THE SEPARATION OF CESIUM, STRONTIUM, AND ACTINIDES FROM ACTUAL ACIDIC RADIOACTIVE WASTE, Solvent Extraction and Ion Exchange, 19 (2001) 23-36.

[93] T.A. Luther, R.S. Herbst, D.R. Peterman, R.D. Tillotson, T.G. Garn, V.A. Babain, I.V. Smirnov, E.S. Stoyanov, N.G. Antonov, Some aspects of fundamental chemistry of the Universal Extraction (UNEX) process for the simultaneous separation of major radionuclides (cesium, strontium, actinides, and lanthanides) from radioactive wastes, Journal of Radioanalytical and Nuclear Chemistry, 267 (2006) 603-613.

[94] V.N. Romanovskiy, I.V. Smirnov, V.A. Babain, T.A. Todd, R.S. Herbst, J.D. Law, K.N. Brewer, THE UNIVERSAL SOLVENT EXTRACTION (UNEX) PROCESS. I. DEVELOPMENT OF THE UNEX PROCESS SOLVENT FOR THE SEPARATION OF CESIUM, STRONTIUM, AND THE ACTINIDES FROM ACIDIC RADIOACTIVE WASTE, Solvent Extraction and Ion Exchange, 19 (2001) 1-21.

[95] E.K. Rzhekhina, V.G. Karkozov, M.Y. Alyapyshev, V.A. Babain, I.V. Smirnov, P.A. Todd, J.D. Law, R.S. Herbst, Reprocessing of spent solvent of the UNEX process, Radiochemistry, 49 (2007) 493-498.

[96] P.K. Sinha, S. Kumar, U. Kamachi Mudali, R. Natarajan, Thermal Stability of UNEX/HCCD-PEG Diluent FS-13, Journal of Radioanalytical and Nuclear Chemistry, 289 (2011) 899-901.

[97] SpringerMaterials Interactive, Dielectric Constant of Phenyl trifluoromethyl sulfone (pure), in, Springer-Verlag Berlin Heidelberg Release 2017, Online, 2017.

[98] C.H. Bartholomew, R.J. Farrauto, Fundamentals of industrial catalytic processes, 2. ed. ed., Wiley, 2006.

[99] M. Carrott, C. Maher, C. Mason, M. Sarsfield, R. Taylor, "TRU-SANEX": A variation on the EURO-GANEX and i-SANEX processes for heterogeneous recycling of actinides Np-Cm, Separation Science and Technology, 51 (2016) 2198-2213.

[100] S. Sinkov, G. Choppin, Acetohydroxamic Acid Complexes with Trivalent f-Block Metal Cations, Journal of Nuclear Science and Technology, 39 (2002) 359-362.

[101] S.I. Sinkov, G.R. Choppin, R.J. Taylor, Spectrophotometry and Luminescence Spectroscopy of Acetohydroxamate Complexes of Trivalent Lanthanide and Actinide Ions, Journal of Solution Chemistry, 36 (2007) 815-830.

[102] R.J. Taylor, S.I. Sinkov, G.R. Choppin, Complexation of lanthanides and actinides by aceto-hydroxamic acid, in: B.A. Moyer (Ed.) Solvent extraction: fundamentals to industrial applications, Proc. ISEC 2008 International Solvent Extraction conference, Can. Inst. Min. Metall. Pet., Montreal, 2008, pp. 527-531.

[103] R.J. Taylor, S.I. Sinkov, G.R. Choppin, I. May, Solvent Extraction Behavior of Neptunium (IV) Ions between Nitric Acid and Diluted 30% Tributyl Phosphate in the Presence of Simple Hydroxamic Acids, Solvent Extraction and Ion Exchange, 26 (2007) 41-61.

[104] E. Macerata, E. Mossini, S. Scaravaggi, M. Mariani, A. Mele, W. Panzeri, N. Boubals, L. Berthon, M.-C. Charbonnel, F. Sansone, A. Arduini, A. Casnati, Hydrophilic Clicked 2,6-Bis-triazolyl-pyridines Endowed with High Actinide Selectivity and Radiochemical Stability: Toward a Closed Nuclear Fuel Cycle, Journal of the American Chemical Society, 138 (2016) 7232-7235.

[105] E. Mossini, E. Macerata, A. Wilden, P. Kaufholz, G. Modolo, N. Iotti, A. Casnati, A. Geist, M. Mariani, Optimization and Single-Stage Centrifugal Contactor Experiments with the Novel Hydrophilic Complexant PyTri-Diol for the i-SANEX Process, Solvent Extraction and Ion Exchange, 36 (2018) 373-386.

[106] R. Malmbeck, D. Magnusson, A. Geist, Modified Diglycolamides for Grouped Actinide Separation, J. Radioanal. Nucl. Chem., 314 (2017) 2531-2538.

[107] H. Chen, R. Taylor, M. Jobson, D. Woodhead, A. Masters, Development and Validation of a Flowsheet Simulation Model for Neptunium Extraction in an Advanced PUREX Process, Solvent Extraction and Ion Exchange, 34 (2016) 297-321.

[108] H. Chen, R.J. Taylor, M. Jobson, D.A. Woodhead, C. Boxall, A.J. Masters, S. Edwards, Simulation of Neptunium Extraction in an Advanced PUREX Process—Model Improvement, Solvent Extraction and Ion Exchange, 35 (2017) 1-18.

[109] F. McLachlan, R. Taylor, D. Whittaker, D. Woodhead, A. Geist, Modelling of Innovative SANEX Process Maloperations, Procedia Chemistry, 21 (2016) 109-116.

[110] J. Brown, F. McLachlan, M.J. Sarsfield, R.J. Taylor, G. Modolo, A. Wilden, Plutonium loading of prospective grouped actinide extraction (GANEX) solvent systems based on diglycolamide extractants, Solvent Extr. Ion Exch., 30 (2012) 127-141.

[111] M. Carrott, K. Bell, J. Brown, A. Geist, C. Gregson, X. Hères, C. Maher, R. Malmbeck, C. Mason, G. Modolo, U. Müllich, M. Sarsfield, A. Wilden, R. Taylor, Development of a New Flowsheet for Co-Separating the Transuranic Actinides: The "EURO-GANEX" Process, Solvent Extr. Ion Exch., 32 (2014) 447-467.

[112] R. Taylor, M. Carrott, H. Galan, A. Geist, X. Hères, C. Maher, C. Mason, R. Malmbeck, M. Miguirditchian, G. Modolo, C. Rhodes, M. Sarsfield, A. Wilden, The EURO-GANEX Process: Current Status of Flowsheet Development and Process Safety Studies, Procedia Chem., 21 (2016) 524-529.

[113] R. Malmbeck, D. Magnusson, S. Bourg, M. Carrott, A. Geist, X. Hérès, M. Miguirditchian, G. Modolo, U. Müllich, C. Sorel, R. Taylor, A. Wilden, Homogenous Recycling of Transuranium Elements from Irradiated Fast Reactor Fuel by the EURO-GANEX Solvent Extraction Process, Radiochim. Acta, 107 (2019) 917-929.

[114] H. Stephan, K. Gloe, J. Beger, P. Muhl, Liquid-Liquid-Extraction of Metal-Ions with Amido Podands, Solvent Extr. Ion Exch., 9 (1991) 459-469.

[115] H. Stephan, K. Gloe, J. Beger, P. Muhl, Liquid-Liquid-Extraction of Strontium with Amido Podands, Solvent Extr. Ion Exch., 9 (1991) 435-458.

[116] Y. Sasaki, R. Choppin, Solvent Extraction of Eu, Th, U, Np and Am with N, N'-Dimethyl-N, N'-dihexyl-3-oxapentanediamide and Its Analogous Compounds, Anal. Sci., 12 (1996) 225-230.

[117] S.A. Ansari, P. Pathak, P.K. Mohapatra, V.K. Manchanda, Chemistry of Diglycolamides: Promising Extractants for Actinide Partitioning, Chemical Reviews, 112 (2012) 1751-1772.

[118] M. Iqbal, J. Huskens, W. Verboom, M. Sypula, G. Modolo, Synthesis and Am/Eu Extraction of Novel TODGA Derivatives, Supramolecular Chemistry, 22 (2010) 827-837.

[119] A. Wilden, G. Modolo, S. Lange, F. Sadowski, B.B. Beele, A. Skerencak-Frech, P.J. Panak, M. Iqbal, W. Verboom, A. Geist, D. Bosbach, Modified Diglycolamides for the An(III) + Ln(III) Co-separation: Evaluation by Solvent Extraction and Time-Resolved Laser Fluorescence Spectroscopy, Solvent Extr. Ion Exch., 32 (2014) 119-137.

[120] A. Wilden, P.M. Kowalski, L. Klaß, B. Kraus, F. Kreft, G. Modolo, Y. Li, J. Rothe, K. Dardenne, A. Geist, A. Leoncini, J. Huskens, W. Verboom, Unprecedented Inversion of Selectivity and Extraordinary Difference in the Complexation of Trivalent *f*-Elements by Diastereomers of a Methylated Diglycolamide, Chemistry – A European Journal, 25 (2019) 5507-5513.

[121] E. Macerata, E. Mossini, S. Scaravaggi, M. Mariani, A. Mele, W. Panzeri, N. Boubals, L. Berthon, M.-C. Charbonnel, F. Sansone, A. Arduini, A. Casnati, Hydrophilic Clicked 2,6-Bis-triazolyl-pyridines Endowed with High Actinide Selectivity and Radiochemical Stability: Toward a Closed Nuclear Fuel Cycle, J. Am. Chem. Soc., 138 (2016) 7232-7235.

[122] C. Wagner, E. Mossini, E. Macerata, M. Mariani, A. Arduini, A. Casnati, A. Geist, P.J. Panak, Time-Resolved Laser Fluorescence Spectroscopy Study of the Coordination Chemistry of a Hydrophilic CHON 1,2,3-Triazol-4-yl pyridine Ligand with Cm(III) and Eu(III), Inorganic Chemistry, 56 (2017) 2135-2144.

[123] E. Mossini, E. Macerata, L. Brambilla, W. Panzeri, A. Mele, C. Castiglioni, M. Mariani, Radiolytic degradation of hydrophilic PyTri ligands for minor actinide recycling, J. Radioanal. Nucl. Chem., 322 (2019) 1663-1673.

[124] E. Mossini, E. Macerata, A. Wilden, P. Kaufholz, G. Modolo, N. Iotti, A. Casnati, A. Geist, M. Mariani, Optimization and Single-stage Centrifugal Contactor Experiments with the Novel Hydrophilic Complexant PyTri-Diol for the *i*-SANEX Process, Solvent Extr. Ion Exch., 36 (2018) 373-386.

[125] T.H. Siddall, E.K. Dukes, Kinetics of HNO2 Catalyzed Oxidation of Neptunium(V) by Aqueous Solutions of Nitric Acid1, Journal of the American Chemical Society, 81 (1959) 790-794.

[126] A. Wilden, G. Modolo, S. Lange, F. Sadowski, B.B. Beele, A. Skerencak-Frech, P.J. Panak, M. Iqbal, W. Verboom, A. Geist, D. Bosbach, Modified diglycolamides for the An(III) + Ln(III) co-separation: evaluation by solvent extraction and time-resolved laser fluorescence spectroscopy, Solvent Extr. Ion Exch., 32 (2014) 119–137.

[127] P. Weßling, U. Müllich, E. Guerinoni, A. Geist, P.J. Panak, Solvent extraction of An(III) and Ln(III) using TODGA in aromatic diluents to suppress third phase formation, Hydrometallurgy, 192 (2020) 105248.

[128] R. Malmbeck, D. Magnusson, A. Geist, Modified diglycolamides for grouped actinide separation, J. Radioanal. Nucl. Chem., 314 (2017) 2531–2538.

[129] C. Ekberg, E. Löfström-Engdahl, E. Aneheim, M. Foreman, A. Geist, D. Lundberg, M. Denecke, I. Persson, The structures of CyMe4-BTBP complexes of americium(III) and europium(III) in solvents used in solvent extraction, explaining their separation properties, Dalton transactions (Cambridge, England : 2003), 44 (2015).

[130] A.V. Ochkin, M.A. Afonina, A.O. Merkushkin, S.Y. Nekhaevskii, Extraction of nitric acid by tributyl phosphate solution in n-dodecane, Russian Journal of Physical Chemistry A, 84 (2010) 1526-1531.

[131] J. Halleröd, C. Ekberg, M. Foreman, E.L. Engdahl, E. Aneheim, Stability of phenyl trifluoromethyl sulfone as diluent in a grouped actinide extraction process, Journal of Radioanalytical and Nuclear Chemistry, 304 (2015) 287-291.

[132] M. Precek, A. Paulenova, B. Mincher, Reduction of Np(VI) in Irradiated Solutions of Nitric Acid, Procedia Chemistry, 7 (2012) 51–58.

[133] S. Chatterjee, S.A. Bryan, A.J. Casella, J.M. Peterson, T.G. Levitskaia, Mechanisms of neptunium redox reactions in nitric acid solutions, Inorganic Chemistry Frontiers, 4 (2017) 581-594.

[134] P.E. Burns, C. Hanson, Distribution of nitric acid between tri-N-butyl phosphate and water, Journal of Applied Chemistry, 14 (1964) 117-121.

[135] D.R. Olander, L. Donadieu, M. Benedict, The distribution of nitric acid between water and tributyl phosphate - hexane solvents, AIChE Journal, 7 (1961) 152-159.

[136] Z. Kolarik, S. Tachimori, T. Nakashima, EXTRACTION OF URANIUM(IV,VI), PLUTONIUM(III) AND NITRIC ACID BY 30% TRIBUTYL PHOSPHATE (TBP) IN DODECANE, Solvent Extraction and Ion Exchange, 2 (1984) 607-620.

[137] K.-W. Kim, K.-C. Song, E.-H. Lee, I.-K. Choi, J.-H. Yoo, Oxidation State and Extraction of Neptunium with TBP, Journal of Radioanalytical and Nuclear Chemistry, 246 (2000) 215-219.

[138] E. Aneheim, C. Ekberg, G. Modolo, A. Wilden, Single Centrifugal Contactor Test of a Proposed Group Actinide Extraction Process for Partitioning and Transmutation Purposes, Separation Science and Technology, 50 (2014) 150527095459001.